공학박사학위논문

슬러리 저감을 위한 중심부 주입 폴리싱

Center Injected Polishing for Slurry Reduction

2023년 2월

서울대학교 대학원

기계항공공학부

김동률

슬러리 저감을 위한 중심부 주입 폴리싱

Center Injected Polishing for Slurry Reduction

지도교수 안 성 훈

이 논문을 공학박사 학위논문으로 제출함

2022년 10월

서울대학교 대학원

기계항공공학부

김 동 률

김동률의 공학박사 학위논문을 인준함

2022년 12월

위 원 장 : 박 희 재 (인)

부위원장 : 안 성 훈 (인)

위 원 : 민 상 기 (인)

위 원 : 전 병 국 (인)

위 원 : 윤 해 성 (인)

Abstract

Silicon carbide has recently attracted considerable attention as an optical component in the space field because of its outstanding material properties. In general, the fabrication of optical components starts with a process with a high material removal rate and ends with a process with a low material removal rate and high surface quality. Polishing which is in the final stage of manufacturing optical components plays a very important role in determining the quality of optics.

Polishing is a time-consuming process due to the low material removal rate. The amount of consumable material required during this long processing time is also enormous; therefore, reducing it is key to reducing the cost of the process and improving the environment.

In the case of slurry, which is one of the main consumables in polishing, an excessive amount of slurry is generally supplied without special consideration to ensure that a sufficient amount is supplied to the process. However, only a fraction of this excess supply participates in the polishing process, and the remainder is discharged as waste. In particular, the centrifugal force generated by the rotating polishing tool during this process prevents slurry from being supplied to the contact surface between the workpiece and tool.

In this study, by supplying the slurry directly at the tool center, the centrifugal force of the tool rotation was utilized to supply the slurry to improve the supply condition of the slurry. Ultimately, it is intended to improve the process performance and reduce slurry consumption by improving the slurry supply performance. The slurry was injected at the center of the tool through a rotary union and an in-house

polishing tool. Polishing experiments were performed at various supply flow rates and tool rotation speeds when the slurry was supplied to different positions, and the material removal and surface roughness were measured after the experiment to evaluate the process performance. In terms of material removal, center-injected polishing resulted in up to 138% higher material removal than that of the tool outside supply. When the slurry reduction performance was evaluated using the amount of material removed and amount of slurry used according to the three criteria, the slurry reduction performance was 54% based on the highest slurry processing efficiency, 58% based on the same process parameters, and 84% based on the maximum material removal performance.

Keyword : Polishing, Slurry reduction, Green manufacturing, Silicon Carbide

Student Number : 2016-20673

Table of Contents

List of Tables

List of Figures

Chapter 1. Introduction

1.1. Benefits of silicon carbide as an optics

Silicon carbide (SiC), one of the hardest materials, is a semiconductor containing silicon and carbon and is produced from moissanite, an extremely rare mineral in nature. SiC was first created in 1824 by Jones Jacobs.

The smallest constituent units of all SiC structures are silicon and carbon. As shown in Figure 1.1, a carbon atom in the center surrounded by four silicon atoms, or vice versa, is a tetrahedral structure. Sic exists in approximately 250 crystalline structures [1]. Its polymorphism can be characterized by its polytypes, indicating a family of similar crystal structures. The polytype is a variant of the same compound, which is the same in two dimensions but different in three dimensions. Therefore, they can be seen as layers stacked in a specific order [2]. Depending on how the tetrahedral structures are stacked, the beta and alpha phases exist [3, 4]. The most commonly encountered polytype, alpha SiC, which has a hexagonal crystal structure, is formed at temperatures above 1700 ℃. The beta SiC is formed at temperatures below 1700 ℃ [5].

As listed in Table 1, SiC has excellent mechanical properties, including high hardness and low density. They are widely used in optical components in aerospace and defense industries because of these properties [6]. However, its excellent mechanical properties render SiC machinability very poor, requiring long times and incurring high costs. This makes it difficult to manufacture optical components [7].

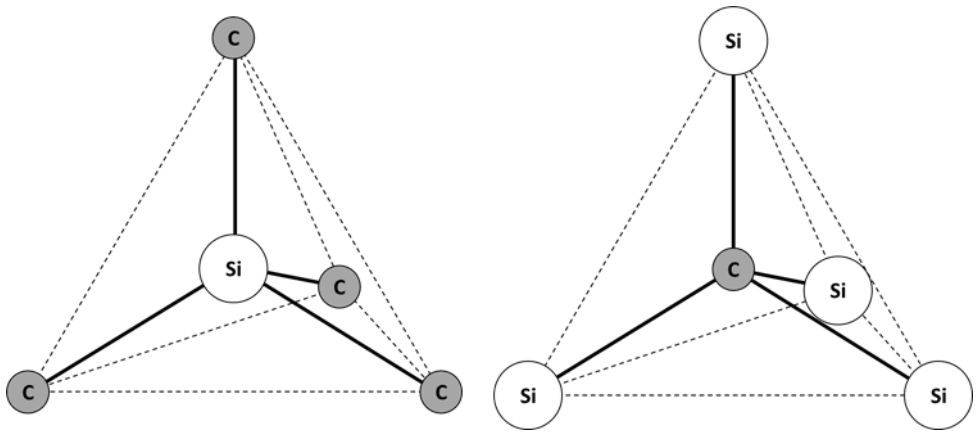

Figure 1.1 Tetrahedral structure of SiC

Table 1.1 Material properties of Silicon carbide [8-12]

Property	**4H-SiC**	**6H-SiC**	**3C-SiC**
Elastic Modulus [GPa]	-	-	433
Density [kg/m^3]	3200		
Moh's Hardness	9		
Thermal Conductivity [W/m•K]	370	490	360
Thermal Diffusivity [$mm^2\ s^{-1}$]	170	220	160
Thermal Expansion (1,000°C) [10^{-6} °C^{-1}]	4.7~5.15	4.6~4.7	3.8

1.2. Polishing in fabrication of optics

The use of optical components with high shape accuracy is increasing in optoelectronics businesses and astronomical observation [13-17]. In general, the manufacturing stage of optical parts starts with a large amount of processing and poor surface quality and ends with a small amount of processing and good surface quality. Therefore, the productivity of the optical components is often determined in the final production stage, which has a low amount of material removal.

Mechanical polishing uses hard abrasive particles such as alumina particles. A polishing pad rubs the abrasive particles against the workpiece and causes it to move. Material removal by abrasive particles occurs through plastic deformation. Because the material is removed very finely, the surface quality after the process is excellent. Therefore, polishing is very useful when high-quality surfaces are required [18, 19].

Various processes are used to manufacture optical components, among which grinding and final polishing are mainly used [20-22]. The demand for polishing in the manufacturing of precision optical components in the aerospace field has recently increased due to the growing popularity of large optical components in optical systems. In particular, owing to increasing surface quality requirements in the aerospace field, the time to manufacture large-diameter optical components has greatly increased to weeks or months[23]. Naturally, the amount of consumables used during this process, such as slurries and polishing pads, increased significantly. As the amount of slurry contaminants discharged from a process over time is very large, reducing it is becoming increasingly important [24].

1.3. Slurry in polishing

The polishing process is indirectly performed using abrasives [25], and it is important to supply a sufficient amount of abrasives. In conventional polishing, a substantial amount of slurry is supplied to ensure that sufficient slurry is supplied. However, because the capacity of the polishing pad is limited, the amount of slurry that actually participates in material removal is very small for a large amount of supplied slurry. An excess slurry supply greatly increases the amount of slurry waste because the remainder is not used for material removal and is immediately discharged as slurry waste as depicted in Figure 1.2. As polishing is a very time-consuming process [26] , the increase in slurry waste due to excessive slurry supply and process cost due to slurry is maximized.

If we take a closer look at the quality of polishing, it is very important to supply the slurry well to the entire area of the tool interface where material removal occurs. As the slurry is supplied to the outside of the contact surface in conventional polishing, centrifugal force prevents the slurry at the outside of the tool from being supplied to the contact surface and causes the slurry to bounce off as depicted in Figure 1.3. Therefore, it is necessary to supply more slurry than the slurry that participates in actual material removal because of this problem. This results in reduced slurry efficiency in terms of material removal.

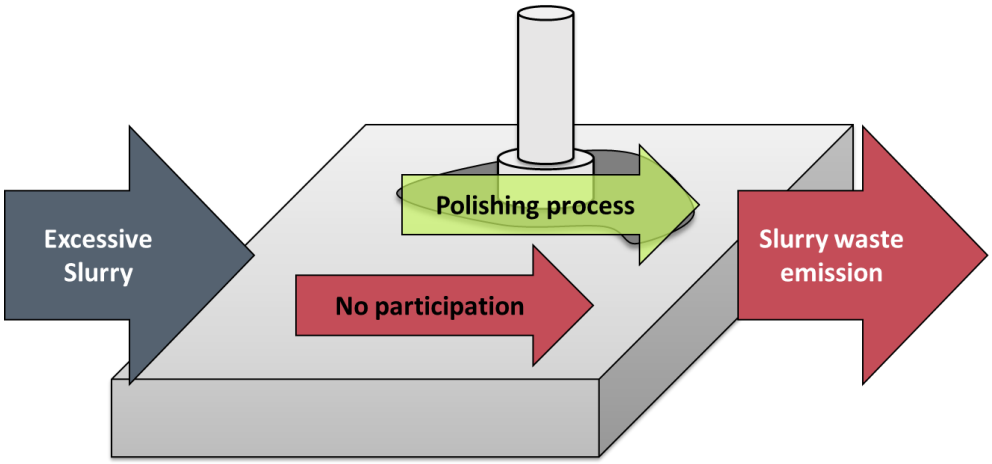

Figure 1.2 Polishing slurry waste emission

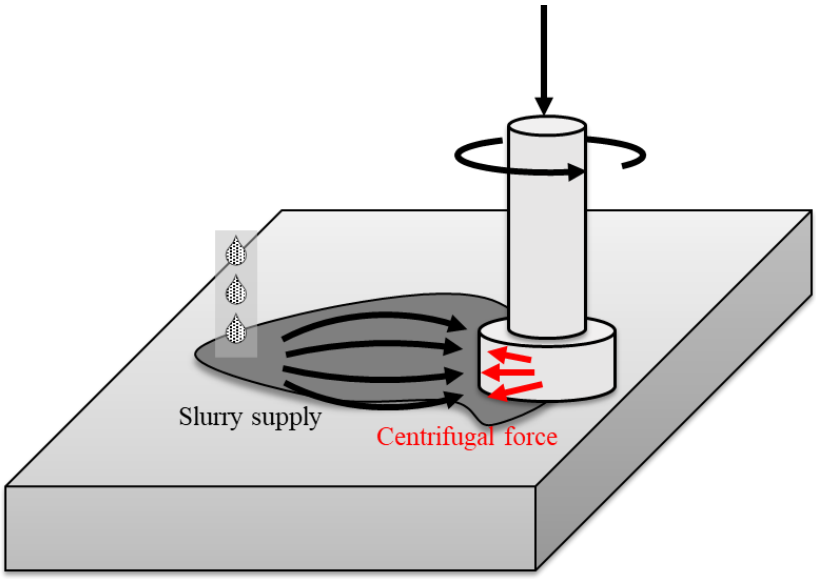

Figure 1.3 Obstruction of slurry supply by centrifugal force

1.4. Green manufacturing in polishing

As the degree of environmental pollution gradually increases, the demand for improved production methods also increases [24]. Green manufacturing approaches product and process design with the following goals:

To reduce the amount of contamination from facilities and processes.

To minimize the population exposed to potential risks, including reduced toxicity.

To improve the usage of material and energy throughout the products and processes.

To maintain economic viability and efficiency.

In the case of polishing, studies to achieve green manufacturing of polishing are actively being conducted [27]. Polishing, the final stage of ultra-precision processing, is critical in achieving high surface quality. However, as mentioned above, the process takes a very long time due to the low material removal rate (MRR), and a significant amount of waste is generated because of the consumables that must be continuously supplied during the process. In particular, slurry reduction reduces process costs as well as environmental pollution. Therefore, many studies have been conducted on reducing slurry use in green manufacturing-related polishing. In polishing, research is underway to reduce slurry in the following three directions.

1. Reducing the amount of slurry used by reducing process time

2. Using abrasive-free slurry
3. Increasing the process participation of the slurry

As for the type of research that reduces processing time, research on improving MRR using mixed abrasive slurry[28-36] and research on reducing additional processing time by improving nonuniformity[37] are being conducted. However, when the composition of the slurry is changed in this manner, the degree of environmental contamination of the new slurry and the reduced amount of environmental contamination due to the reduction in processing time should be considered. Chemical mechanical polishing (CMP) of metals has been studied using abrasive-free slurry, which removes the material using a chemical reaction instead of mechanical removal [38-41]. As these studies depend on chemical reactions, they cannot be utilized in mechanical polishing. A study has also been conducted to make the slurry supply to the retaining ring efficient using a crescent-shaped slurry injector [42].

Studies related to slurry recycling have been actively conducted on CMP. However, in the case of mechanical polishing using a slurry containing fine particles, although slurry waste may cause serious environmental pollution, research on reducing slurry waste is insufficient.

In conventional mechanical polishing, there are cases in which slurry is circulated and recycled to reduce slurry consumption. As the circulation of slurry is impossible in high-end processing, such as the production of precision parts where surface quality is important, research to reduce this is necessary.

1.5. The goal of this research

As previously stated, the demand for green manufacturing in polishing is increasing as the processing time required to manufacture high-quality and large-area optical parts has increased in recent years. However, considering the amount of slurry used in conventional polishing, an excessive amount of slurry, which is a processing consumable, is supplied without special consideration, thereby maximizing the discharge of slurry waste.

This dissertation aims to develop a polishing system capable of center-injected polishing and improve the process performance to reduce slurry consumption and waste discharge.

For this purpose, in the case of the conventional polishing method, the externally supplied slurry is prevented from being supplied to the polishing tool by the centrifugal force caused by tool rotation. It was hypothesized that improving the slurry supply across the tool would improve process performance. The slurry supply flow rate was controlled at various tool rotation speeds during polishing experiments to supply the inside and outside of the polishing tool. When the slurry was injected at the center of the tool, it was directly supplied to the contact surface at the center of the polishing tool through a rotary union. Finally, the process performances, such as material removal, surface roughness, and slurry supply, were compared, and the performance of reducing the amount of slurry used was evaluated.

1.6. Outline of dissertation

Chapter 2 presents the mechanisms acting throughout the material removal during polishing. Mechanisms related to material removal by abrasive particles and the flow mechanisms of the slurry supplying the abrasive particles are also presented.

Chapter 3 introduces the slurry flow difference between supplying the slurry at the center of the tool and supplying the slurry outside the tool in terms of fluid flow. Through simulation, the flow difference of the slurry was first predicted, and this was visually confirmed in the experiment.

Chapter 4 focuses on the tool center slurry-supplying polishing system. A detailed introduction of the equipment comprising the entire system is provided.

In Chapter 5, the performance of the polishing process based on the slurry supply method was evaluated. The process performance is evaluated in terms of the material removal amount, roughness, slurry supply state, and slurry usage by performing polishing experiments in various slurry supply methods, flow rates, and RPM environments, and measuring the surface of the workpiece.

In Chapter 6, the limitations of this study and further experiments and analysis of results were discussed. The entire study is summarized in Chapter 7.

Chapter 2. Principles of Polishing Process

2.1. Contact theory

The process of removing materials by rubbing a workpiece with free abrasive particles is called free-abrasive machining. Mechanical polishing is the best example of free-abrasive machining [43, 44]. The mechanism of polishing consists of the following four elements: polishing pad, fluid, abrasive particles, and workpiece [45]. Among the four elements, because the fluid plays the role of transporting the abrasive particles, the actual material removal occurs by the interaction of the three elements, except the fluid [45, 46]. As depicted in Figure 2.1, the contact of these three components during the polishing process is governed by contact theory [47-50].

$$a = \sqrt{R^2 - (R-d)^2} = \sqrt{2Rd - d^2} \approx \sqrt{2Rd} \tag{2-1}$$

$$F = \frac{4}{3} E^* R^{1/2} d^{3/2} \tag{2-2}$$

$$\mathrm{E}^* = \left(\frac{1-\nu_1^2}{E_1} + \frac{1-\nu_2^2}{E_2} \right)^{-1} \tag{2-3}$$

$$p(r) = p_0 \left(1 - \frac{r^2}{a^2}\right)^{1/2} \tag{2-4}$$

$$p_0 = \frac{3F}{2\pi a^2} = \frac{1}{\pi}\left(\frac{6FE^{*2}}{R^2}\right)^{1/3} \tag{2-5}$$

$$a^3 = \frac{3FR}{4E^*} \tag{2-6}$$

$$d = \frac{a^2}{R} = \left(\frac{3FR}{4E^*}\right)^{2/3}\frac{1}{R} = \left(\frac{9F^2}{16E^{*2}R}\right)^{1/3} \tag{2-7}$$

where E_1, E_2 : Elastic modulus

ν_1, ν_2 : Poisson's ratio

F : Force

$p(r)$: Normal pressure distribution (contact surface)

p_0 : Maximum pressure

d : Depth of indentation. [49, 51]

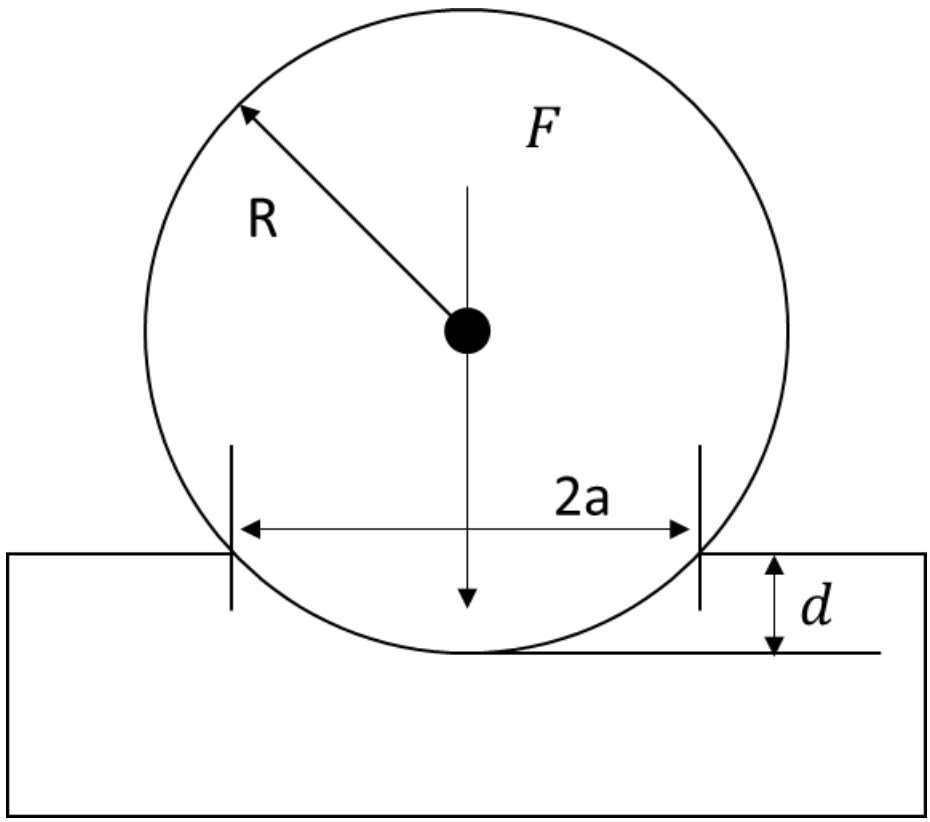

Figure 2.1 Schematic diagram of contact between sphere particle and workpiece

2.2. Abrasive Wear

Material removal during polishing occurs mainly by abrasive wear and not by direct contact between the tool and the workpiece. Abrasive wear, a type of wear mechanism, causes degradation of the workpiece surface material using hard particles in contact with the workpiece. In addition, it occurs when a smooth surface interacts with a hard particle or surface [52]. Abrasive wear can occur on surfaces that contain hard particles under any condition. For example, automobile tires wear very easily when interacting with a road surface that has a higher hardness than tires. Initially, abrasive wear was known to be caused by cutting by objects with sharp edge or wear particles. However, microscopic analyses have revealed many other mechanisms involved in its initiation. This includes particle removal by not only cutting, but also fatigue, fracture, and grain formation. Grain pull-out occurs particularly in ceramic materials, such as SiC, used in this study. It occurs at grain boundaries where the surface is weak [53].

Abrasive wear can be classified into 2- and 3-body abrasive wear as depicted in Figure 2.2. Two-body abrasive wear occurs when the surface material is removed by sharp or hard particles. In this case, displacement of the material occurs by plowing or cutting operations [54]. 3-body abrasive wear is caused by non-constrained grit motion at the interface of the wear-causing surface. This is very slow compared to two-body abrasive wear. In this case, grit slides and rolls freely at the interface. As 2-body abrasive wear can lead to 3-body abrasive wear when hard abrasives are dislocated from the surface, and vice versa [55-58], these two modes are not mutually exclusive.

The removal rate is inversely proportional to the fracture toughness and hardness and is directly proportional to the sliding distance and pressure [56, 59]. When the abrasives are caught on the pad, they act as one body, resulting in 2-body abrasive wear between the workpiece and the abrasives [58].

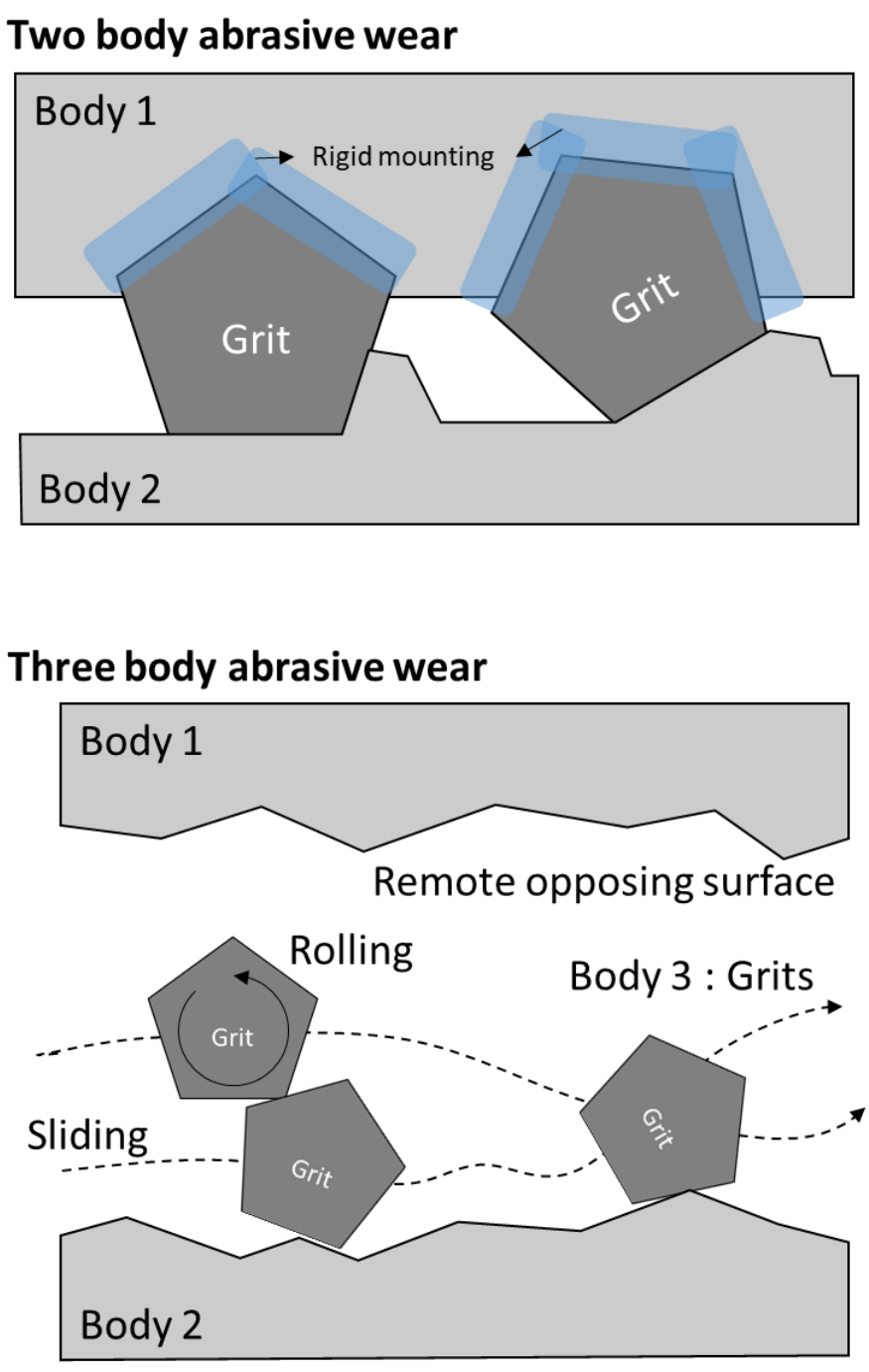

Figure 2.2 Two modes of abrasive wear

2.3. Preston model

Preston's wear equation is commonly used as an approximation of the MRR of polishing [60]. Accordingly, the MRR is proportional to the strength, speed, and length of the workpiece [61]. The approximation for material removal during polishing can be expressed as follows:

$$\Delta \mathrm{V} = k_p P v \Delta t \tag{2-8}$$

where P : Pressure

v : Relative velocity

Δt : Dwell time.

The amount of material removed was proportional to the pressure, relative velocity, workpiece, and dwell time.

2.4. Slurry abrasive in material removal

When both the surfaces of the workpiece, and tool are flat and the tool moves on the surface of the workpiece, the relative velocity v_s between two arbitrary points on each can be defined as follows:

$$v_s = v_{tool} - v_{workpiece} \tag{2-9}$$

$$v_{workpiece} = 0 \tag{2-10}$$

$$v_s = v_{tool} \tag{2-11}$$

As the movement of an arbitrary point of the polishing tool moving on the XOY plane is the superposition of linear and circular motions depicted in Figure 2.3, the velocity of the tool v_{tool} can be expressed as follows:

$$v_{rot} = (v_{rot}sin\theta, v_{rot}cos\theta) \tag{2-12}$$

$$v_{tool} = v_{rot} + v_{tra} = (v_{tra} + v_{rot}sin\theta, v_{rot}cos\theta) \tag{2-13}$$

The magnitude of v_s can be expressed as follows:

$$|v_s| = \sqrt{v_{tra}^2 + v_{rot}^2 + 2v_{tra}v_{rot}sin\theta} \tag{2-14}$$

where v_s : Relative velocity

v_{tra} : Velocity due to the transverse movement of tool

v_{rot} : Velocity due to the rotation of tool

θ : Angle between transverse movement direction and arbitrary point

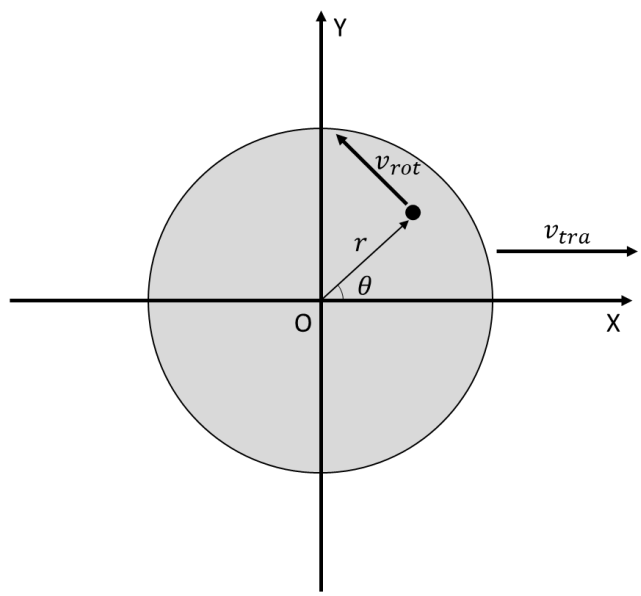

Figure 2.3 The motion of an arbitrary point on polishing tool

The abrasives that exist in the flat area of the pad, rather than in the pores, move in accordance with the movement of the tool. It is assumed that all the abrasives have same spherical shape with radius R and same height except for the pores of the pad. The abrasive particles are not abraded while the polishing process is in progress, and the shape is kept constant. When the contact state of one abrasive particle is as shown in Figure 2.4, each element can be expressed as follows. The contact force F_{cf} between the workpiece and the abrasives can be expressed as follows [62, 63]:

$$F_{cf} = H_w \pi R \lambda_w \tag{2-15}$$

where H_w : Hardness of the workpiece

R : Radius of abrasive particles

λ_w : Depth of invasion

The adhesive forces can be expressed as follows[64]:

$$F_{Apa} \approx 1.5\pi W_{pa} R \tag{2-16}$$

$$F_{Awa} \approx 2\pi W_{wa} R \tag{2-17}$$

where F_{Awa} : Adhesive force (Workpiece & Abrasive particles)

F_{Apa} : Adhesive force (Pad & Abrasive particles)

W_{Awa} : Adhesive work (Workpiece & Abrasive particles)

W_{Apa} : Adhesive work (Pad & Abrasive particles)

R : Radius of abrasive particles

The force between the pad and abrasives $\mathrm{F_{pa}}$ can be expressed as follows according to contact theory [65, 66]:

$$\mathrm{F_{pa}} = \frac{4}{3} E_{pa} R^{\frac{1}{2}} \lambda_p^{\frac{3}{2}} \tag{2-18}$$

$$\mathrm{E_{pa}} = \left(\frac{1-\gamma_a^2}{E_a} + \frac{1-\gamma_p^2}{E_p} \right)^{-1} \tag{2-19}$$

where E_a, E_p : Young's modulus (abrasive particle, pad)

γ_a, γ_p : Poisson ratio (abrasive particle, pad)

λ_{p} : Depth of invasion to the polishing pad

The forces on the pad, abrasives, and workpiece satisfy the following equation.

$$\mathrm{F_{pa}} + F_{Awa} = F_{Apa} + F_{cf} \tag{2-20}$$

$$\frac{4}{3} E_{pa} R^{\frac{1}{2}} \lambda_p^{\frac{3}{2}} + 2\pi W_{wa} R = 1.5\pi W_{pa} R + H_w \pi R \lambda_w \tag{2-21}$$

λ_{p} can be expressed as follows:

$$\lambda_p = 2R - \lambda_w \tag{2-22}$$

Therefore, the equation above can be expressed as:

$$\frac{4}{3}E_{pa}R^{\frac{1}{2}}(2R-\lambda_w)^{\frac{3}{2}} + 2\pi W_{wa}R = 1.5\pi W_{pa}R + H_w\pi R\lambda_w \tag{2-23}$$

The depth of invasion to the workpiece λ_w can be obtained through the above equation.

Where the width of abrasive wear by an abrasive particle is 2a, the length of the scratch by this particle is x, the abrasive wear coefficient is k_s and the number of abrasives under the tool is N, the material removal can be expressed as:

$$V_{\text{single particle}} = 2k_s a\lambda_w x \tag{2-24}$$

$$V_{\text{total particle}} = 2k_s a\lambda_w xN \tag{2-25}$$

where the polished area of the workpiece is A_p. The MRR is expressed as:

$$MRR_{\text{total particle}} = \frac{dV_{total\ particle}}{A_p dt} = \frac{2k_s a\lambda_w N}{A_p}\frac{dx}{dt} = \frac{2k_s a\lambda_w N}{A_p}V_s \tag{2-26}$$

The workpiece does not make static contact with the abrasives that are trapped in the pore; therefore, the amount of material removed by it can be neglected.

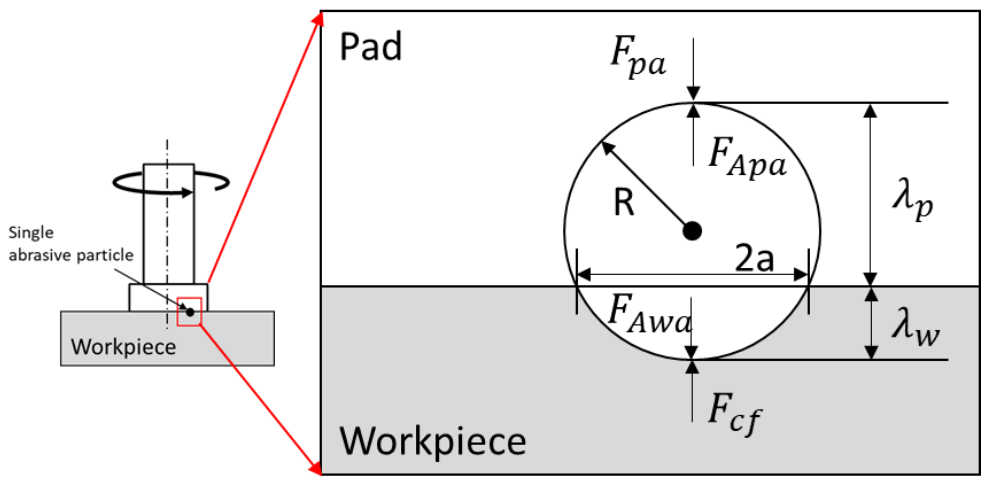

Figure 2.4 Schematic diagram of a single abrasive particle contact

Chapter 3. Slurry flow analysis

As shown in Chapter 2, the MRR of polishing is determined by the number of abrasives at the bottom of the polishing tool. Assuming that the abrasives were evenly distributed in the slurry, the number of abrasives was proportional to the volume of the slurry. The flow of the slurry ultimately determines the MRR. Therefore, it is necessary to identify the slurry flow to improve the polishing performance.

3.1. Flow model of polishing slurry

The transport mechanism of the slurry has a significant influence on the polishing process performance and slurry consumption. Therefore, fluid transfer at the contact surface is one of the most important issues in polishing.

The slurry flow during the polishing process can be simplified as Couette flow. The slurry was trapped and dragged by two boundaries (polishing pad and workpiece surface). As these two boundaries have different velocities, the slurry located near the pad follows the movement of the pad, and the slurry located on the workpiece surface follows the movement of the surface of the workpiece. However, the fluid flow can be determined by considering the average velocity of the fluid at a certain location. The flow of a fluid is analyzed in a way that ignores terms with very small parameters in the Naiver–Stokes equation.

In the Navier–Stokes equation, the boundary conditions for the coordinate system shown in Figure 3.1, are given as follows.

Radial component:

$$v_{\mathrm{r}}(z=0)=0 \tag{3-1}$$

$$v_{\mathrm{r}}\left(z=\bar{h}\right)=v_{tra} \tag{3-2}$$

Tangential component:

$$v_{\theta}(z=0)=0 \tag{3-3}$$

$$v_{\theta}\left(z=\bar{h}\right)=v_{rot}=\omega r \tag{3-4}$$

As the distance between the workpiece and polishing tool is small and the workpiece is horizontal, the following assumptions are made:

$$v_{\mathrm{z}}(r,\theta,z)=0 \tag{3-5}$$

$$\mathrm{g_r}=g_{\theta}=0 \tag{3-6}$$

where $\bar{h}$: Average gap between workpiece and polishing pad

v_{tra} : Velocity due to the transverse movement of tool

v_{rot} : Velocity due to the rotation of tool

ω : Angular velocity of polishing tool

r : Radius of polishing tool

The N-S equations can be simplified to the following:

Radial component:

$$\rho\left(\frac{\partial v_r}{\partial t}+v_r\frac{\partial v_r}{\partial r}+\frac{v_\theta}{r}\frac{\partial v_r}{\partial \theta}-\frac{v_\theta^2}{r}\right) = -\frac{\partial p}{\partial r}+\mu\left(\frac{\partial}{\partial r}\left(\frac{1}{r}\frac{\partial}{\partial r}(rv_r)\right)+\frac{1}{r^2}\frac{\partial^2 v_r}{\partial \theta^2}+\frac{\partial^2 v_r}{\partial z^2}-\frac{2}{r^2}\frac{\partial v_\theta}{\partial \theta}\right) \quad (3\text{-}7)$$

Tangential component:

$$\rho\left(\frac{\partial v_\theta}{\partial t}+v_r\frac{\partial v_\theta}{\partial r}+\frac{v_\theta}{r}\frac{\partial v_\theta}{\partial \theta}+\frac{v_r v_\theta}{r}\right) = -\frac{\partial p}{\partial \theta}+\mu\left(\frac{\partial}{\partial r}\left(\frac{1}{r}\frac{\partial}{\partial r}(rv_\theta)\right)+\frac{1}{r^2}\frac{\partial^2 v_\theta}{\partial \theta^2}+\frac{\partial^2 v_\theta}{\partial z^2}+\frac{2}{r^2}\frac{\partial v_r}{\partial \theta}\right) \quad (3\text{-}8)$$

Z component:

$$0 = -\frac{\partial p}{\partial z}+\rho g_z \quad (3\text{-}6)$$

A non-dimensional analysis can be used to find negligible terms in the above equation. If negligible terms are neglected by applying the parameters generally used

in the polishing environment to the non-dimensional analyzed equation, the N-S equation is changed as follows:

Radial component:

$$\frac{\partial \mathrm{p}}{\partial \mathrm{r}} = \mu \frac{\partial^2 v_r}{\partial z^2} \tag{3-10}$$

Tangential component:

$$\frac{\partial \mathrm{p}}{\mathrm{r}\,\partial \theta} = \mu \frac{\partial^2 v_\theta}{\partial \mathrm{z}^2} \tag{3-11}$$

Z component:

$$\frac{\partial \mathrm{p}}{\partial \mathrm{z}} = 0 \tag{3-12}$$

To solve these equations, boundary conditions (3-1, 3-2, 3-3, and 3-4) are required. Integrating both sides of the equations and applying the following boundary conditions:

Radial component:

$$\mathrm{v_r} = \frac{1}{2\mu}\frac{\partial p}{\partial r} z^2 - \left(\frac{\bar{h}}{2\mu}\frac{\partial p}{\partial r} - \frac{v_{tra}}{\bar{h}}\right) z \tag{3-13}$$

Tangential component:

$$v_\theta = \frac{1}{2r\mu}\frac{\partial p}{\partial \theta}z^2 - \left(\frac{\bar{h}}{2r\mu}\frac{\partial p}{\partial \theta} - \frac{\omega r}{\bar{h}}\right)z$$

(3-14)

Both components of the fluid velocity are functions of r, θ, z. z dependent terms, which can be eliminated by introducing the mean flow velocity term. The average flow velocity is defined as follows:

Radial component:

$$\overline{v_r} = \frac{1}{\bar{h}}\int_0^{\bar{h}} v_r dz$$

(3-15)

Tangential component:

$$\overline{v_\theta} = \frac{1}{\bar{h}}\int_0^{\bar{h}} v_\theta dz$$

(3-16)

Integrating the two equations yields two components of the average fluid velocity vector field under the pad:

$$\overline{v_r} = -\frac{\partial p}{\partial r}\frac{\bar{h}^2}{12\mu} + \frac{v_{tool\cdot tra}}{2}$$

(3-17)

$$\overline{v_\theta} = -\frac{\partial p}{r\partial\theta}\frac{\bar{h}^2}{12\mu} + \frac{\omega r}{2}$$

(3-18)

Neglecting the flow due to the pressure difference between the outside(atmospheric pressure) and pores of the pad provides a very simple solution:

$$\frac{\partial \mathrm{p}}{\partial \mathrm{r}} = \frac{\partial \mathrm{p}}{\mathrm{r}\,\partial\theta} = 0$$

(3-19)

$$\overline{v_r} = \frac{1}{2} v_{tool\cdot tra}$$

(3-20)

$$\overline{v_\theta} = \frac{1}{2}\omega r$$

(3-21)

The Couette flow model cannot account for all flows that actually occur at the abrasive interface. The assumption that the slurry used in this model was transported between two smooth moving surfaces was incorrect. In practice, a polishing pad is a rough surface that contacts the workpiece at many points. Because the fluid encounters many obstacles along the path, it does not have the same degrees of freedom as those assumed for the Couette flow. In actual polishing, the flow is disturbed as shown in Figure 3.2 by the rough part of the polishing pad, which is quite different from the assumption in the Couette flow model.

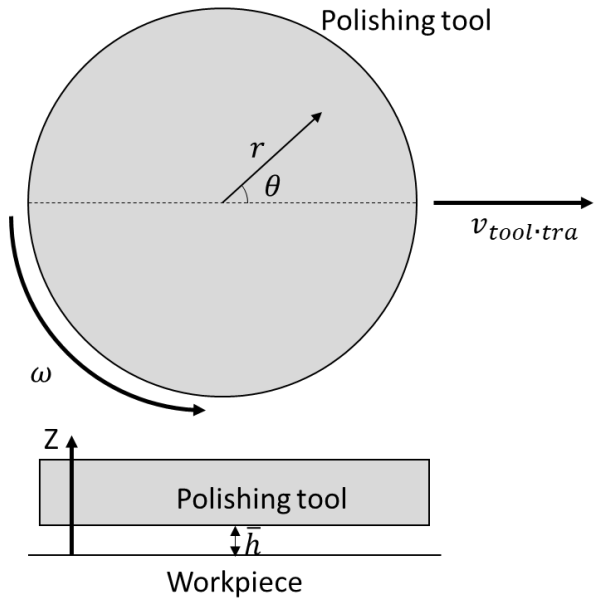

Figure 3.1 The coordinate system of polishing tool

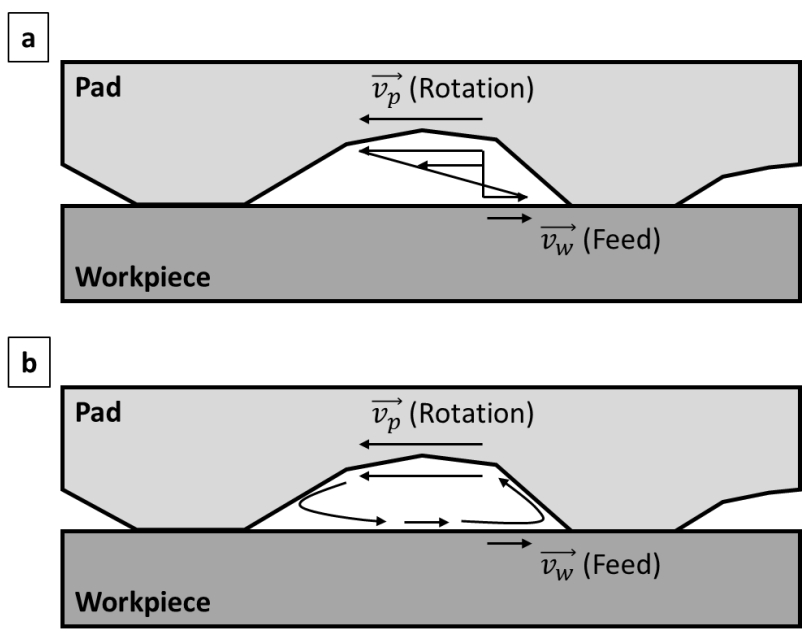

Figure 3.2 Slurry flow (a)Couette flow model (b)Actual polishing

3.2. Effect of slurry in material removal rate

As described in Section 2.4, MRR is proportional to the number of abrasives present in the contact surface. Assuming that the abrasives are evenly distributed, the material removal by polishing is proportional to the volume of the slurry present at the contact surface of the polishing pad and workpiece. Therefore, if a sufficient amount of slurry is not supplied to the bottom of the polishing tool, the number of abrasives participating in material removal may decrease, resulting in a decrease in the polishing process performance. Therefore, it is not yet clear how the MRR is affected by the slurry supply rate. However, it seems intuitive to expect the MRR to change in two steps as the supply flow rate increases.

When the slurry supply is increased to a certain level in the first stage (slurry starving state), the abrasive particle starvation under the polishing tool decreases, and the MRR increases.

As the slurry supply rate exceeds the capacity of the polishing pad, the number of abrasives and the MRR no longer increase and are maintained at a constant level in the second stage (slurry sufficient state).

3.3. Center slurry injection

As the amount of slurry supplied to the bottom of the polishing tool is ultimately determined by the slurry flow, it is necessary to investigate the modification of the slurry flow depending on the slurry supply method.

In this dissertation, the slurry is supplied in two ways.

First, when supplying the slurry at the outside of the tool:

The slurry is supplied outside the polishing interface and to the contact surface by the transverse movement of the tool and the flow of the supplied slurry. In this case, as described above, only a portion of the supplied slurry enters the contact surface and participates in material removal. The majority of the slurry does not enter the contact surface and is immediately discharged as waste. In addition, the centrifugal force resisted a portion of the slurry entering the contact surface. Therefore, as the rotational speed of the tool increased, the slurry supply condition deteriorated. Furthermore, as the Couette flow due to tool rotation is offset by the flow from one direction from the outside, an imbalance in the slurry supply occurs inside the contact surface, as shown in Figure 3.3.

Second, when supplying the slurry at the center of the tool:

It was supplied directly to the contact, regardless of tool movement. Unlike when the slurry is supplied externally, the entire supplied slurry is supplied to the contact surface where material removal occurs, so the entire slurry participates in material removal with no unused slurry. As the supply amount of the slurry is

independent of the centrifugal force, the supply state of the slurry is not affected, even if the rotation speed of the tool increases. In addition, the slurry spreads evenly from the center of the tool to the entire contact surface, such that an uneven supply of the slurry does not occur.

In summary, supplying the slurry at the center of the tool has the following advantages. First, as the entire slurry supplied participates in the material removal, the efficiency of using the slurry can be increased without wasting the slurry. Second, unlike conventional polishing, centrifugal force prevents the slurry from supplying the slurry to the contact surface. When the slurry is injected at the center of the tool, this centrifugal force can be used to supply the slurry. Therefore, the effect of the rotation of the tool on the slurry supply is minimized so that better process performance can be obtained without spraying more slurry at a high RPM. This advantage can also shorten the processing time owing to increasing the MRR using the high RPM. Therefore, it is possible to reduce the slurry due to the process time reduction in addition to the increase in the slurry supply efficiency as depicted in Figure 3.4. Third, as the velocity term of the Couette flow inside the tool is not canceled owing to the slurry flow from the constant direction outside the tool, the asymmetry of the slurry supply does not occur over the entire machining surface.

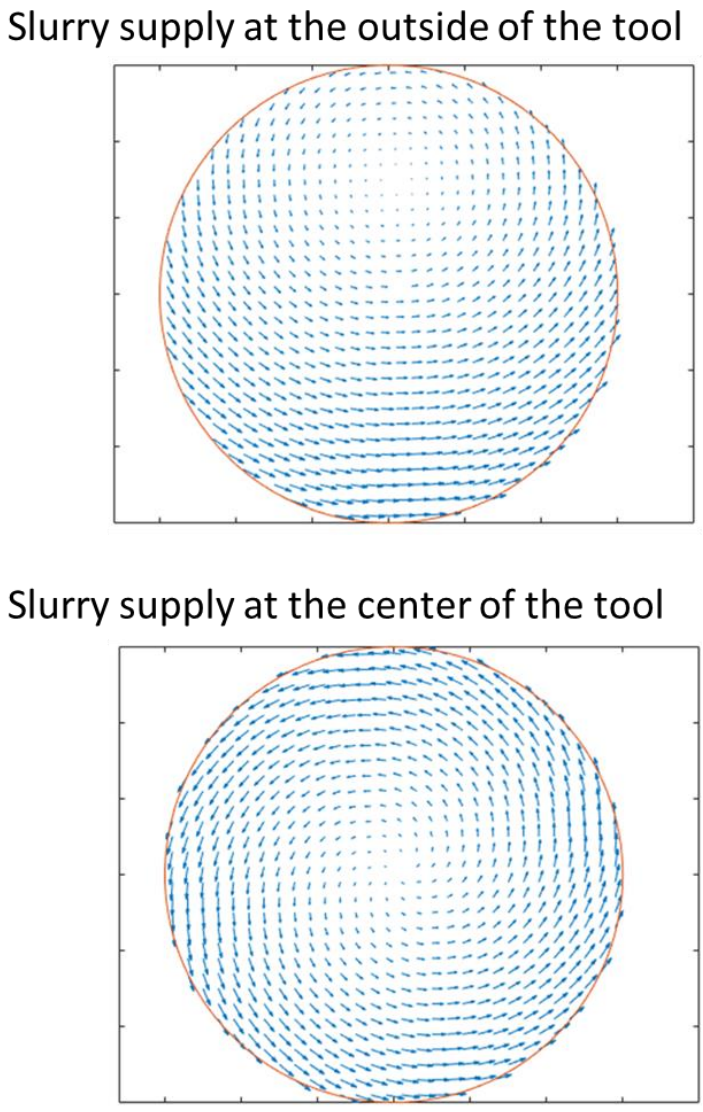

Figure 3.3 Schematic of slurry flow according to supply method

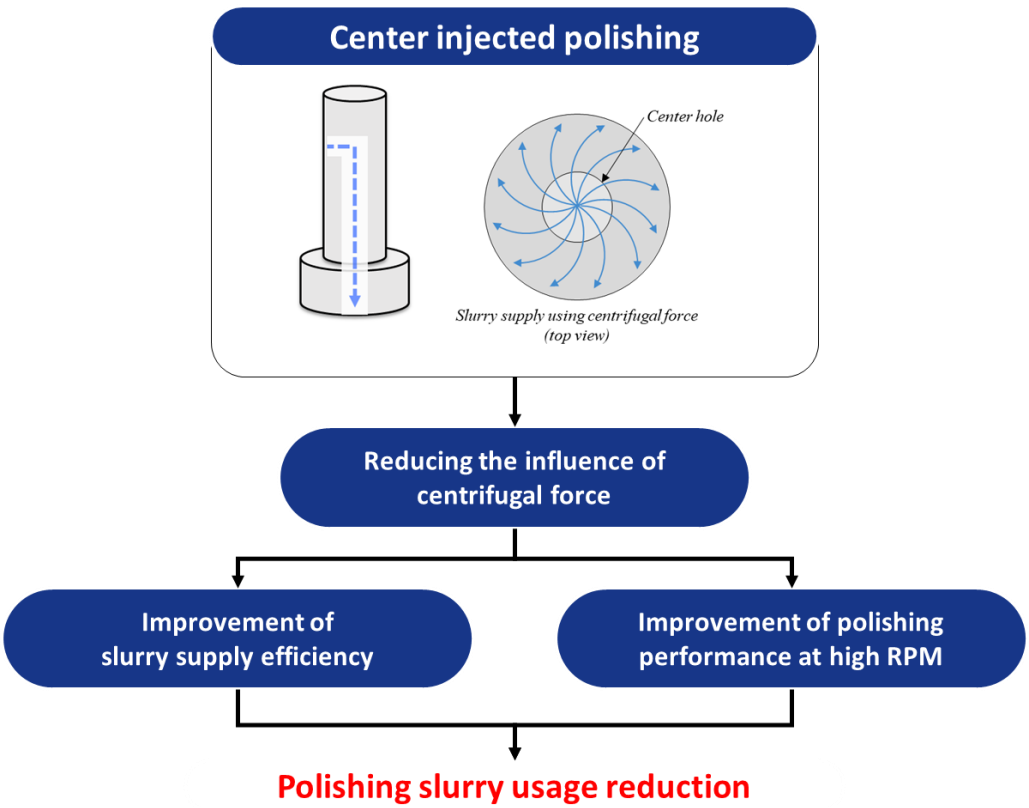

Figure 3.4 Concept of center injected polishing

3.4. Slurry flow characterization

In the polishing process, hydrodynamic analysis is an important measure to investigate the slurry supply in the polishing process. In this section, the computational fluid dynamics (CFD) model is discussed. For the convenience of the simulation process, the assembly model was simplified under the following assumptions:

First, the gap between the two parts is simplified to have a uniform gap, unlike the actual non-uniform gap owing to the rough pad surface. Second, the slurry velocity distribution in the slurry supply channel was uniform. Third, the space between the two parts was filled with a slurry. Fourth, it was assumed that the fluid had the same properties as water for the convenience of calculation, because it was difficult to implement a fluid containing fine particles.

Ansys software was used to simulate the polishing slurry flow during polishing, and the parameters used for the simulation were the same as those in Table 3.1. The polishing environment was simplified and simulated, as shown in Figure 3.5.

Table 3.1 CFD simulation parameter

Simulation parameter	
Tool diameter	26 mm
Rotational speed	1500 RPM
Slurry flow rate	5 ml/min
Distance between tool & supply point	10 mm
Model	K-omega SST
Solution	Coupled (Least-square)

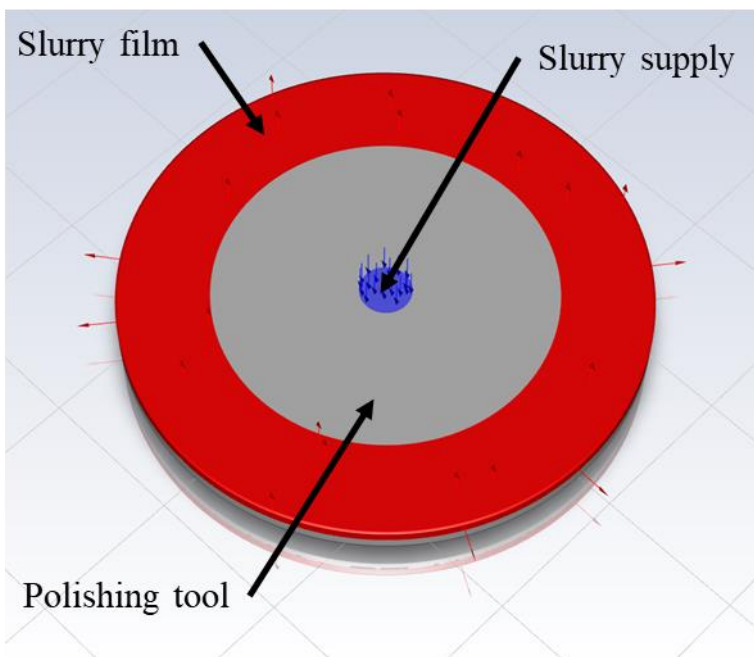

Figure 3.5 Slurry flow model for CFD simulation

The CFD results are shown in Figure 3.6 and 3.7. In the case of center-injected polishing, a symmetric flow was observed both at the bottom and outside of the polishing tool. However, when the slurry was supplied outside the tool, an asymmetric flow distribution was observed depending on the location of the external supply channel. The rotational flow was dominant at the bottom of the tool in both supply methods; therefore, changes in the radial direction of the slurry supply were difficult to observe. However, when observing the streamline, there was a flow supplied from the outside of the tool to the inside in addition to the supply from the inside in the case of supply inside the tool. Therefore, when compared to conventional polishing, in which only a part of the total supplied flow rate is supplied internally, the actual amount of slurry supplied by center-injected polishing, in which additional slurry is supplied externally in addition to the total supplied internally supplied amount, is greater.

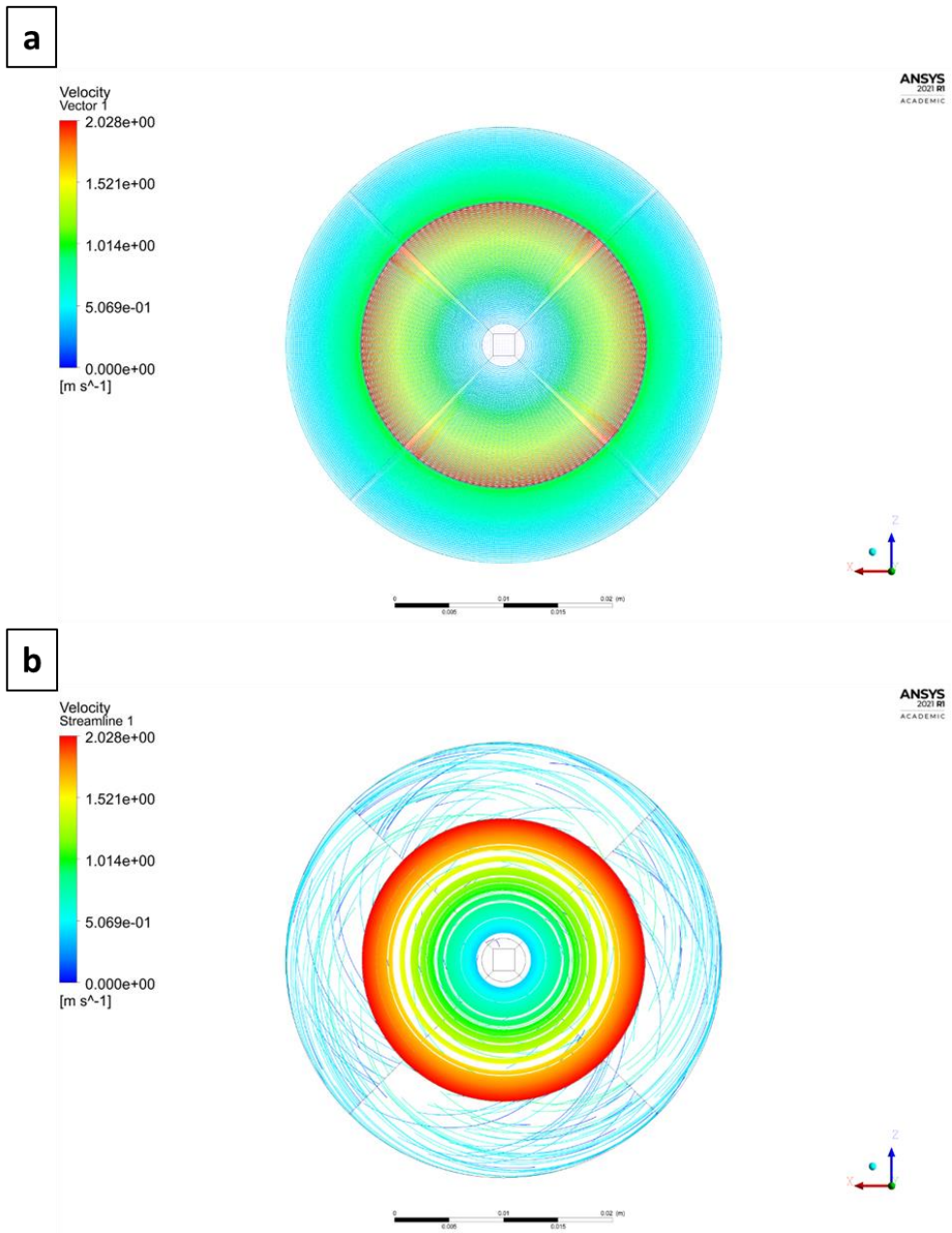

Figure 3.6 CFD result of center injected polishing

(a) Velocity vector map (b) Stream lines

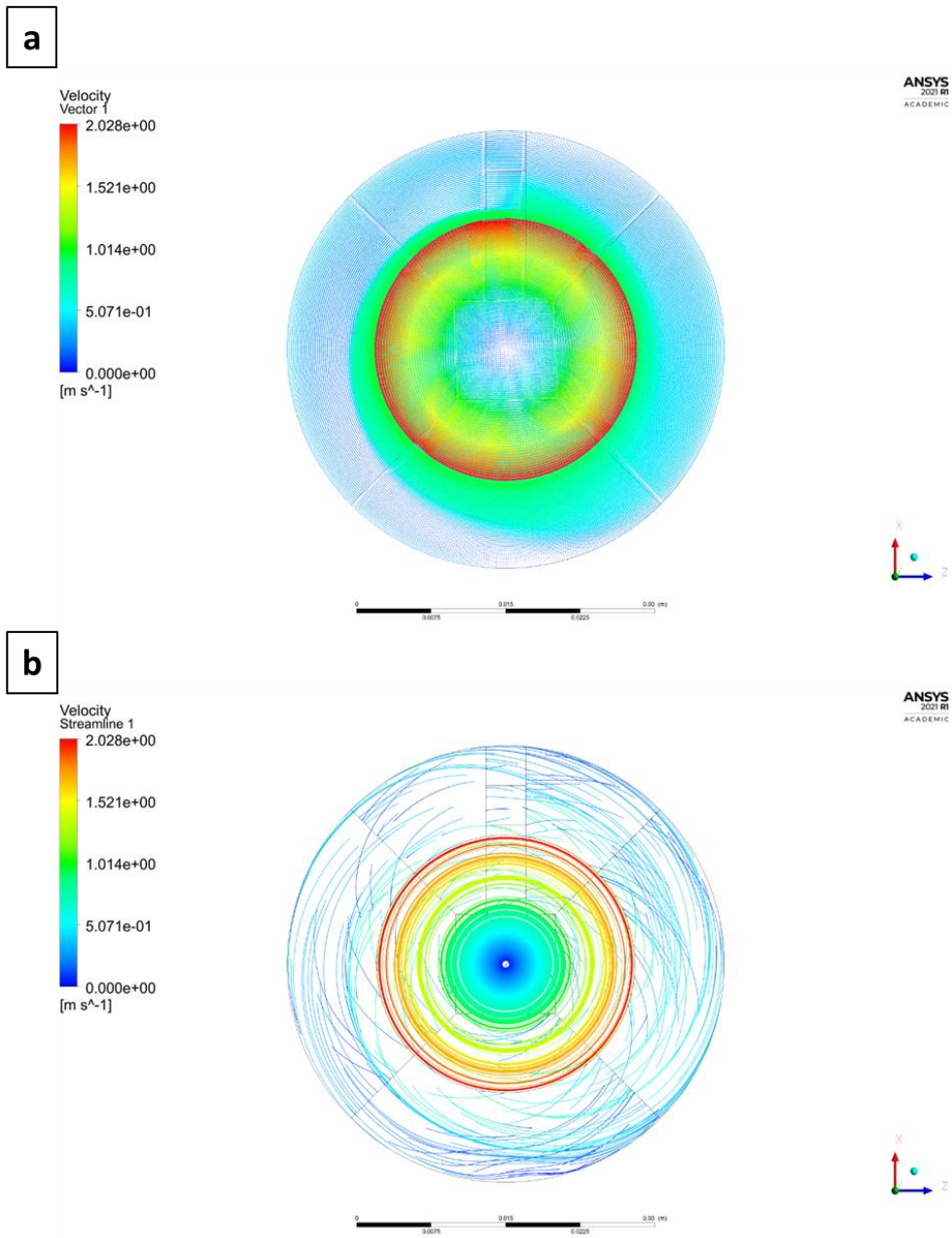

Figure 3.7 CFD result of conventional polishing

(a) Velocity vector map (b) Stream lines

In addition to the simulation results, experiments were performed to confirm the slurry flow during the polishing process. During the polishing process, ink was mixed and supplied to the slurry supply process to determine how the actual slurry moved. The system was configured to check the flow at the contact surface. In this dissertation, a transparent specimen other than SiC was selected as a workpiece, which was subjected to a processing experiment, and a camera was placed at the bottom to photograph how the slurry moved on the contact surface during polishing. The system setup used at this time is shown in Figure 3.8. To prevent tool marks, the ink was mixed with distilled water instead of the slurry.

The flow test results for the tool outside the supply are shown in Figure 3.9. First, when the slurry was supplied to the outside of the tool, rotating at 1500 RPM without transverse movement, hardly any slurry was observed entering the tool, as shown in Figure 3.9 (a). The flow when the fluid is supplied to the outside of the tool that moves at a feed of 2.5 and 25 mm/s and rotates at 1500 RPM is shown in Figure 3.9 (b) and (c). A slight improvement in supply was observed at higher feed levels, but the effect was insignificant. However, a clear supply improvement effect was observed when the rotation speed was lowered. As shown in Figure 3.9(d), when the tool rotational speed was lowered to 600 RPM, the fluid supply into the tool occurred very smoothly, and black ink was supplied to most of the area at the bottom of the tool.

The result of the center-injected polishing was very different from that of the tool outside supply as shown in Figure 3.10. It was clearly observed that the fluid from the hole in the center of the tool spread outward from the case where the fluid was supplied to the tool rotating at 1500 RPM in situ without transverse movement

of the tool.

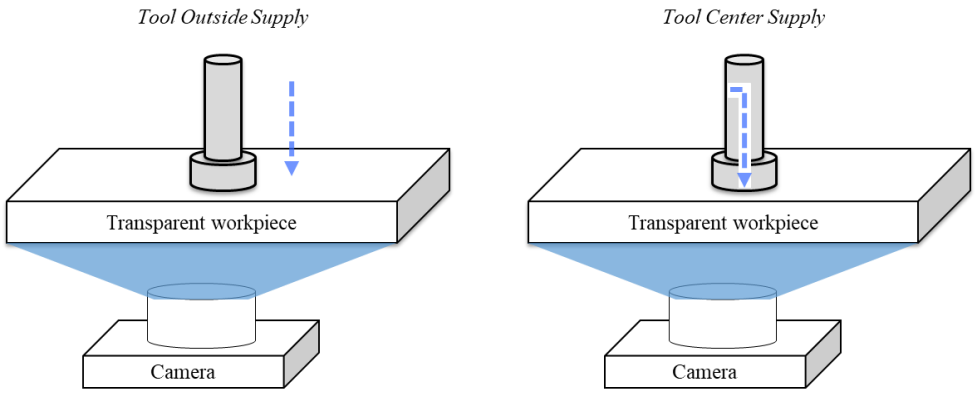

Figure 3.8 | Schematic diagram of slurry observation experiment

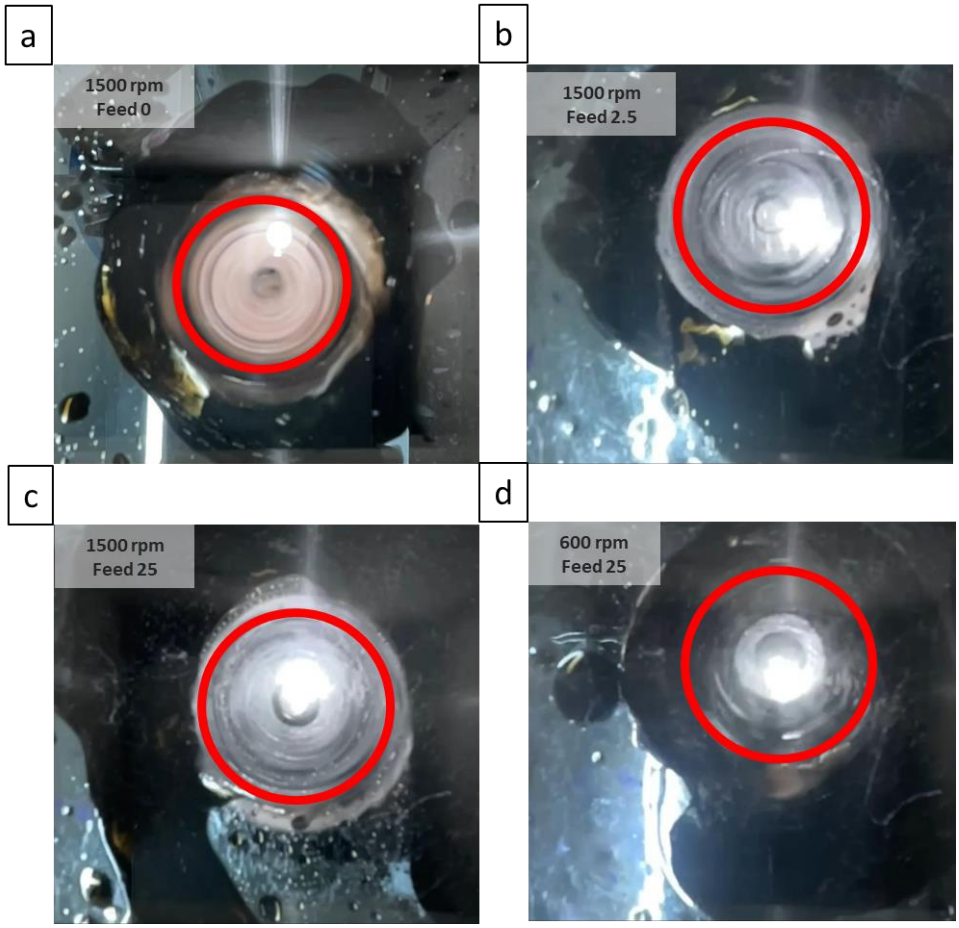

Figure 3.9 Flow observation result of conventional polishing

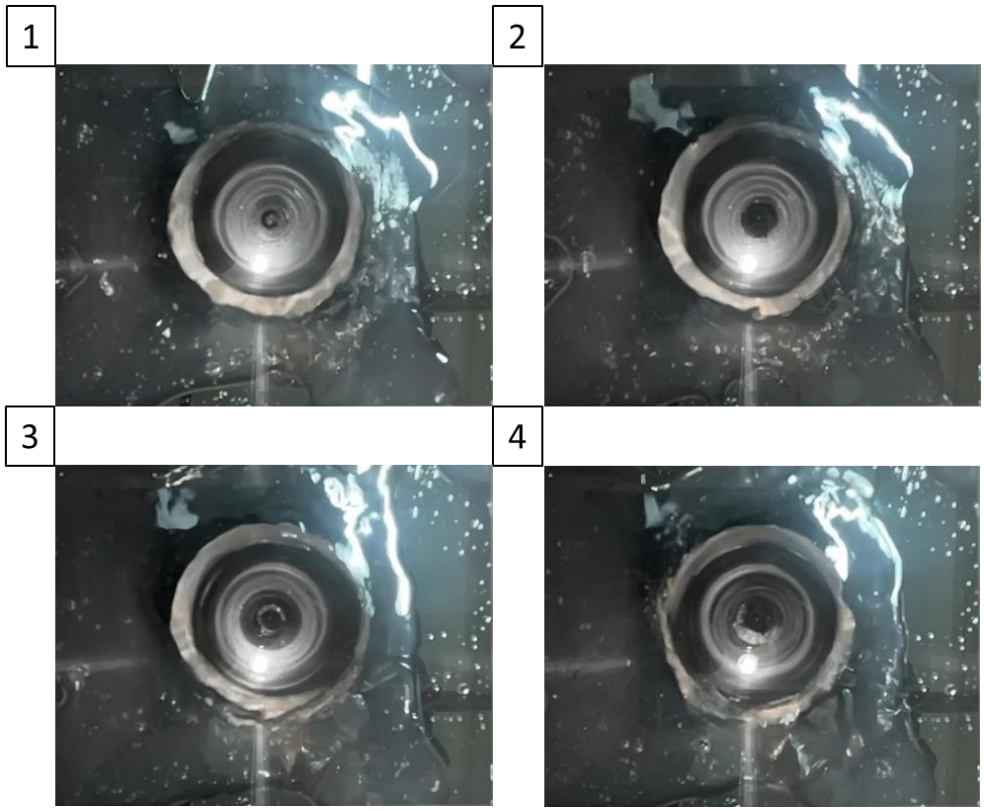

Figure 3.10 Flow observation result of center injected polishing (order by time)

Polishing experiments were conducted to investigate the material removal characteristics. The polishing experiments were conducted by making only rotational movements at the same position, without transverse movement of the polishing tool. I attempted to identify the material removal and flow characteristics of each supply method by measuring the surface profile of the workpiece. When polishing is performed without transverse movement of the tool, the polished surface becomes w-shaped according to the relative speed distribution at the bottom of the tool. The change in the width of the central peak confirms that the slurry has been well supplied to the center of the tool as shown in Figure 3.12.

Figure 3.11 shows the result of the center-injected polishing. In this case, even if the rotation speed increased, the width of the unpolished area in the center did not change, and only the polishing depth increased. Therefore, only material removal was increased by increasing the rotational speed without a significant change in the slurry supply to the center of the tool. In contrast, in the case of conventional polishing, the width of the unpolished central area increased as the rotation speed increased, as shown in Figure 3.14. The results of comparing the maximum material removal depth and the width of the center peak are shown in Figure 3.13 and Figure 3.15. Therefore, the slurry supply to the center of the tool deteriorated, and the removal depth increased as the rotational speed increased outside, where the supply of slurry was smooth. This is because the centrifugal force prevents the slurry from entering the center. The removal depth outside where the slurry was supplied increased as the rotational speed increased.

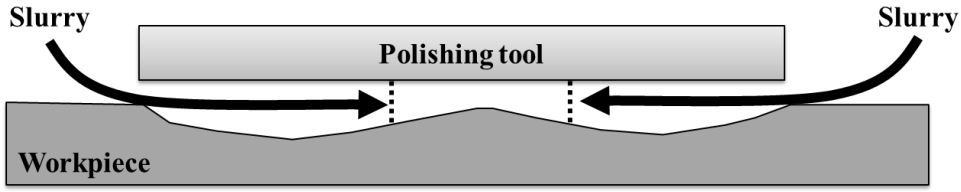

Figure 3.12 Schematic diagram of material removal characteristic experiment

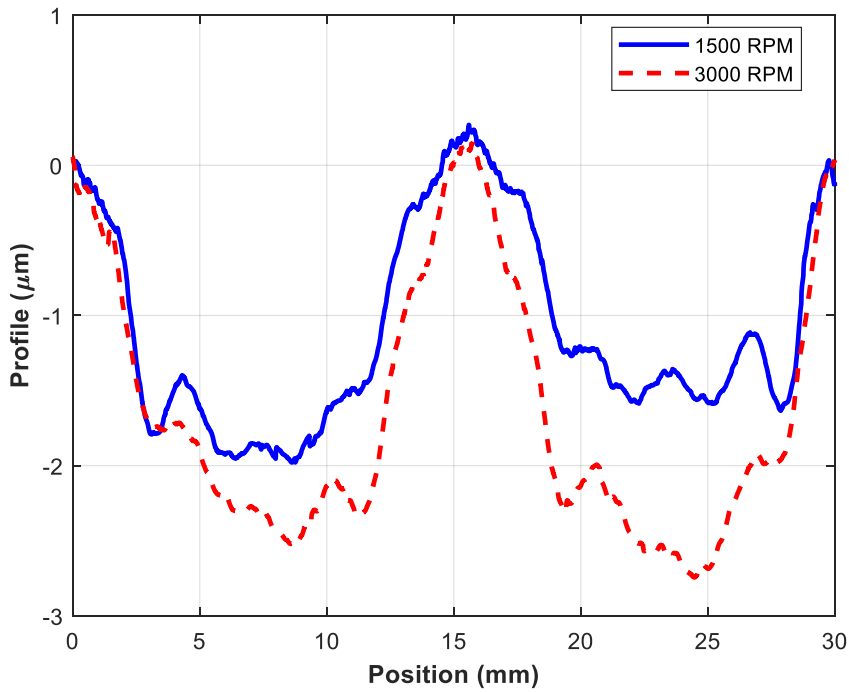

Figure 3.11 Surface profile of center injected polishing

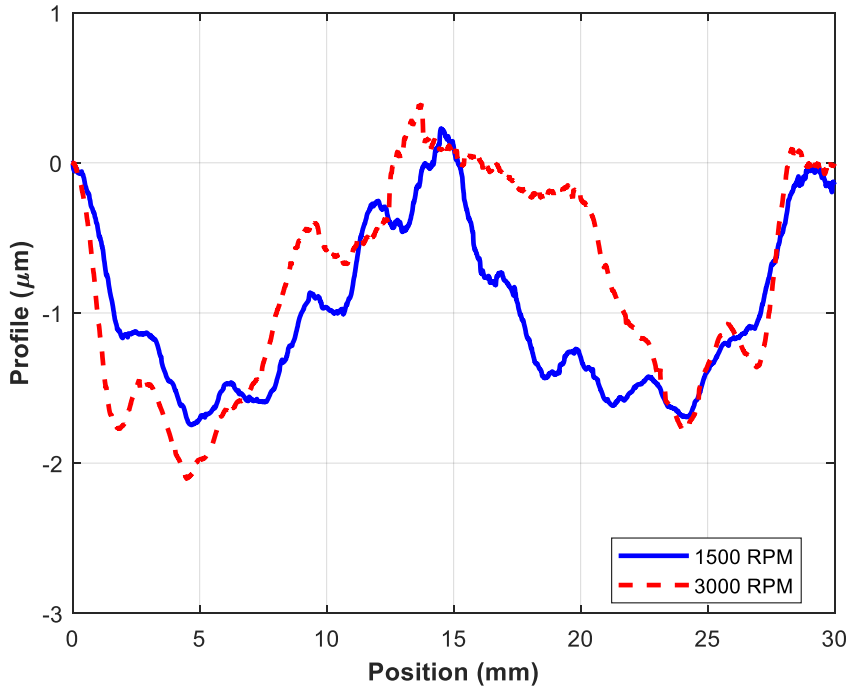

Figure 3.14 Surface profile of conventional polishing

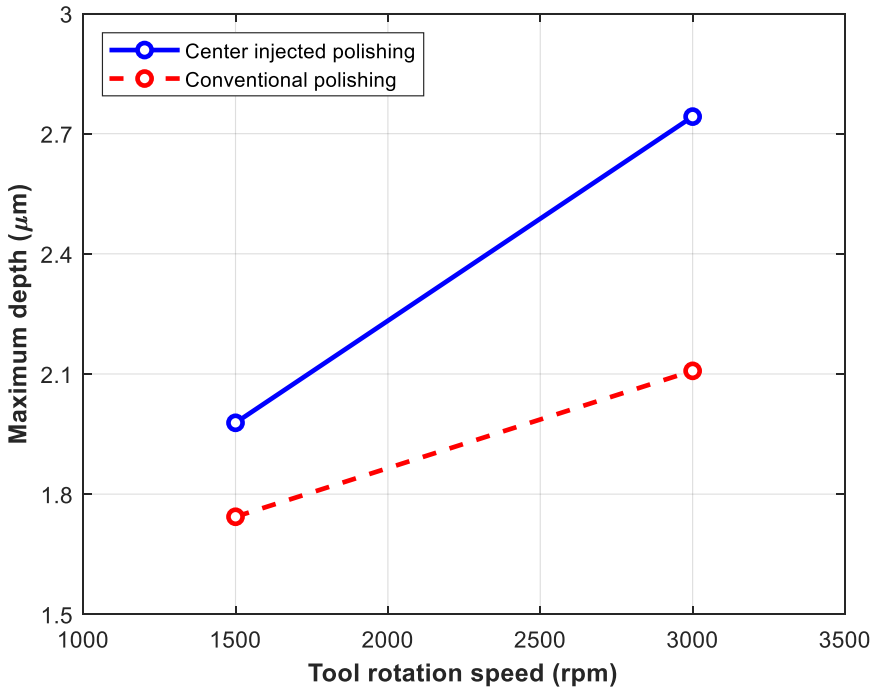

Figure 3.13 Maximum removal depth according to tool rotational speed

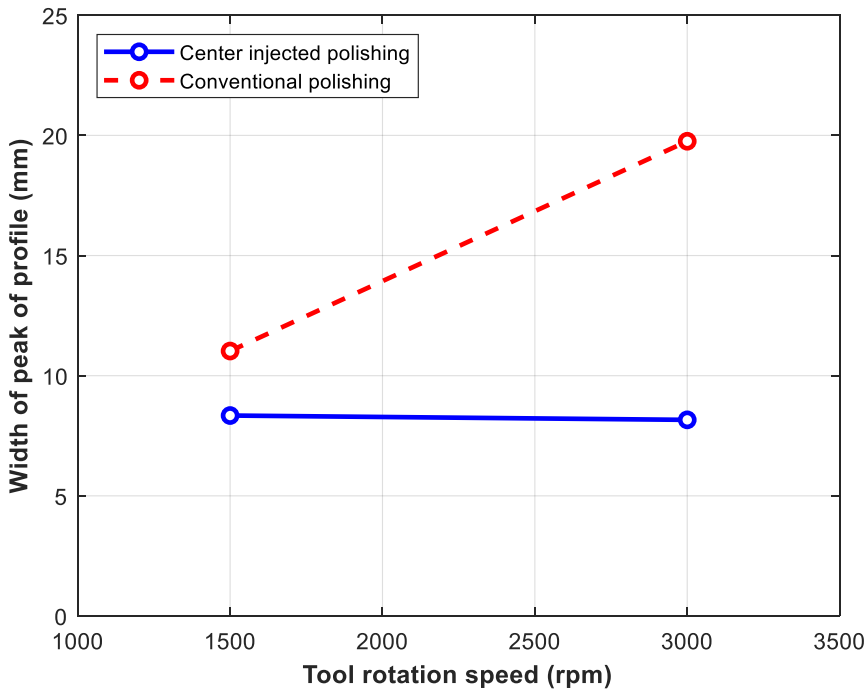

Figure 3.15 Width of the peak according to tool rotational speed

Chapter 4. System Design and Integration

This section describes the polishing system used in the study. The entire system was composed of a polishing system and a slurry supply system to supply the center injection. The system was composed of a stage, spindle, dynamometer for measuring the polishing pressure, and slurry supply system. A detailed description of each component is provided below:

4.1. Polishing system

The polishing system was based on a gantry-type 3-axis stage. A linear guide was used for the x-direction movement, two linear guides were used for the y-direction movement, and a ball-screw guide was used for the z-direction movement. The X-axis and Y-axis are mounted on one structure to take charge of the movement of the XZ plane, and the Y-axis is located at the lower end of the structure so that the entire system performs a movement in the three-axis direction.

To explain the system in more detail, the spindle was mounted on a structure responsible for movement on the XZ plane, and a slurry reservoir was mounted on the Y-axis structure to fix the workpiece. A polishing tool including the rotary union, polydimethylsiloxane (PDMS) elastomer, and a polishing pad (polyurethane), was mounted at the end of the spindle. The slurry reservoir prevents the supplied slurry from being thrown out during the fixing and polishing of the workpiece. A

dynamometer was mounted on the lower part of the bed that fixed the workpiece to measure the polishing pressure. The schematic diagram and picture of the entire system are shown in Figure 4.1. The detailed specifications of the entire system are listed in Table 4.1.

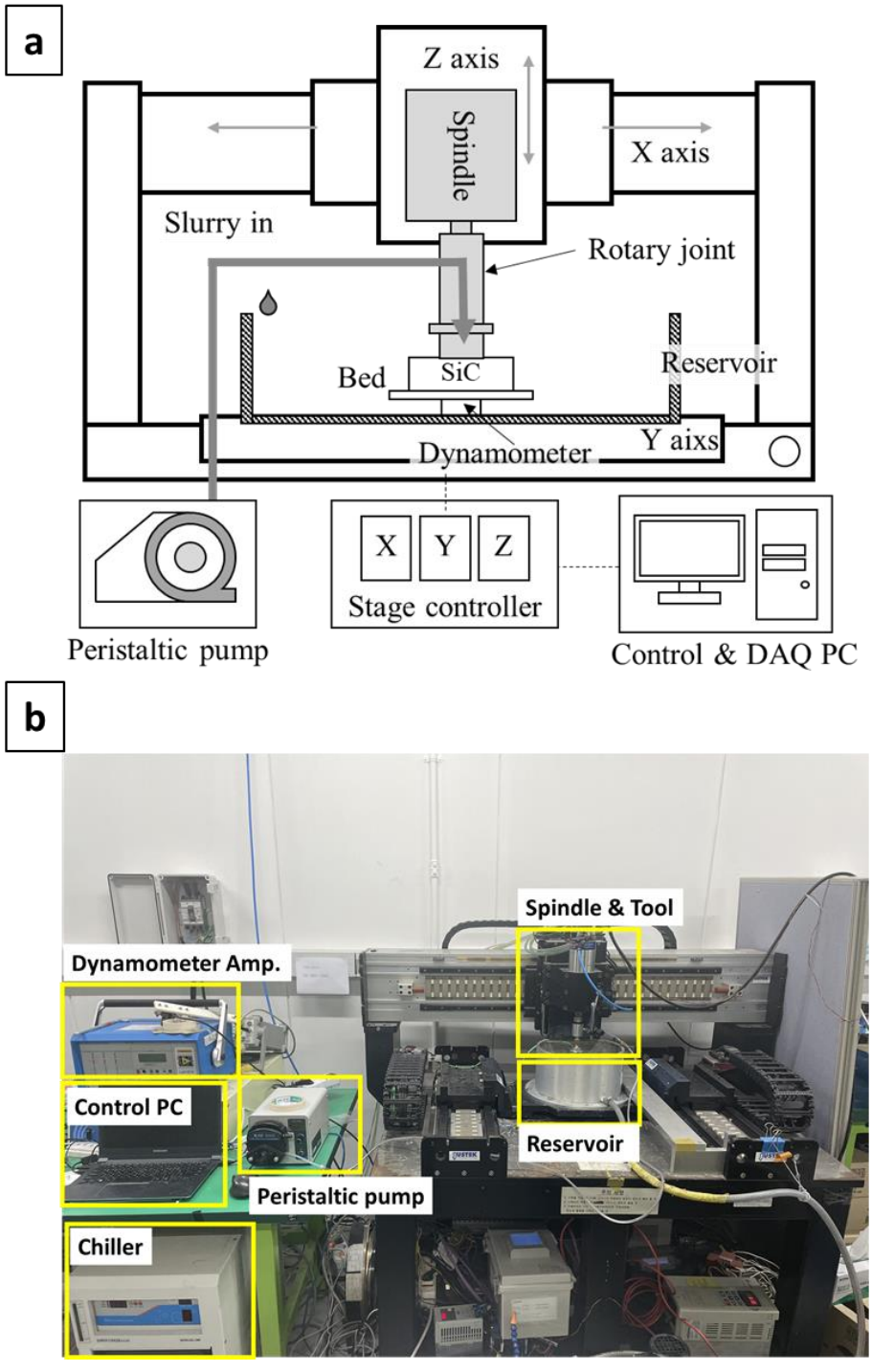

Figure 4.1 Experimental apparatus (a) schematic diagram (b) photograph

Table 4.1 Polishing system specifications

3-axis stage (JTM-30 / Justek, Korea)	
Resolution	1 μm (encoder)
Repeatability	±0.5 μm
Accuracy	2 μm / 4 μm
Spindle (SW80 / SAMWOO hitech., Korea)	
Motor power	1.3 kW
Torque	1.1 Nm
Speed	12,000 RPM
Chiller (DLC-1000, Dawoncooler, Korea)	
Flow rate	10 L/min
Cooling capacity	1,000 kcal/h
Dynamometer (9251A, Kistler, Switzerland)	
Sensitivity	-4 pC/N
Range	-5.0 ~ 5.0 kN
Resolution	1 μN

4.2. Slurry supply system

The slurry was supplied using a peristaltic pump to control the amount of slurry supplied accurately A peristaltic pump is a positive displacement pump. Inspired by intestinal peristalsis in animals, it refers to a pump that can repeatedly deliver a variety of fluids in precise amounts.

As depicted in Figure 4.2, the mechanism by which the fluid was supplied is as follows. The supplied fluid was then placed in a flexible tube mounted inside the pump. The pump alternately compressed and relaxed the tube to draw it in and push the fluid out of the pump. A roller was rotating inside the casing of the pump and passed in the longitudinal direction of the tube to create a sealed space. As the rotor of the pump rotates, the sealing pressure travels along the tube, causing the fluid to move along the pump's discharge line. When the pressure was released, a vacuum was created inside the tube, and fluid was drawn from the inlet of the pump. By repeating this suction and discharge process, the pump delivers a fluid and is generally used to deliver a certain amount of a variety of fluids at a predetermined time. Detailed specifications of the pump used in this study are shown below.

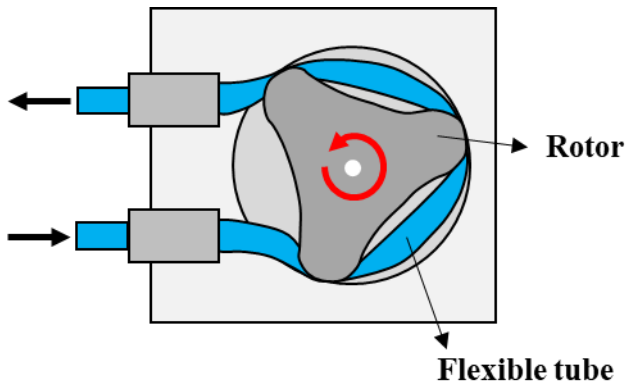

Figure 4.2 Schematic diagram of peristaltic pump

Table 4.2 Peristaltic pump specification

Peristaltic Pump	
Model	BT100M
Maker	Baoding Chuangrui Precision Pump Co., Ltd. (China)
Speed range [RPM]	0.1~100
Resolution [RPM]	0.1
Flow range [ml/min]	0.0015~380
Pump head	YZ1515x
Tube diameter	Inner diameter 1.6 Outer diameter 4.8
Flow range considering tube size [ml/min]	0.27~27

The slurry was supplied to the process through the center of the tool. For this purpose, a rotary union was used to supply fluid to the rotating part. As shown in Figure 4.3, the rotary union consists of an aluminum housing, a shaft core with holes on the side, a bearing to prevent rotation of the spindle from being transmitted to the slurry supply tube, and a rubber seal. The fluid supplied from the side channels is allowed to flow along the axis to the center through the hole in the shaft core. The rotary union was equipped with a polishing tool with through-holes drilled along the center of the shaft, as shown in Figure 4.4.

Figure 4.3 Polishing tool capable of center injection

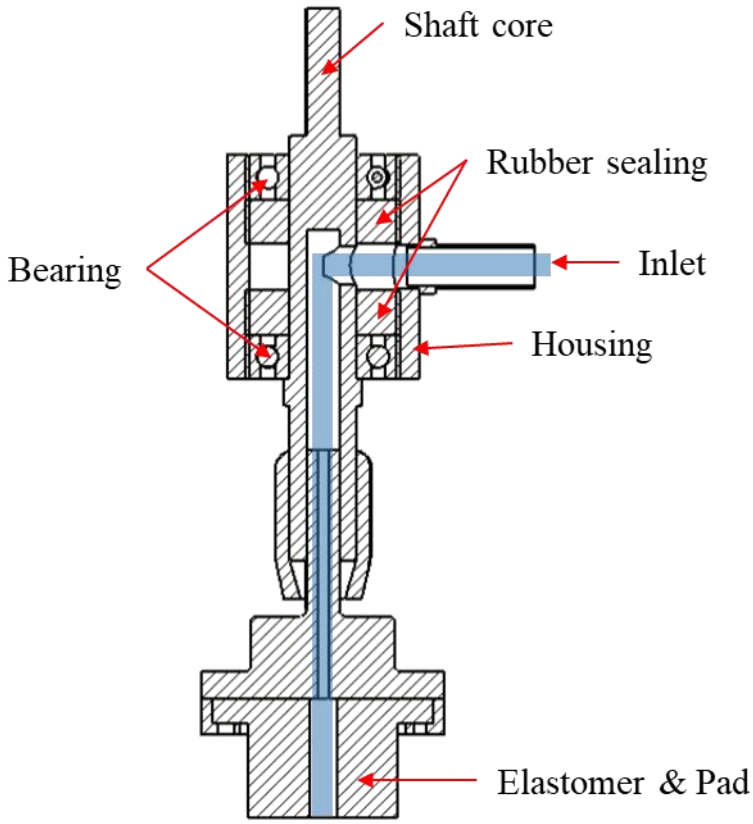

Figure 4.4 Cross section of tool for center injected polishing

Chapter 5. Process Evaluation

5.1. Process design

Polishing experiments were designed and performed as follows to investigate the process performance of the tool center slurry supply.

As shown in Figure 5.1, the entire experiment consists of a case that supplies the slurry to the center of the tool and a case that supplies the slurry to the outside. When the slurry was injected at the center of the tool, the nozzle of the pump was connected to the rotary union so that the entire slurry supplied was injected at the center. In the other case, where the slurry was supplied outside the tool, the pump nozzle was placed approximately 10 mm away from the polishing tool rather than being connected to the rotary union, allowing the entire slurry to be supplied outside the contact surface.

In addition, a method was designed to evaluate the process performance when the tool rotation speed changed. The entire experiment was performed at three rotational speeds: 900, 1500, and 3000 RPM.

Finally, the flow rate of the supplied slurry was included in the control value. The polishing experiment was designed by setting the slurry supply flow rate in four steps: 2.5, 5, 10, and 15 ml/min.

After successive polishing experiments, the MRR, slurry supply state, surface roughness, and slurry usage were compared by measuring the surface of the polished workpiece. The detailed experimental parameters are presented in Table 5.1. As

shown in Figure 5.3, , polishing was performed for 52 min along the raster tool path. A photograph of the workpiece before and after polishing is shown in Figure 5.2. The SiC workpiece used in this study was fabricated via surface grinding after hot-press sintering. The details are listed in Table 5.2.

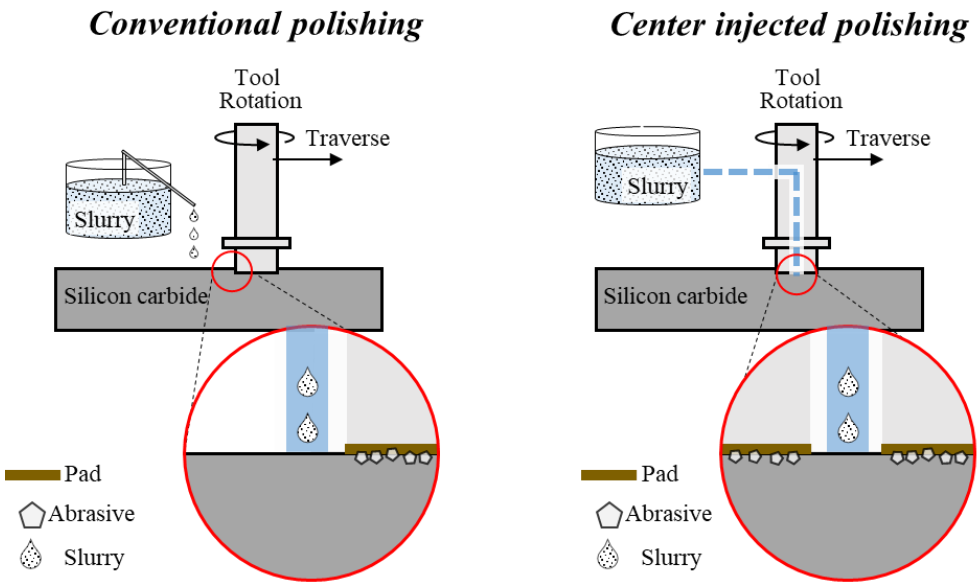

Figure 5.1 Experimental paradigm of polishing process

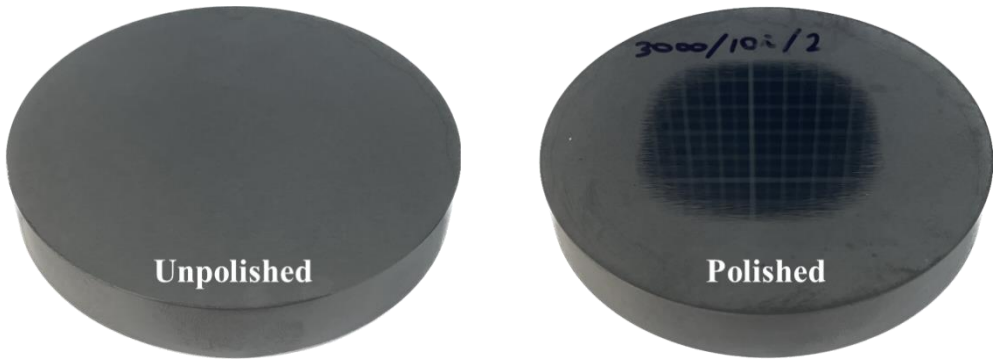

Figure 5.2 SiC workpiece before and after polishing

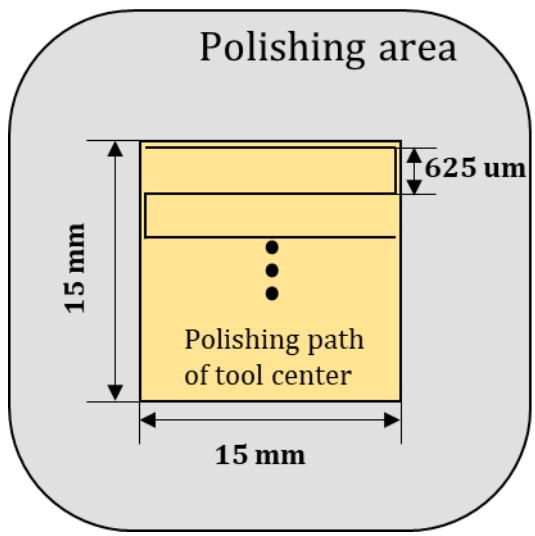

Figure 5.3 Tool path for performance evaluation experiment

Table 5.1 Polishing process parameter

Polishing process parameter	
Normal force [N]	22.5
Tool diameter [mm]	26
Tool speed [RPM]	900, 1500, 3000
Dwell time [min]	52
Feed rate [mm/s]	2.5
Slurry	Diamond and ceria (~1 μm diameter)
Polishing Pad	Polyurethane
Slurry flow rate [ml/min]	2.5, 5, 10, 15

Table 5.2 Properties of SiC workpiece

Properties of SiC workpiece	
Fabrication process	Hot-press sintering α-SiC (6H)
Density [kg/m^3]	3210
Elastic modulus [GPa]	410
Compression strength [MPa]	4600
Fracture toughness [$MPa \cdot m^{1/2}$]	4.6

5.2. Evaluation of material removal

In general, material removal during polishing is measured through the change in the mass of the workpiece before and after polishing. This was calculated by inversely calculating the material density. However, owing to the very low processability and low density of SiC, it is difficult to measure the processing volume using this method. Instead, the material removal in each experiment was determined by measuring the surface profile of the workpiece. In the case of polishing, where the pressure and relative velocity are uniform over the entire surface, the MRR can be expressed as the removal depth per unit time [67]. Measurements were performed using ET200 equipment (Kosaka Laboratory Ltd., Japan). The photographs and specifications of the equipment used for the measurement are as follows: Surface measurements were performed from outside the polished area, through the polished area, and out of the polished area on the opposite side. The removal depth of the polished area was measured after correcting the inclination of the workpiece using the value measured outside the polished area.

Table 5.3 Specification of surface profilometer

Specification of surface profilometer	
Model	ET200
Maker	Kosaka Laboratory Ltd. (Japan)
Moving direction axis	
Measuring range	Maximum 10 mm
Straightness	0.2 μm / 100 mm
Scan speed	200 μm / sec
Scale resolution	0.1 μm
Detector	
Measurement range	600 μm
Resolution	0.1 nm
Measuring force	50 μN
Tip radius	2 μm, diamond, 60 deg
Step reproducibility	1 nm

The processing depth was measured and used to calculate the MRR in a successful polishing experiment. When the slurry was supplied to the center of the tool (2.5, 5, 10, and 15 ml/min at 900 RPM), the material removal was 4.13, 4.73, 4.49, and 4.81 μm, respectively. When the slurry was supplied to the outside, the MRRs were 2.80, 3.15, 5.06, and 4.65 μm, respectively, under the same process parameters. In internal supplying at 1500 RPM, the values were 6.34, 6.04, 5.79, and 6.03 μm, respectively, under the same process parameters. When the slurry was supplied to the outside of the tool with 1500 RPM, the removal depth was 3.57, 4.67, 4.51, and 4.45 μm, respectively, under the same process parameters. In the case of 3000 RPM, the value of center injected polishing was 7.72, 7.55, 7.66, and 7.00 μm, respectively, under the same process parameters. When the slurry was supplied at the outside of the tool, the material removal was 3.24, 3.54, 3.74, and 4.88 μm, respectively, under the same process parameters. The MRR was calculated by dividing the removal depth by a dwell time of 52 min.

As shown in the graph, the effect of the tool-center slurry supply was maximized as the tool rotational speed increased. At 900 RPM, the amount of material removed converging on both sides was 5 μm; however, at 1500 RPM, when the slurry was injected at the center, the amount of material removed was 7 μm, whereas when it was supplied to the outside, the amount of material removed was 4 μm. Consequently, the MRR was lower than that at 900 RPM. In the case of 3000 RPM, as in 1500 RPM, the material removal increased when the slurry was injected inside, but the material removal decreased when the slurry was supplied from the outside. When spraying from the inside, the supplied flow rate is supplied to the machining surface regardless of the rotation speed of the tool. However, when

supplying the slurry outside, the supply condition deteriorates due to the centrifugal force.

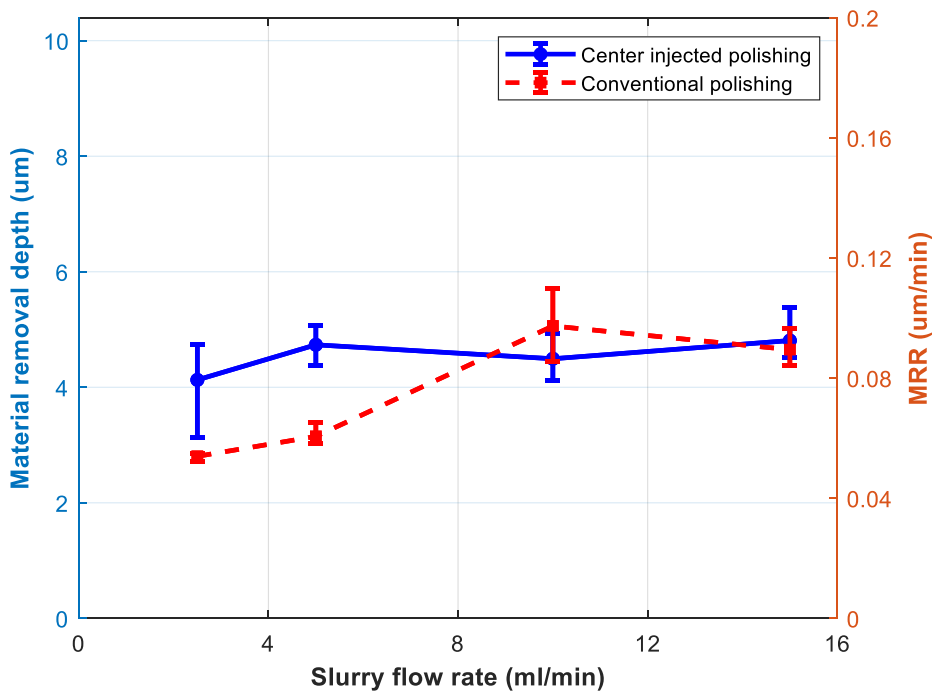

Figure 5.4 Material removal performance (900RPM)

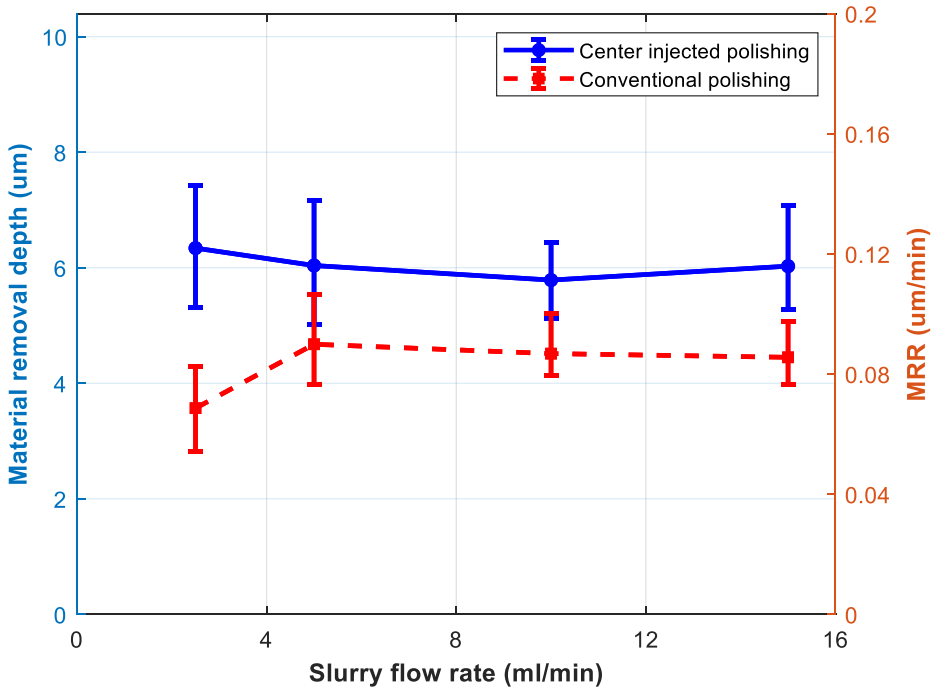

Figure 5.6 Material removal performance (1500RPM)

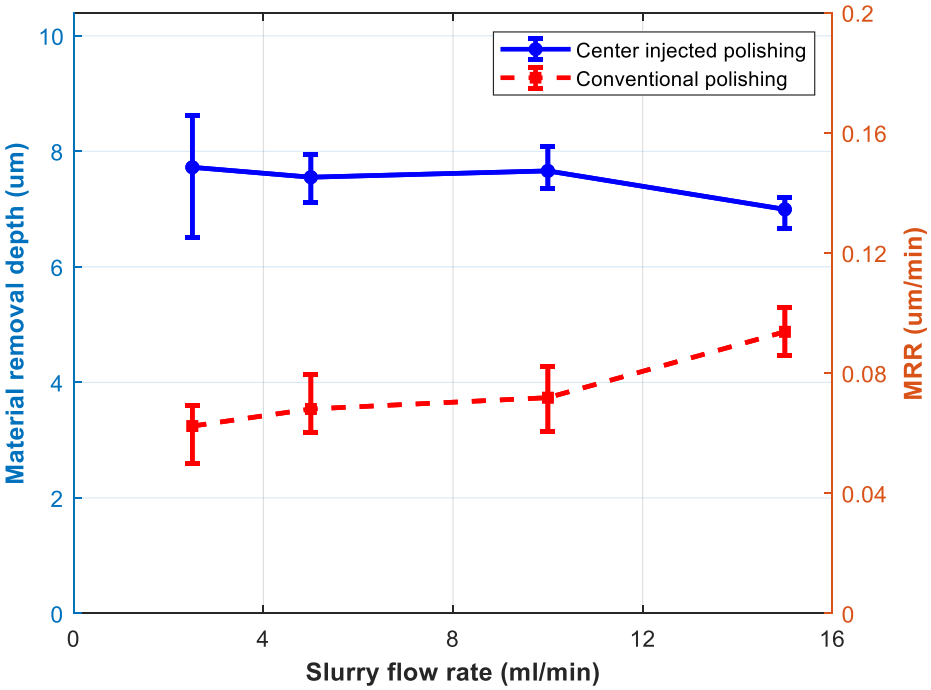

Figure 5.5 Material removal performance (3000RPM)

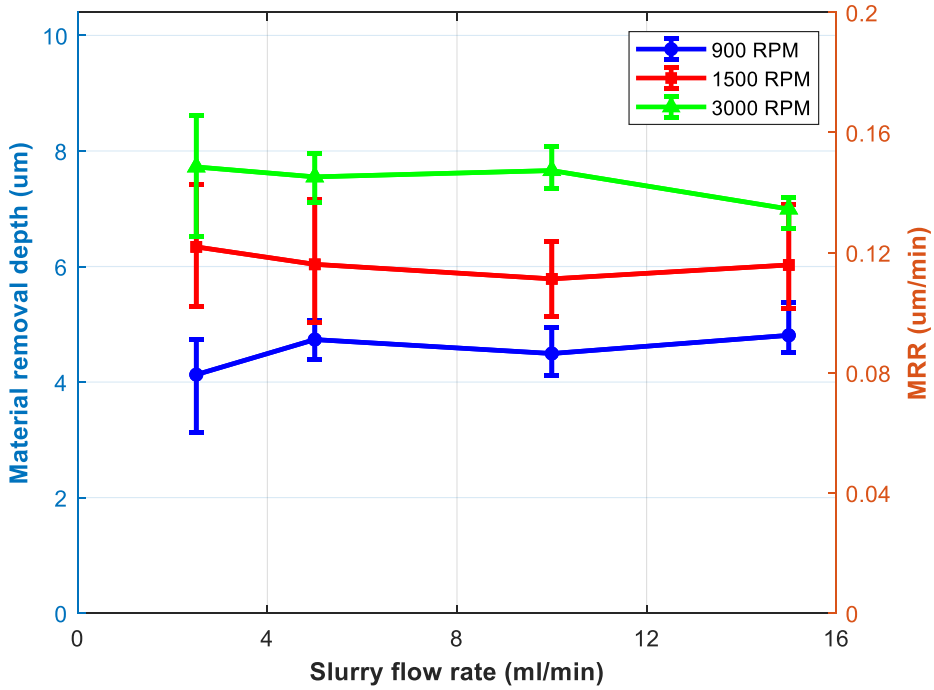

Figure 5.7 Material removal performance of center injected polishing

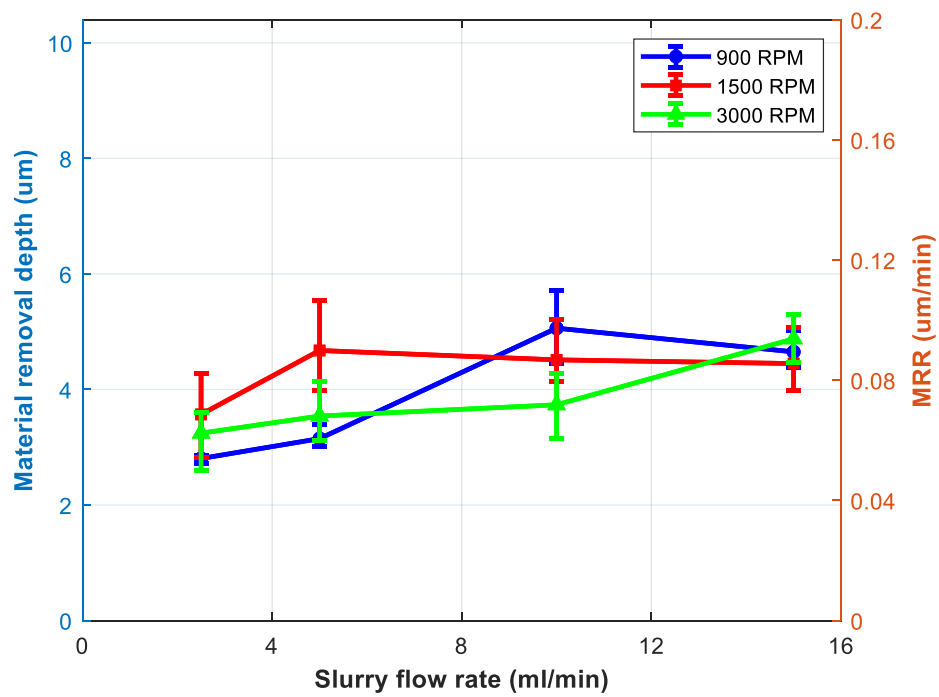

Figure 5.8 Material removal performance of conventional polishing

5.3. Evaluation of slurry supply performance

According to Eqn. 2-8, MRR must be proportional to the relative velocity. However, the results presented in Chapter 5.2. was not proportional. As all other parameters were the same, it was assumed that this was a problem with the slurry supply. In addition, according to Eqn. 2-26, MRR is proportional to the number of particles. Therefore, it is necessary to evaluate not only the MRR but also the state of the slurry supply.

The Preston constant is ideal for evaluating the slurry supply state of polishing when other process parameters are constant. As a process with an insufficient slurry supply will have a low Preston constant, the slurry supply state of each process can be evaluated based on the size of this constant. For ease of calculation, assume that the polished surface has the same depth across the entire processing area and the relative speed by feed rate can be neglected; the Preston constant is calculated as follows:

$$\mathrm{k_p} = \frac{\Delta h}{p|v|\Delta t} \tag{5-1}$$

The results of calculating and comparing the Preston constants of each process using the above equation are shown in the figure below: When the slurry was supplied to the center (2.5, 5, 10, and 15 ml/min at 900 RPM), the Preston constants of each process were 2.54×10^{-14}, 2.92×10^{-14}, 2.77×10^{-14}, and 2.96×10^{-14}(1/Pa), respectively. When the slurry was supplied at the outside of the tool,

Preston constants of each process were 1.73×10^{-14}, 1.94×10^{-14}, 3.12×10^{-14}, and 2.87×10^{-14} (1/Pa), Respectively, under the same process parameters.

In center injected polishing at 1500 RPM, the values were 2.35×10^{-14}, 2.24×10^{-14}, 2.14×10^{-14}, and 2.23×10^{-14} (1/Pa), respectively, under the same process parameters. When the slurry was supplied at the outside of the tool, the Preston constants of each experiments were 2.54×10^{-14}, 2.58×10^{-14}, 2.30×10^{-14}, and 2.38×10^{-14} (1/Pa), respectively, under the same slurry flow rate.

In the case of 3000 RPM, the Preston constants of each center injected polishing experiments were 1.43×10^{-14}, 1.38×10^{-14}, 1.42×10^{-14}, and 1.29×10^{-15} (1/Pa), respectively, under the same process parameters. When the slurry was supplied at the outside of the tool, the Preston constants of each experiments were 6.00×10^{-15}, 6.55×10^{-15}, 6.91×10^{-15}, and 9.02×10^{-15} (1/Pa), respectively, under the same process parameters.

When the slurry was injected at the center, a similar size was maintained, regardless of the rotation speed. The external slurry supply exhibited a continuous decrease in the Preston constant as the process RPM increased. As a result, for the center supply, the material removal increased at a rate similar to the increase in the tool rotation speed, and for conventional polishing, the material removal did not increase when the rotation speed increased.

The slurry supply condition deteriorated due to the high centrifugal force in the conventional polishing. However, when the slurry was injected at the center of the tool, the centrifugal force was not significantly affected. As previously stated, as the rotational speed of the tool increases, the centrifugal force increases and the slurry outside the tool is prevented from being supplied to the inside of the tool. The amount

of slurry supplied to the bottom of the tool is maintained regardless of the number of revolutions in the case of the center supply; therefore, this does not seem to be the case.

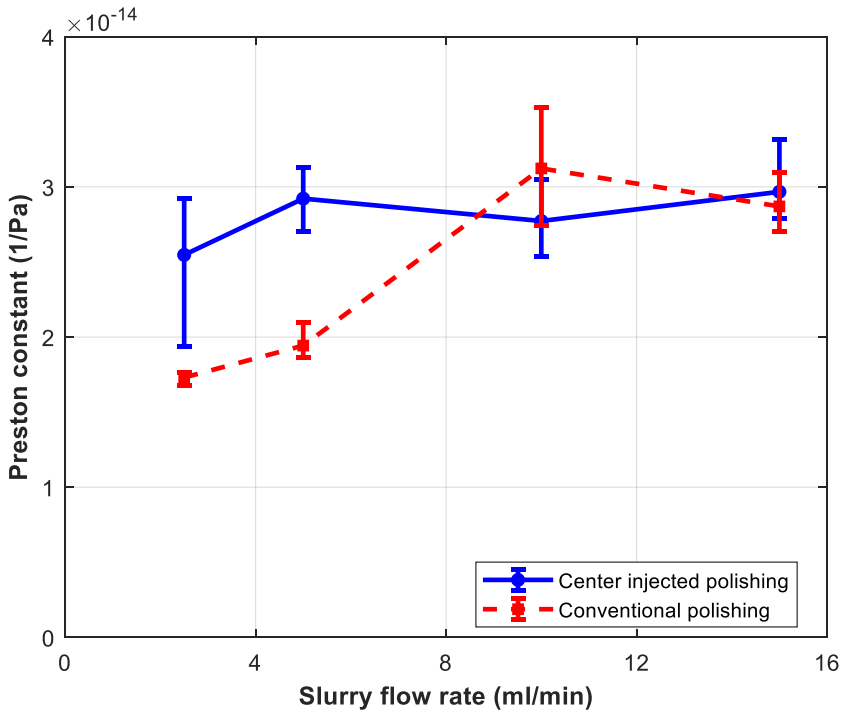

Figure 5.9 Preston constant comparison (900RPM)

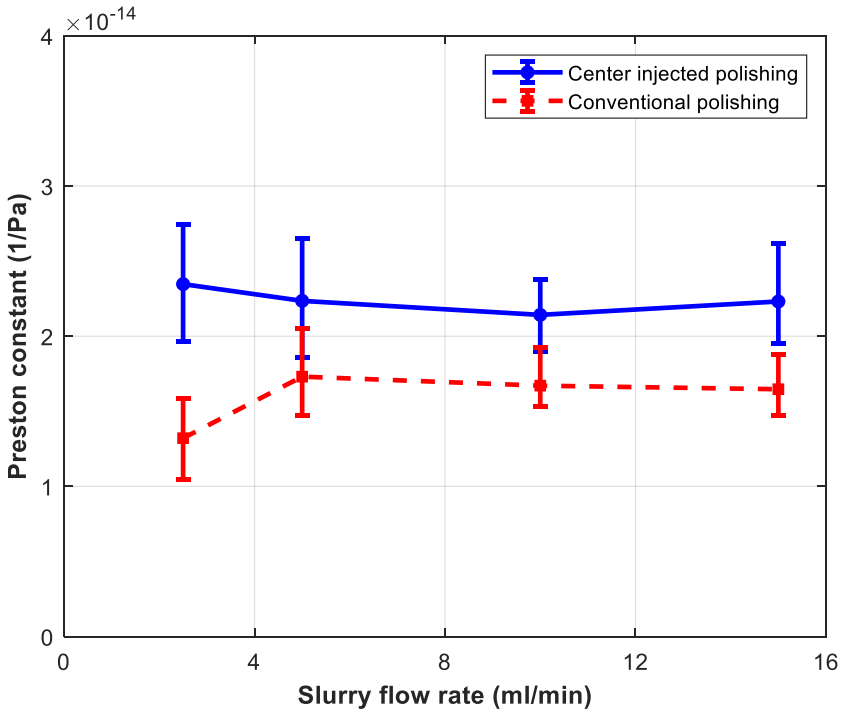

Figure 5.10 Preston constant comparison (1500RPM)

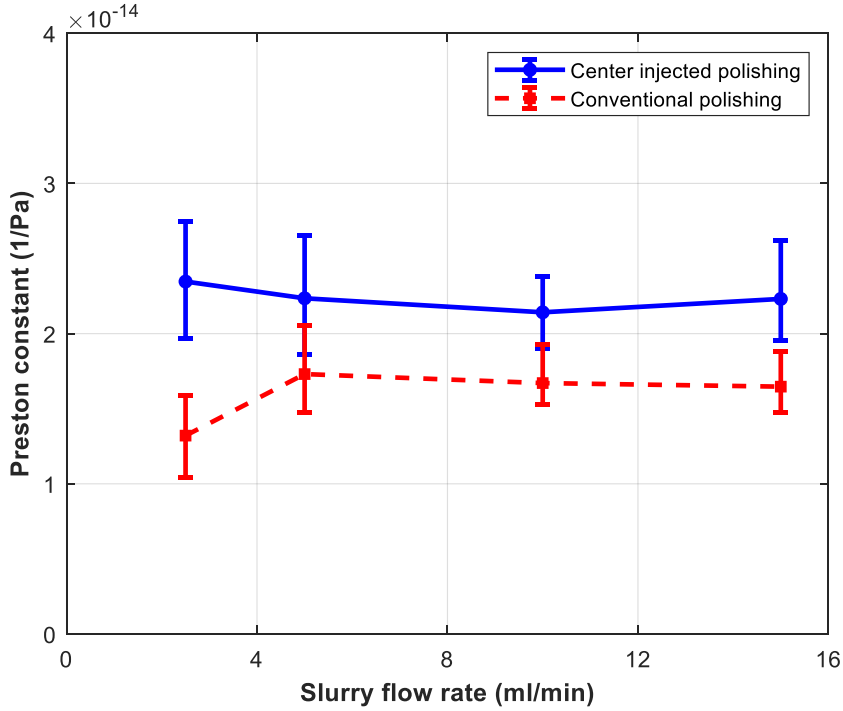

Figure 5.11 Preston constant comparison (3000RPM)

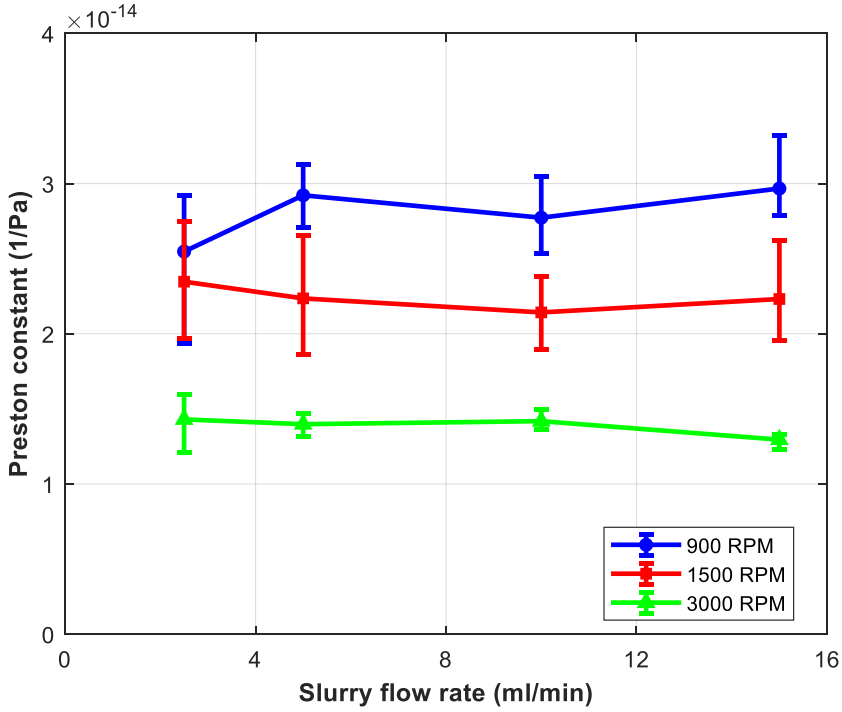

Figure 5.12 Preston constant comparison of center injected polishing

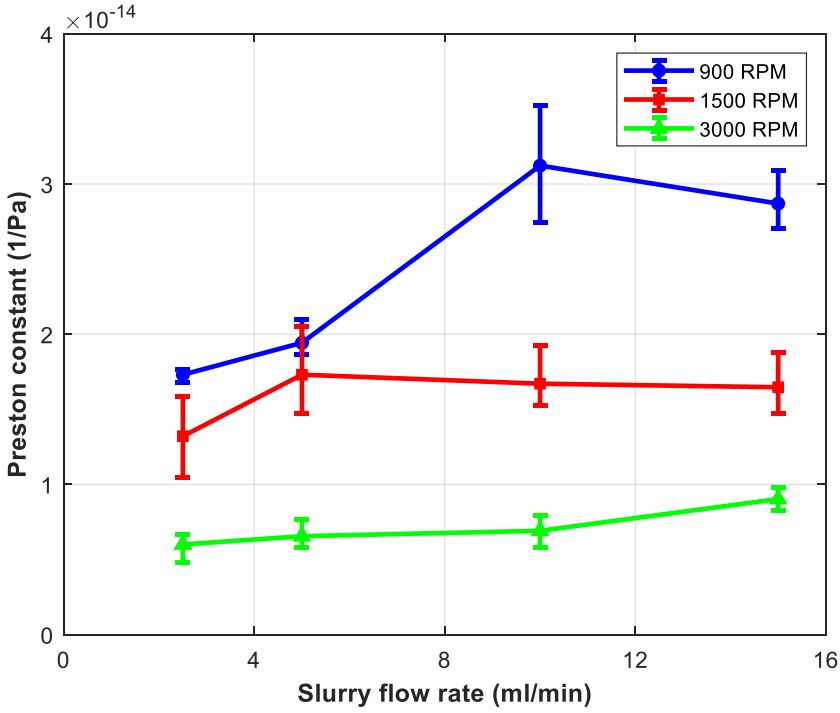

Figure 5.13 Preston constant comparison of conventional polishing

5.4. Evaluation of surface roughness

As the goal of polishing is generally to obtain high surface quality [68], not only the MRR but also the surface roughness after the process is one of the main performances of the process. Therefore, it is necessary to evaluate the surface conditions after the process as well as the MRR. In this study, a three-dimensional Sa value was measured instead of a two-dimensional Ra value for surface quality evaluation. The Sa value is defined as follows:

$$\mathrm{S_a} = \frac{1}{S_M}\int_0^{L_x}\int_0^{L_y}|f(x,y)|\,dx\,dy \tag{5-2}$$

$$\mathrm{S_M} = L_x L_y \tag{5-3}$$

In general, the final roughness of polishing is dependent on the slurry particle size [69]. In this study, as the same slurry was used in all the experiments, the surface roughness by polishing converged to a similar level. However, the specimen used in this study was manufactured through grinding, and if the material removal in the polishing experiment was insufficient to remove all surface damage caused by grinding, the surface roughness value of the corresponding point might be high. As shown in Figure 5.14, there was an area where grinding damage remained after polishing. The results of measuring the area where the grinding damage remains are shown in Figure 5.15. The roughness of this area was 47 nm, and it was confirmed that the surface roughness changed significantly because of the remained damage.

However, the roughness value was changed by the amount of material removed, and the amount of material removed was compared in the previous section. Therefore, the roughness of the area without any damage was measured.

The surface roughness was measured using an interferometer, and the photographs and specifications of the equipment used for the measurement were as follows:

Table 5.4 Specification of interferometer

Specification of Interferometer	
Model	SURFIEW Academy series
Maker	GLTECH.CO.,LTD (Korea)
Vertical resolution	VSI, VEI < 0.5 nm, VPI < 0.1nm
Pixel resolution	0.03 ~ 7.2 um
Step height repeatability	≤ 0.3% 1sigma
Scan range	≤ 100 um
Sample reflectivity	0.05 ~ 100%

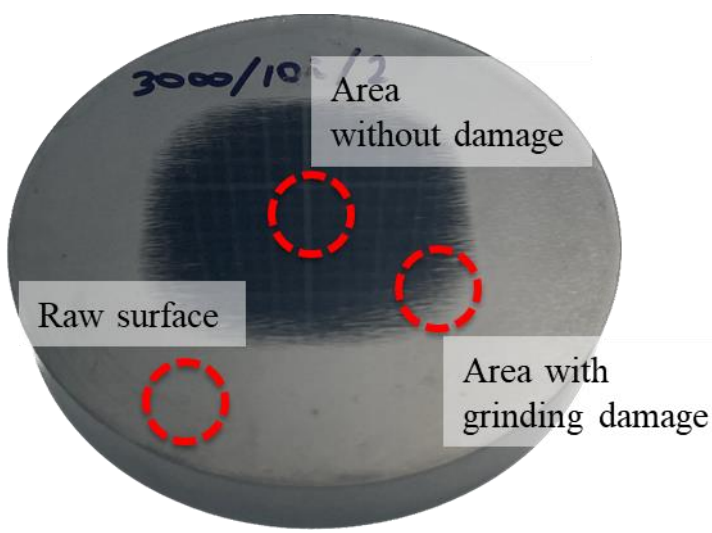

Figure 5.14 Surface after polishing (grinding damage)

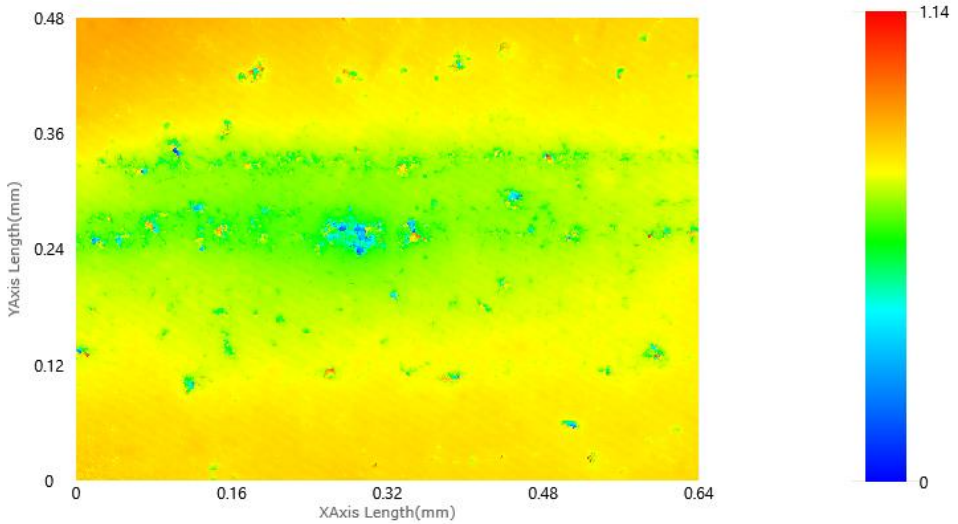

Figure 5.15 Surface measurement result of area with damage

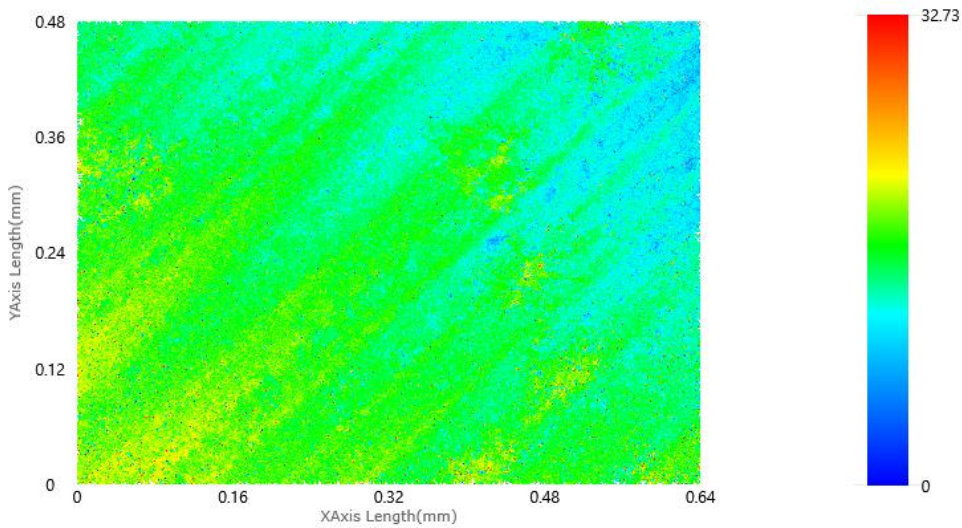

Figure 5.16 Surface measurement result of raw material

When the slurry was injected at the center of the tool (2.5, 5, 10, and 15 ml/min at 900 RPM), the surface roughness values were 8, 10, 14, and 13 nm, respectively. When the slurry was supplied outside the tool, the material removal was 10, 10, 7, and 9 nm, respectively, under the same process parameters. The values of the central supply at 1500 RPM were 8, 11, 13, and 14 nm, respectively, under the same process parameters. When the slurry was supplied outside the tool, the surface roughness values were 8, 8, 9, and 7 nm, respectively, under the same process parameters. At 3000 RPM, the center supply was 11, 10, 8, and 12 nm, respectively, under the same process parameters. When the slurry was supplied outside the tool, the surface roughness values were 11, 9, 10, and 8 nm, respectively, under the same process parameters.

The results of the evaluation of the surface roughness were as expected. As the surface roughness of polishing depends on the particle size of the slurry, if the surface roughness reaches a convergence value after a certain period of processing, the surface roughness value converges to a level of approximately 10–15 nm throughout the experiment, as in previous experiments. This is intuitively reasonable because the surface roughness on the polishing surface remains only a part of the scratches caused by abrasive particles when the amount of processing reaches a depth sufficient to remove the subsurface damage caused by grinding. A graph comparing the surface roughness measurement values by RPM and the slurry supply method is shown in the figure below.

As shown in Figure 5.16, the surface roughness of the workpiece before polishing is 1.5 micrometers. The surface roughness value before and after polishing decreased significantly and remained below 18 nm throughout the polishing experiment, indicating that there was no difference in the surface roughness

improvement performance depending on the supply method, as expected. In this study, a non-contact area was created at the center of the polishing tool. Therefore, there may be concerns such as surface pattern generation after polishing. However, there were no traces of patterns other than some residual damage on the surface after polishing, as shown in the images of the surface measurement results (Figures 5.19 – 5.24).

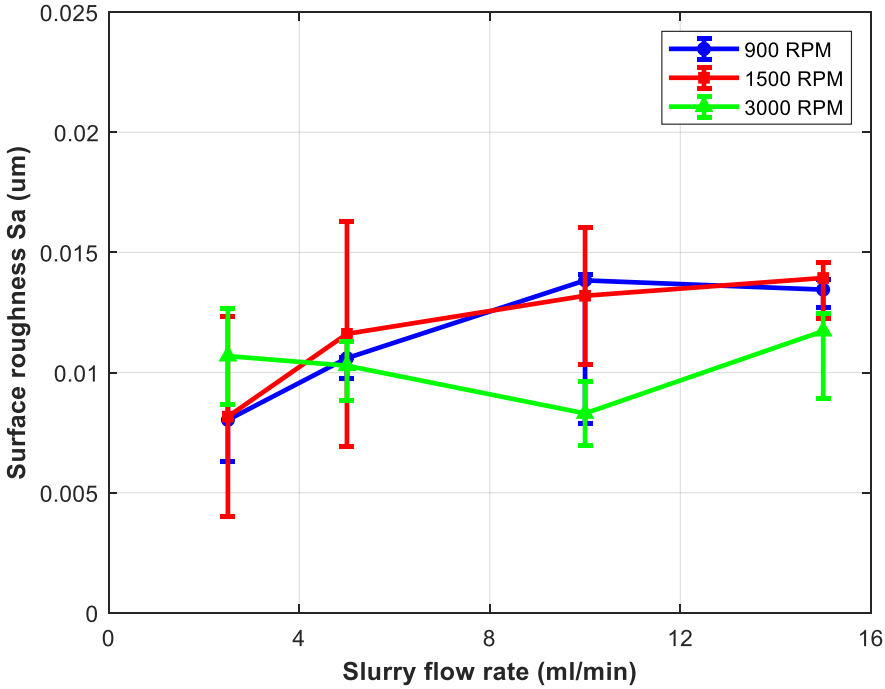

Figure 5.17 Surface roughness of center injected polishing

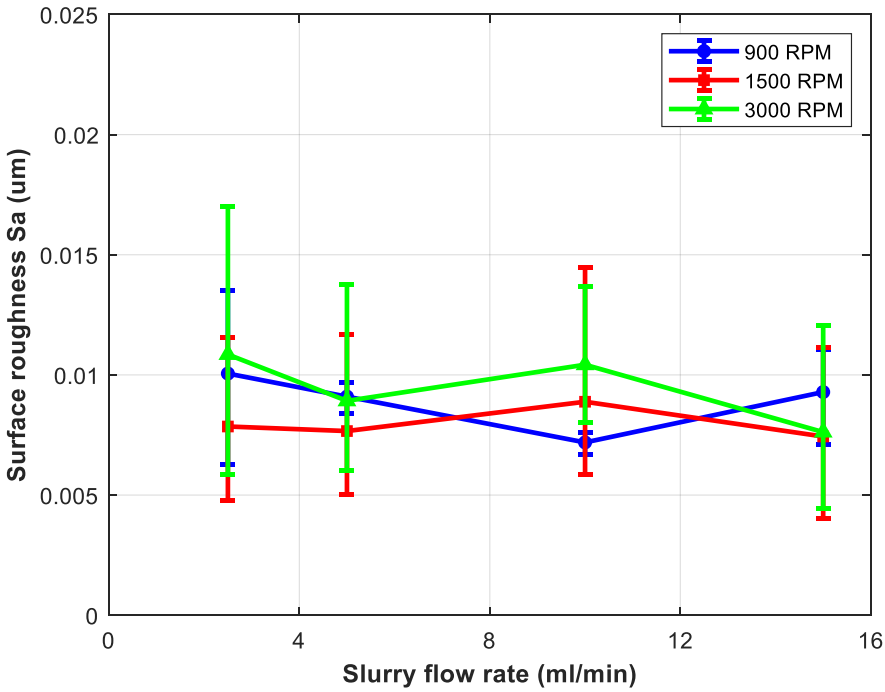

Figure 5.18 Surface roughness of conventional polishing

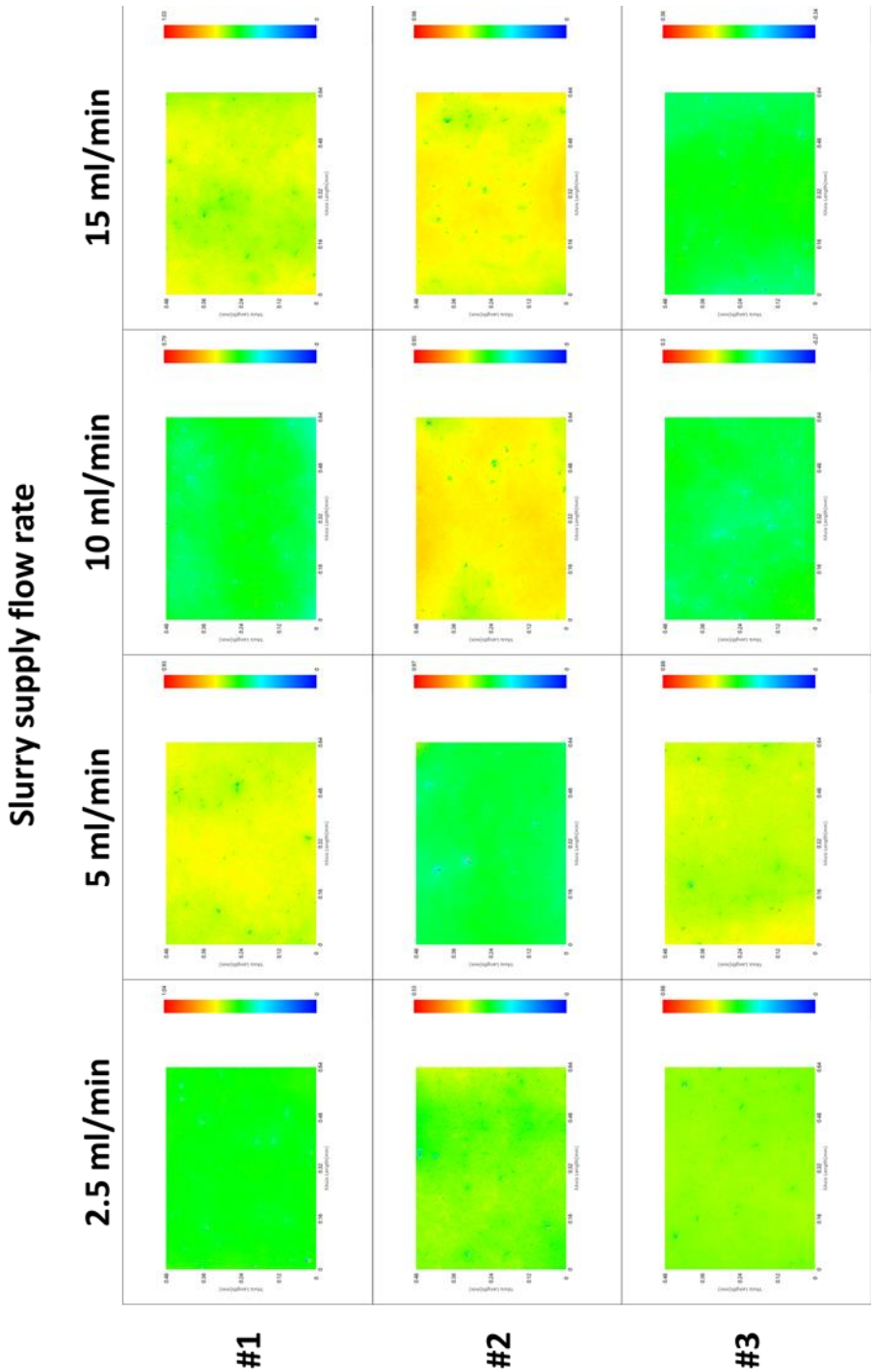

Figure 5.19 Surface roughness (900 RPM center injected)

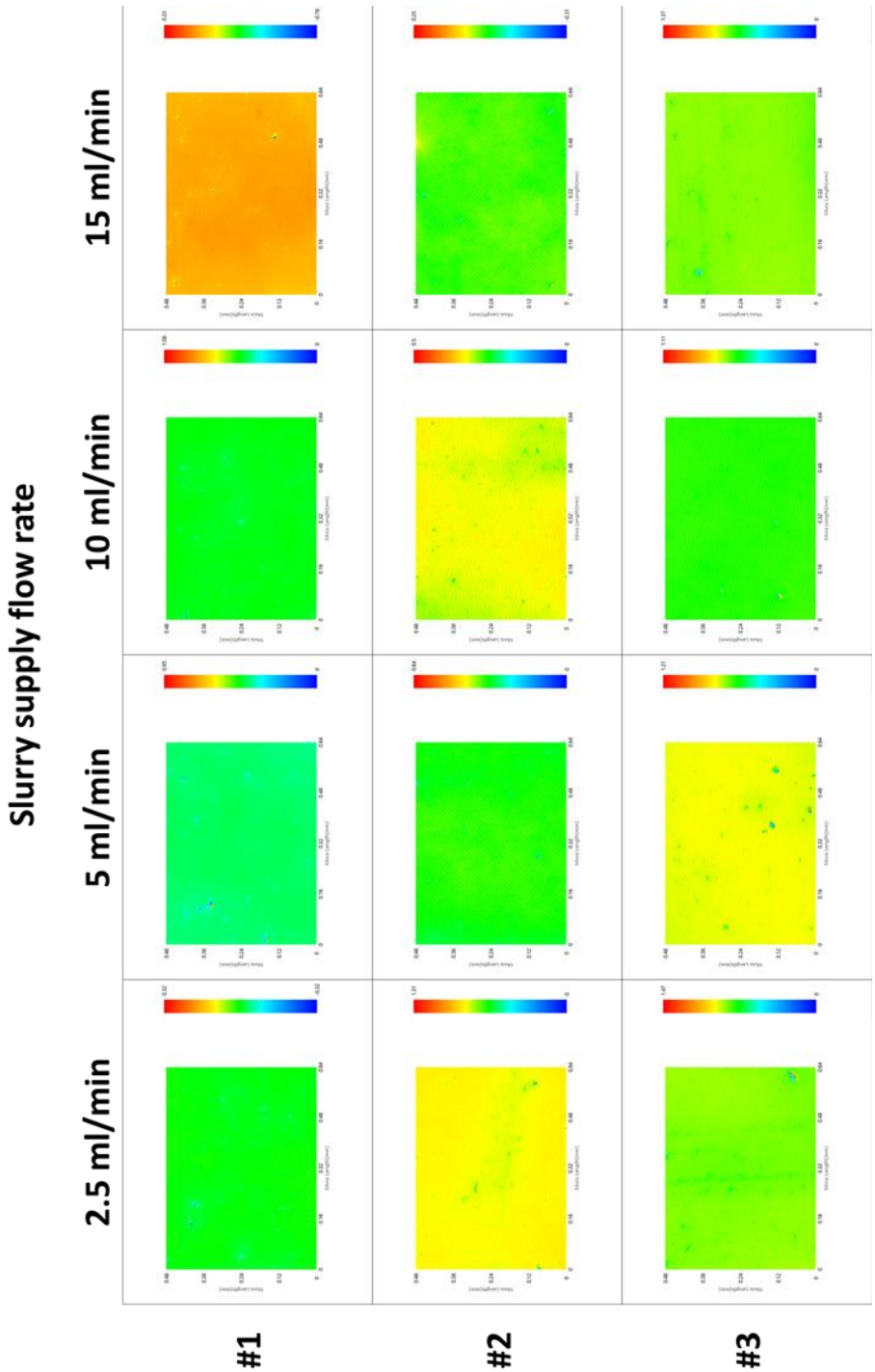

Figure 5.20 Surface roughness (900 RPM conventional polishing)

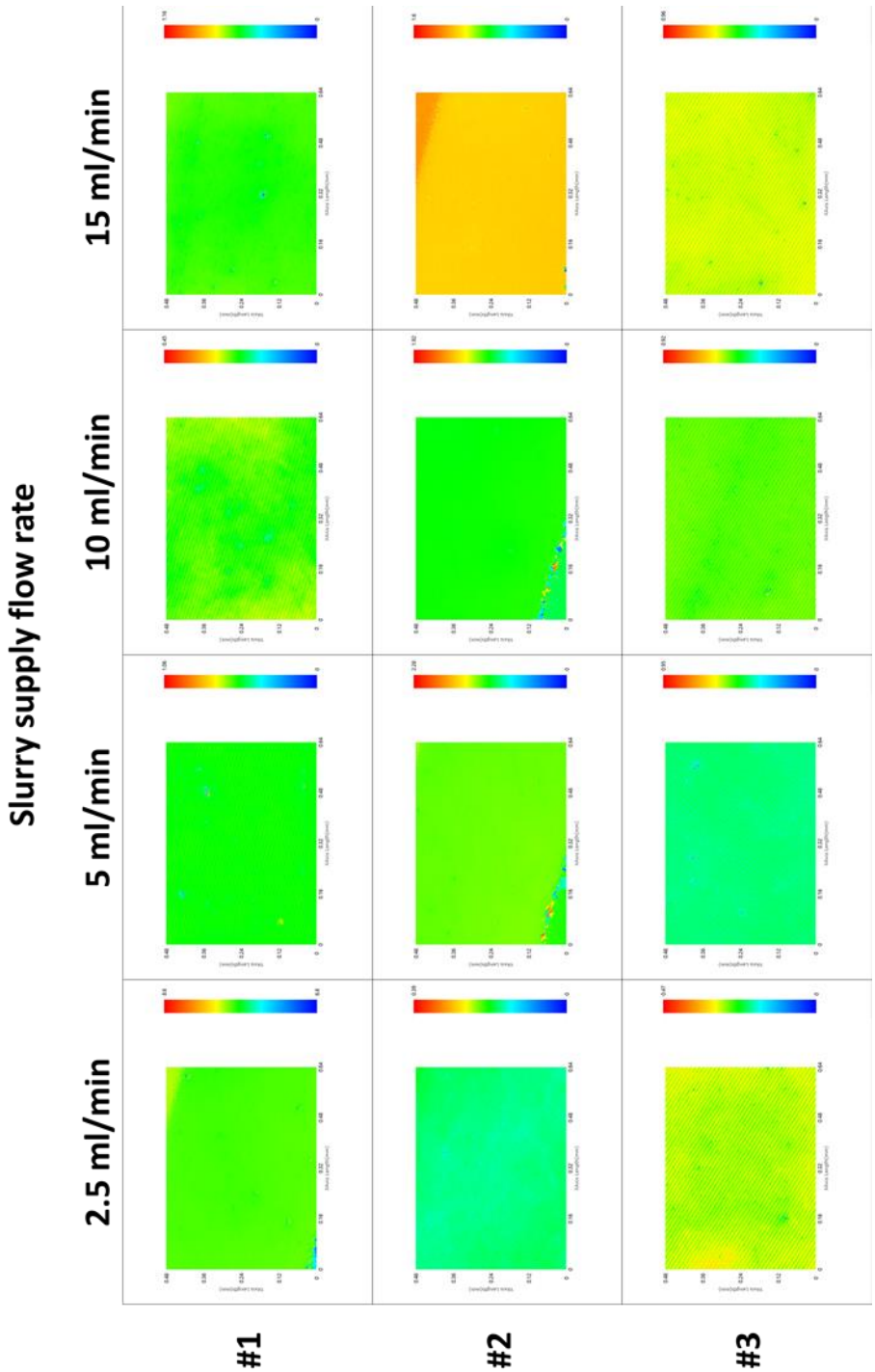

Figure 5.21 Surface roughness (1500 RPM center injected)

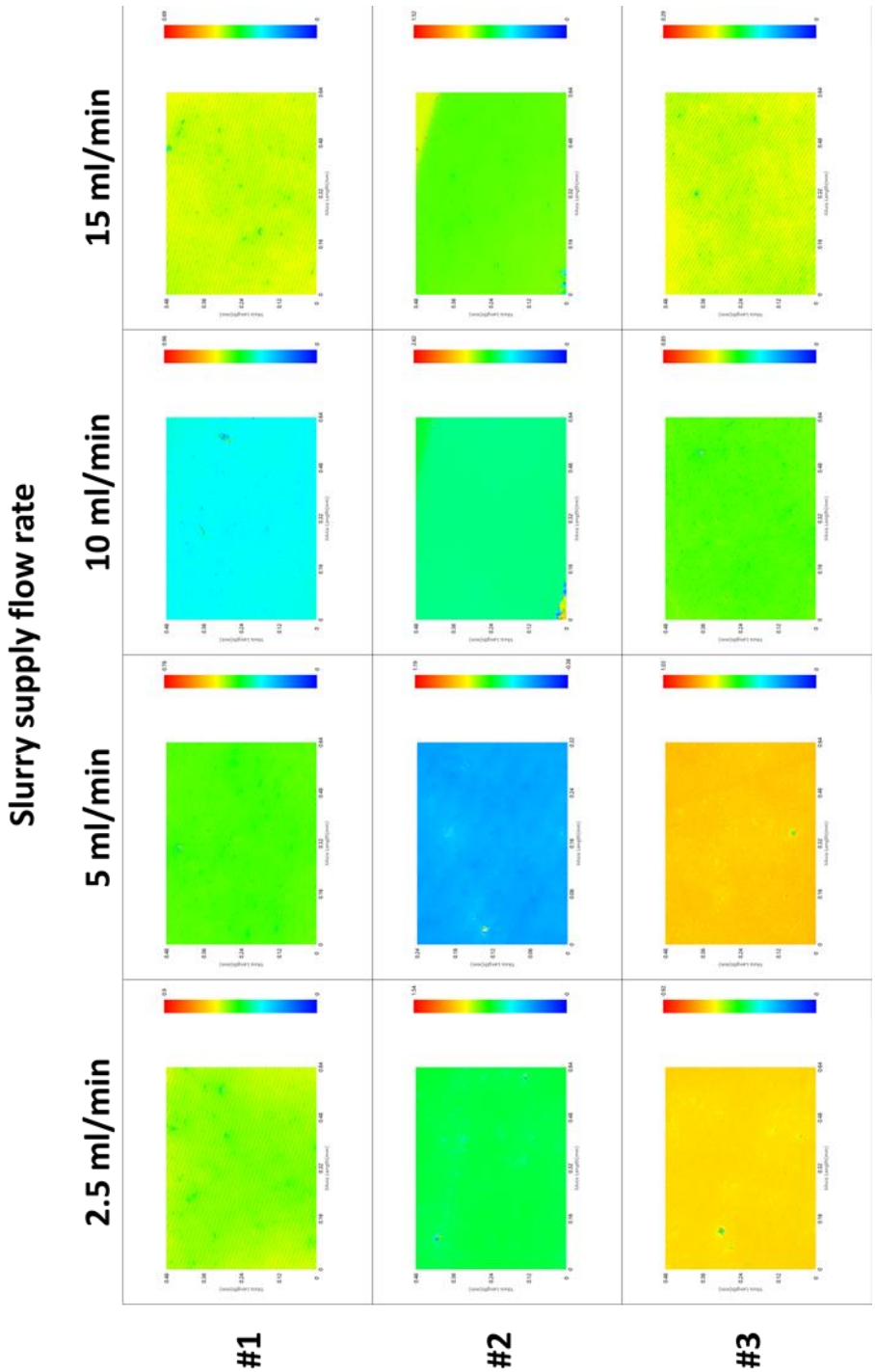

Figure 5.22 Surface roughness (1500 RPM conventional polishing)

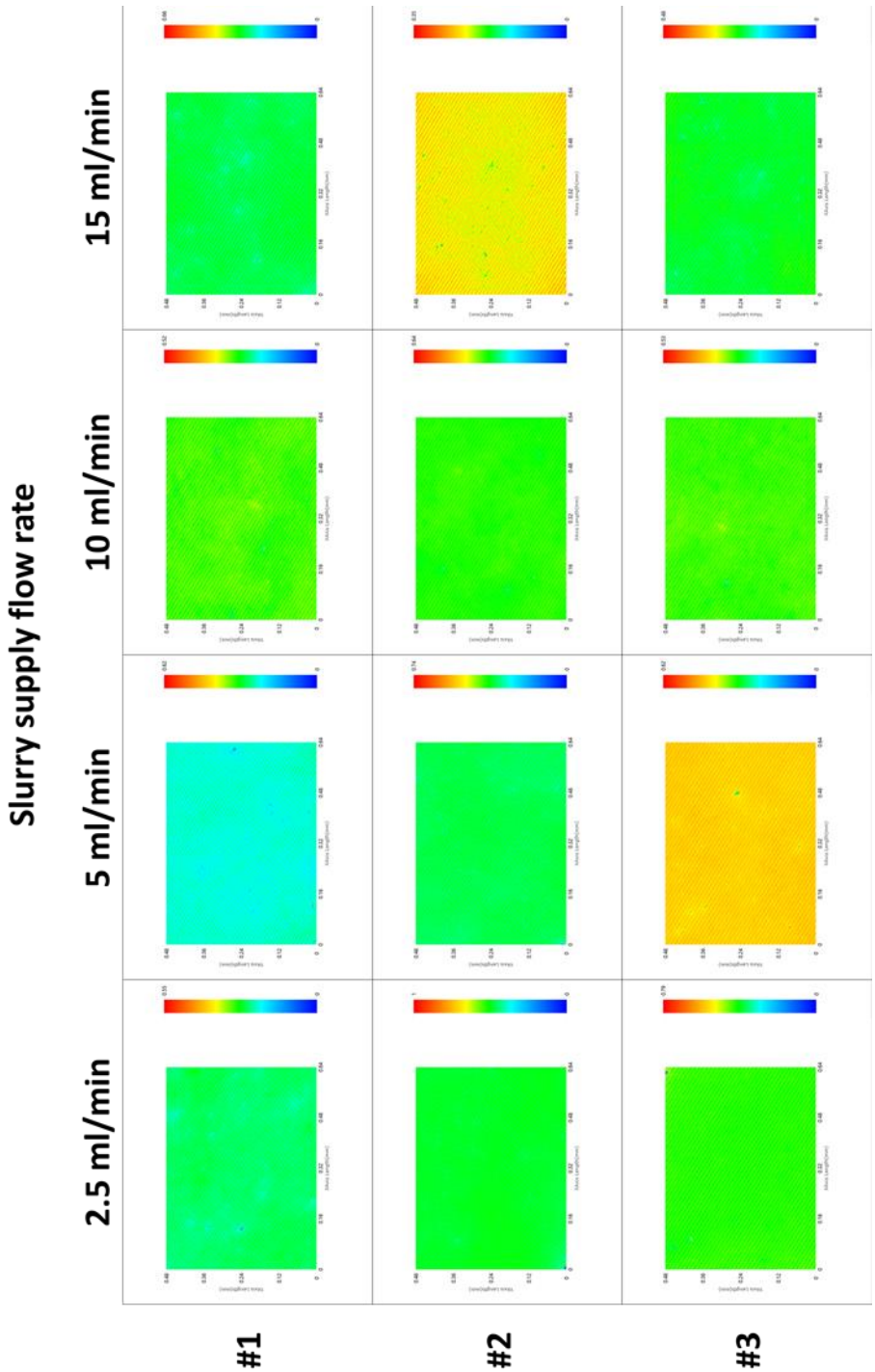

Figure 5.23 Surface roughness (3000 RPM center injected)

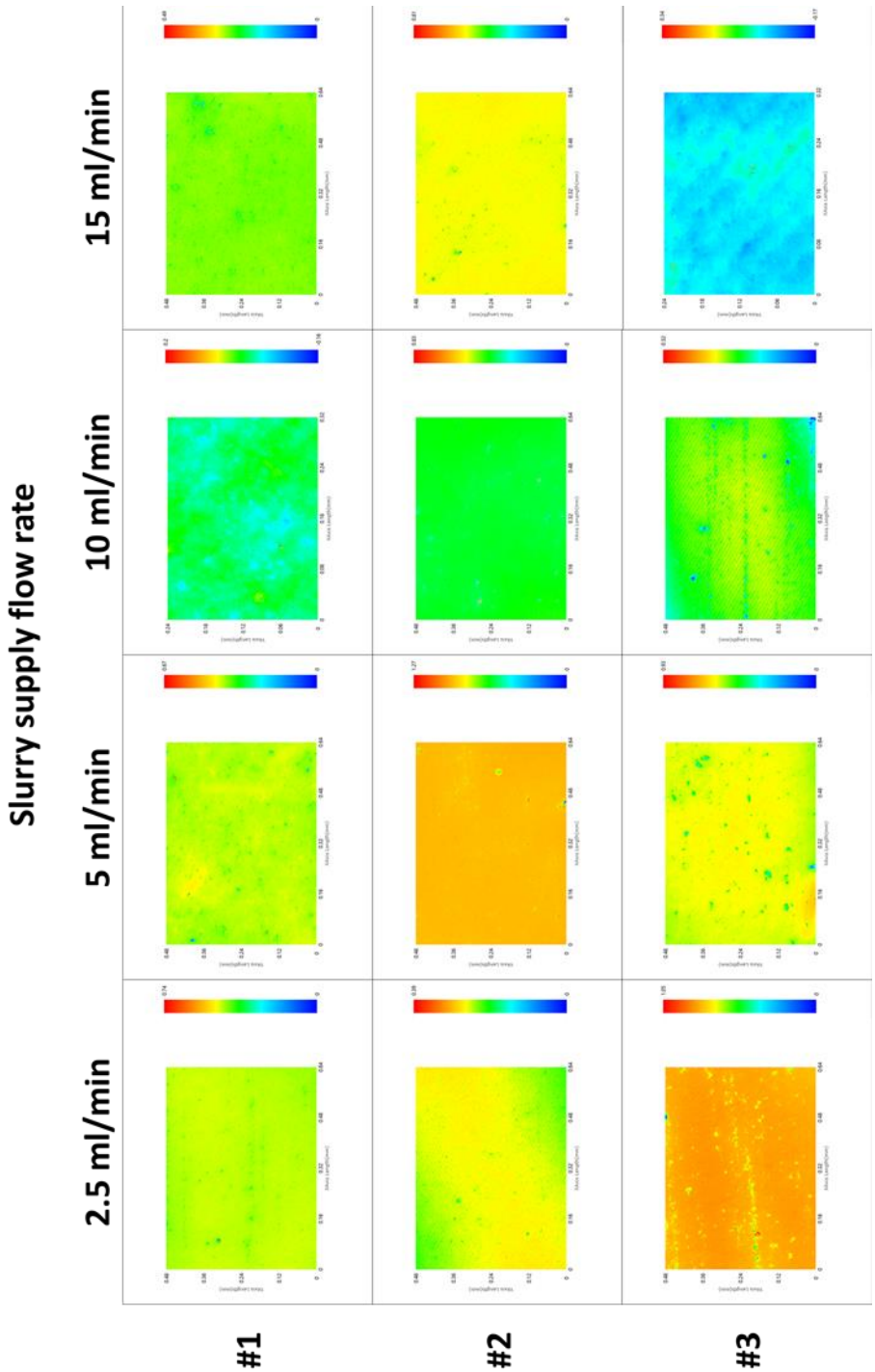

Figure 5.24 Surface roughness (3000 RPM conventional polishing)

5.5. Evaluation of slurry usage

The purpose of this study was to reduce slurry consumption through center-injected polishing. Therefore, it is also necessary to evaluate how much slurry can be reduced in the overall process by reducing the processing performance and processing time. First, the material-removal efficiencies of each experiment were compared. In this study, the slurry efficiency was defined as follows:

$$\text{Efficiency}_{\text{slurry}} = \frac{\Delta h}{Q \Delta t} \tag{5-4}$$

where Δh : Polished depth (material removal)

Q : Slurry supply flow rate

Δt : Dwell time

The results of the calculation-based comparison of slurry efficiency are shown in the graph below. As material removal is not proportional to the slurry supply flow rate, slurry material removal efficiency is decreased as the slurry supply is increased. When the rotation speed of the polishing tool was considered, the material removal increased according to the rotation speed when the slurry was injected into the center. However, when the slurry is supplied externally, the MRR does not increase, even if the rotation speed is increased. Therefore, the efficiency of the slurry also increased as the number of rotations increased in the case of center-injected polishing, whereas

conventional polishing did not. As a result, in the case of the center injected polishing, the amount of slurry reduction is greatest when processing at a high RPM. This seems to be because the difference in the slurry supply state is larger at high RPM, as determined by evaluating the Preston constant.

This difference is clear when comparing the efficiency of the slurry according to the supply method rather than the slurry supply flow rate. In both center-injected polishing and conventional polishing, the higher the supply flow rate, the lower the removal efficiency of the slurry. However, as the efficiency is different in the first place, the difference in efficiency according to the supply method is very clear. For example, supplying 5 ml/min of slurry to the tool center rotating at 1500 RPM has the same efficiency as supplying 2.5 ml/min to the outside of the tool. The material removal efficiency of the slurry when 15 ml/min of slurry is injected into the center of the tool is similar to when 10 ml/min of slurry is supplied outside the tool. The maximum processing efficiency observed when 2.5 ml/min of the slurry was supplied inside the tool at 1500 RPM was approximately 92% higher than the maximum efficiency observed when the slurry was supplied outside the tool.

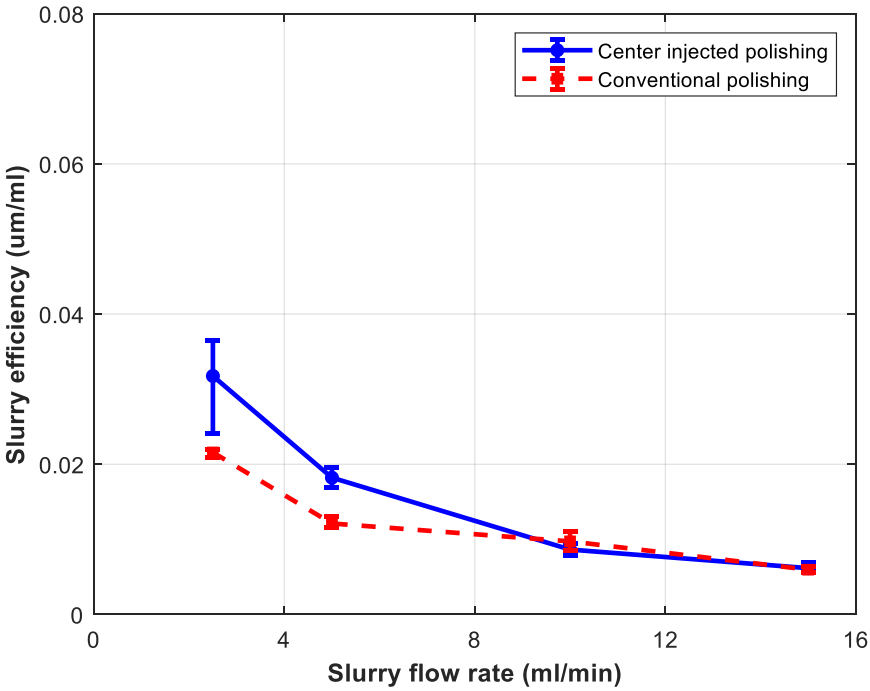

Figure 5.25 Slurry efficiency comparison (900RPM)

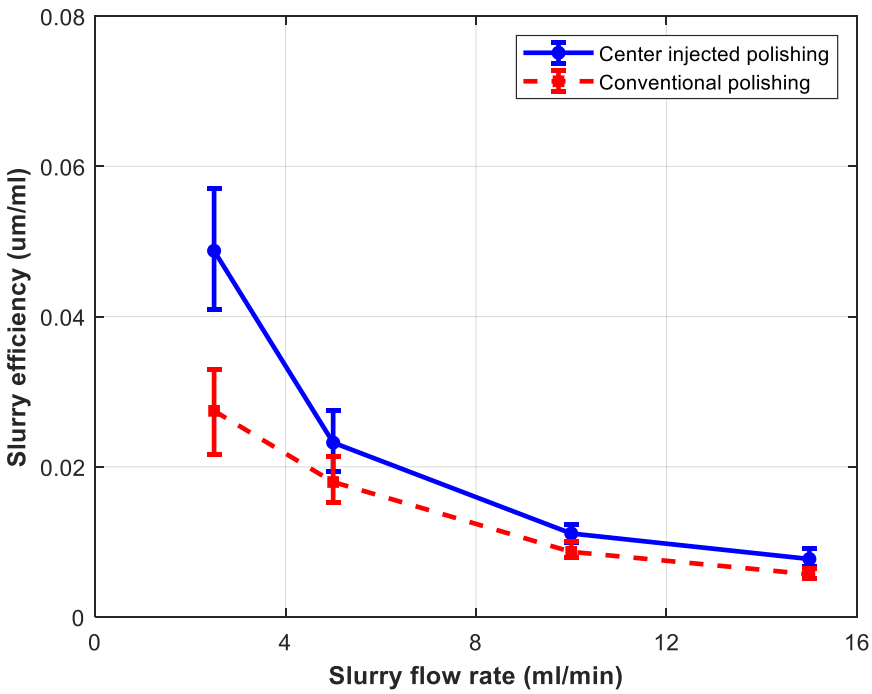

Figure 5.26 Slurry efficiency comparison (1500 RPM)

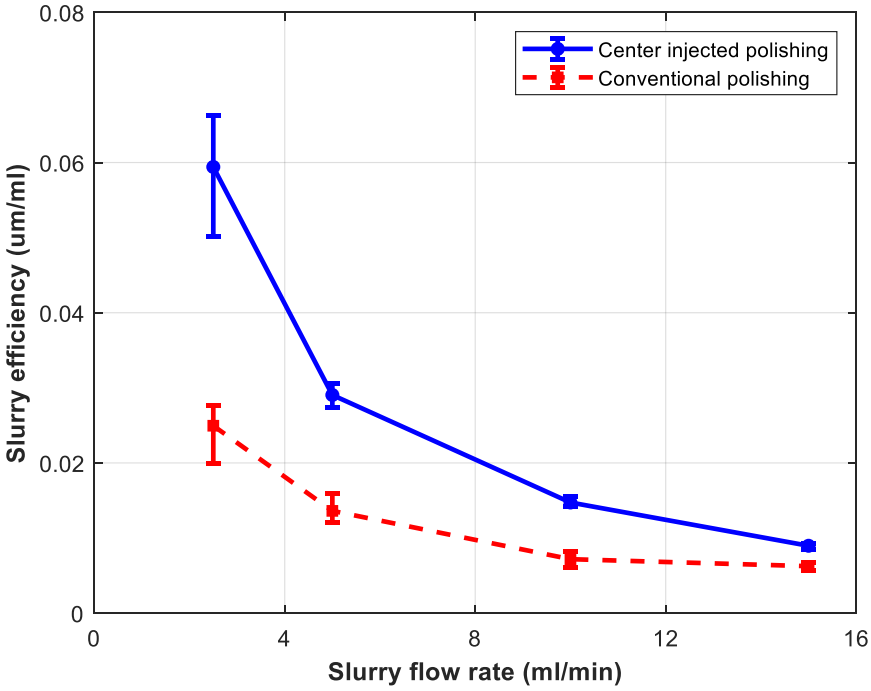

Figure 5.27 | Slurry efficiency comparison (3000RPM)

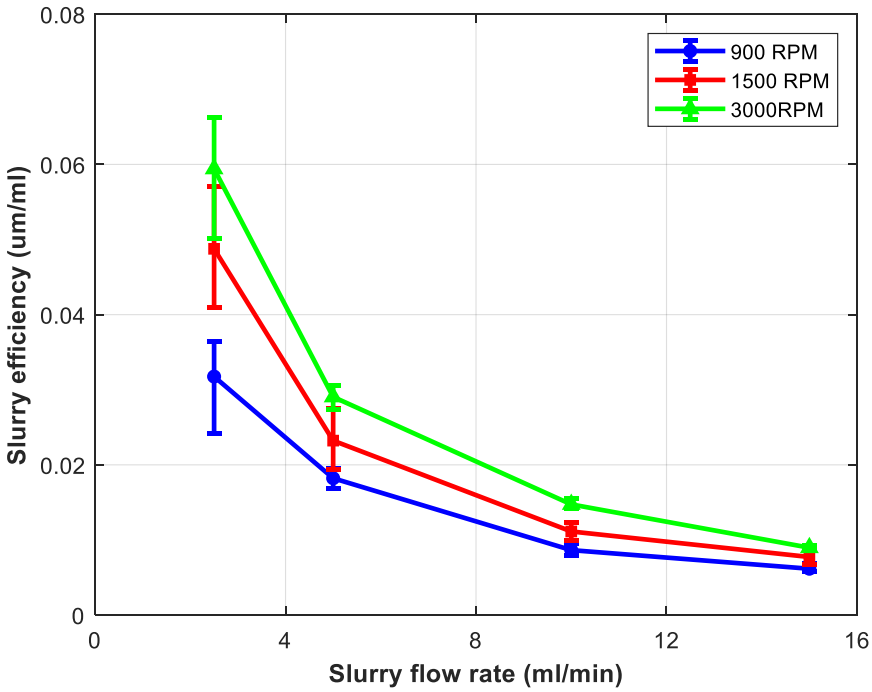

Figure 5.28 Slurry efficiency comparison of center injected polishing

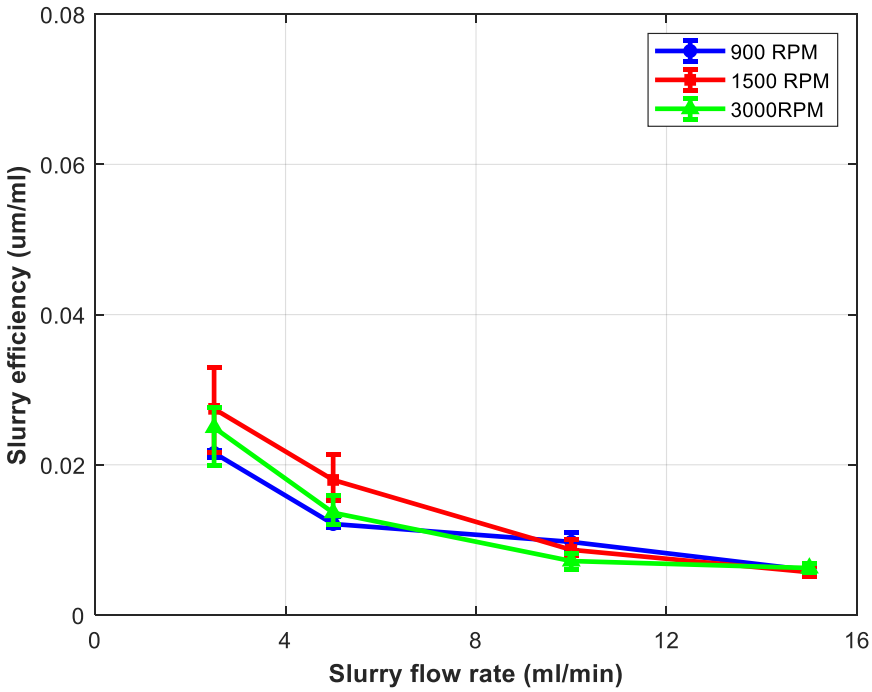

Figure 5.29 Slurry efficiency comparison of conventional polishing

The amount of slurry required to remove a certain volume of the workpiece was estimated using the calculated slurry efficiency, and the slurry reduction effect of the proposed system was evaluated. The experimental parameters were selected based on the following three criteria from the center-injected polishing and tool outside supply, and the amount of slurry used was compared.

1. Based on the parameter with the highest slurry efficiency
2. Based on the same polishing parameters
3. Based on the parameter with the maximum MRR

The comparison results are shown in the following graph. Comparing the experiments with the highest slurry efficiency, it is possible to reduce the slurry by 54% while increasing the MRR by 116% using center-injected polishing. Based on the same process parameters, it was possible to reduce the slurry by up to 58% while increasing the MRR by 138% using center-injected polishing. Finally, when comparing the experiments with the highest material removal performance, it was possible to reduce the slurry by up to 84% while increasing the MRR by 53% when using center-injected polishing.

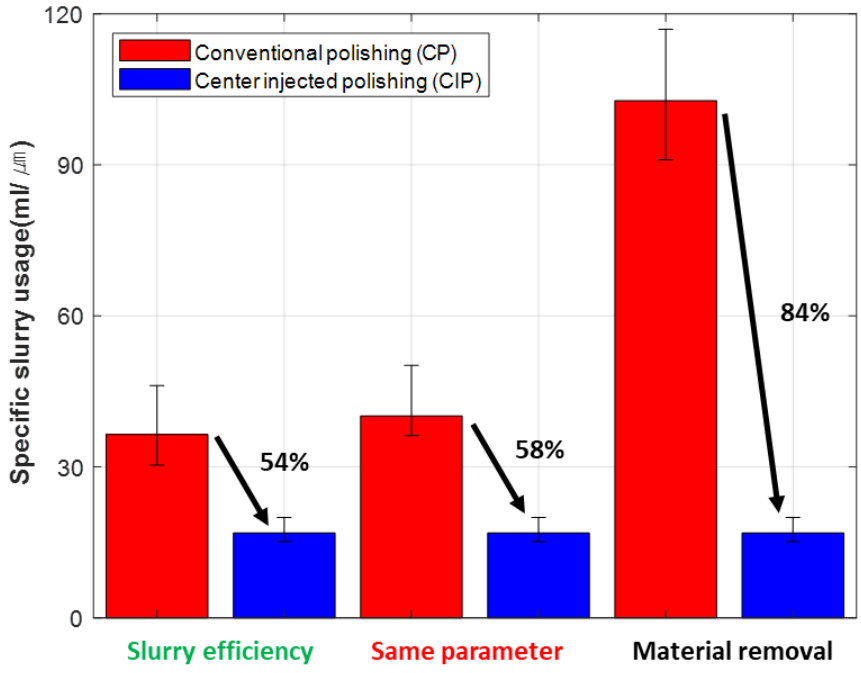

Figure 5.30 Specific slurry usage comparison

Chapter 6. Discussion

6.1. Limitations

The supplied polishing slurry condenses around the polishing tool due to surface tension and rotates together. Therefore, if a low flow rate is continuously supplied, a large amount of slurry is present around the tool, potentially distorting the slurry supply amount. In the case of supplying the slurry from the inside, there is a possibility that conventional polishing may be performed simultaneously by the slurry that forms together from the outside in addition to the internal supply. It is possible to determine the effect when more than the supply flow rate is supplied. In addition, the surface tension can act as a centripetal force at the bottom of the rotating tool. Therefore, when the surface tension changes, there is a possibility of changing the slurry flow under the rotating tool. As the surface tension of the slurry containing a large amount of water increases as the temperature decreases, the polishing performance may change when the temperature of the slurry is lowered, and polishing is performed. The design of the polishing tool tip is another factor that can affect slurry supply conditions. This study confirms that the slurry supply position has a significant influence on the performance. Therefore, design factors, such as the location and number of supply channels of the polishing tool, can also significantly affect the slurry supply status of center-injected polishing. In addition, it affects the slurry flow inside the polishing tool, which can have a significant impact on

important conditions, such as the vibration characteristics according to rotation. However, this study was conducted using a simple channel without considering the design elements. Significant problems such as vibration did not occur during the experimental process used in this study. However, additional research on the design of the polishing tool and the resulting vibration characteristics is required.

In addition, there are many cases in which a curved surface is processed during the manufacture of an optical system. The polishing tool was tilted to create a curved surface. In this case, as the interface characteristics change, the performance of center-injected polishing may also change. Depending on the design of the optical system, the performance in the case of low curvature, may be similar to that shown in this study. However, for processing an optical system with a large curvature, additional research on the processing performance of the system proposed in this study is required.

6.2. Effect of polishing pressure on the slurry supply

The polishing pressure can also affect the slurry supply conditions. If the polishing pressure is high, the size of the microchannels of the pad may be reduced as the polishing pad is pressed against the workpiece. Therefore, the supply state of the slurry may deteriorate. However, in the case of center-injected polishing, as the slurry is supplied by the pressure of the pump through the channel connected to the center of the tool, there is a possibility that the slurry can be supplied more smoothly than external injection that supplies the slurry without any special pressure.

According to the governing equation of polishing, the MRR is proportional to the polishing pressure and relative velocity. However, as mentioned above, a polishing pressure above a certain level may interfere with the slurry supply (see Section 5.3) may show results similar to those of RPM.

Additional polishing experiments were conducted to identify the effect of the polishing pressure. The experiments were performed by changing only the normal force in the polishing experiments using polishing parameters of 3000 RPM and 2.5 ml/min. Polishing was performed by changing the normal force from 22.5 N to 35 and 47.5 N. The experiment parameters are listed in Table 6.1.

The measurement results are shown in the Figure 6.1 and Figure 6.2. Material removal varied linearly according to the normal force (polishing pressure). The MRR increased linearly up to 3000 rpm, and then decreased at 4000 rpm. The MRR exhibited a linear increase when the normal drag force increased. Similar to the tool rotation speed, this also increases the MRR to a certain level. However, it is expected that the MRR will decrease owing to the deterioration of the slurry supply.

Table 6.1 Process parameters of the pressure experiment

Polishing (pressure experiment)	
Normal force [N]	35, 47.5
Tool diameter [mm]	26
Tool speed [RPM]	3000
Dwell time [min]	52
Feed rate [mm/s]	2.5
Slurry flow rate [ml/min]	2.5

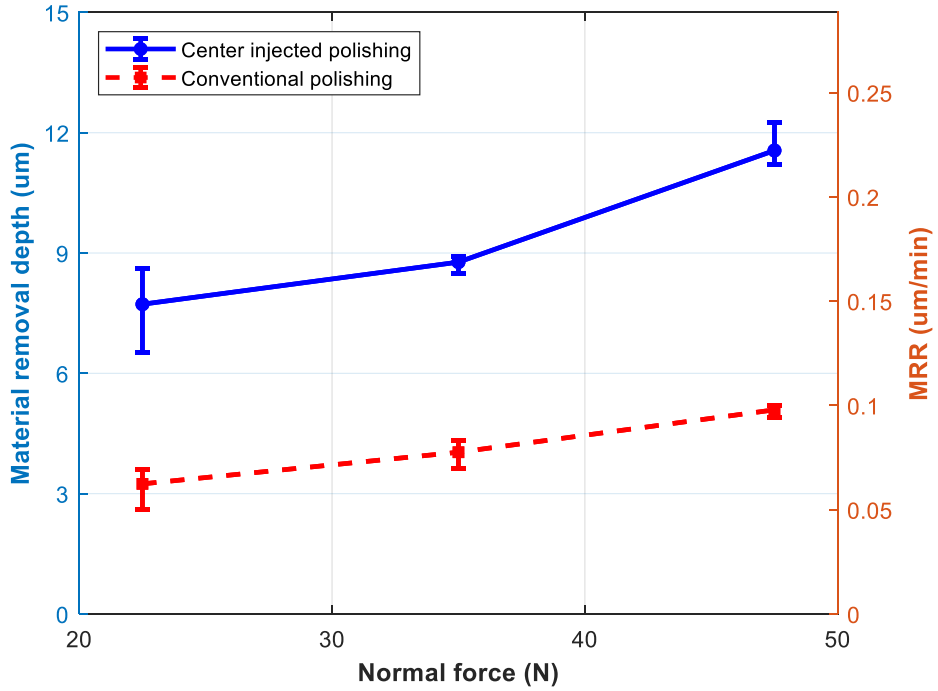

Figure 6.1 Material removal according to polishing pressure

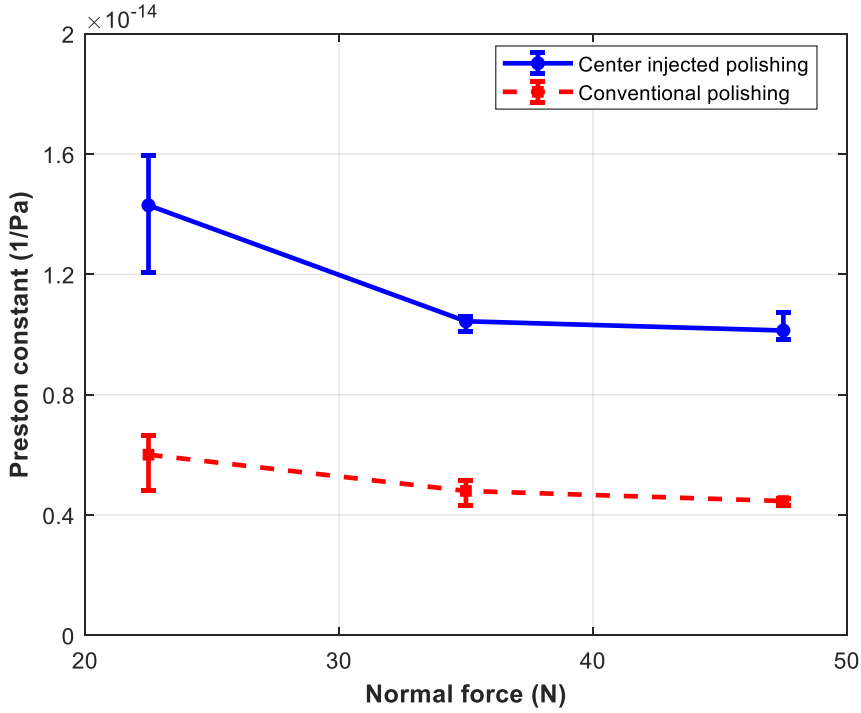

Figure 6.2 Preston constant according to polishing pressure

6.3. Model for Preston constant

In general, the governing equation for polishing is the Preston equation (Eq. 2-8). According to this equation, the Preston constant is independent of polishing pressure and speed. The graph in section 5.3 of this dissertation shows the Preston constant changes with the tool rotation speed.

This is because the material removal mechanism changes according to the ratio between relative velocity and pressure. As described in Section 2.2, the main material removal mechanisms for polishing are two-body sliding and three-body rolling. In the low V/P band, the amount of material removed by two-body sliding is dominant; therefore, the existing Preston equation fits well. However, according to Liu et al., in the high V/P region, material removal by three-body rolling increases during polishing [70]. Therefore, the governing equation must be modified to reflect this phenomenon. Where V is the relative velocity and P is the polishing pressure, the governing equation for polishing is modified in the form below [71]:

$$\mathrm{MRR} = (\mathrm{C}_1 P + C_2)V + C_3 \tag{6-1}$$

When the governing equation is modified in the above form, if the Preston constant is obtained in the same form as before, the constant is no longer independent of speed and pressure. (There is still no problem comparing the slurry supply conditions between processes with the same process parameters).

In this section, we intend to create an empirical model to predict the Preston constant using this equation. Based on the 10 ml/min slurry supply at the center

supply, an empirical model was created using existing performance comparison data. The experiment parameters are listed in Table 6.2.

Table 6.2 Process parameters of Preston constant prediction

Polishing (Preston constant prediction)	
Normal force [N]	22.5
Tool diameter [mm]	26
Tool speed [RPM]	2000, 2500, 4000
Dwell time [min]	52
Feed rate [mm/s]	2.5
Slurry flow rate [ml/min]	10

The results of predicting the Preston constants at 2000, 2500, and 4000 RPM, which were not tested, are shown in Figure 6.4. At 2000 and 2500 RPM, the prediction results of the model fit well. The MRR increased linearly up to 3000 rpm, and then decreased at 4000 rpm. In the case of the experiment performed at 4000 rpm, it appears that the slurry is in the starving state because the MRR drops rapidly. The Preston Constant in the slurry-starvation state is unpredictable. As the Preston constant is an empirical value, a model must be created empirically for prediction. However, in the slurry starting state, because the slurry supply state also changes whenever the parameter changes, the target model also changes every time.

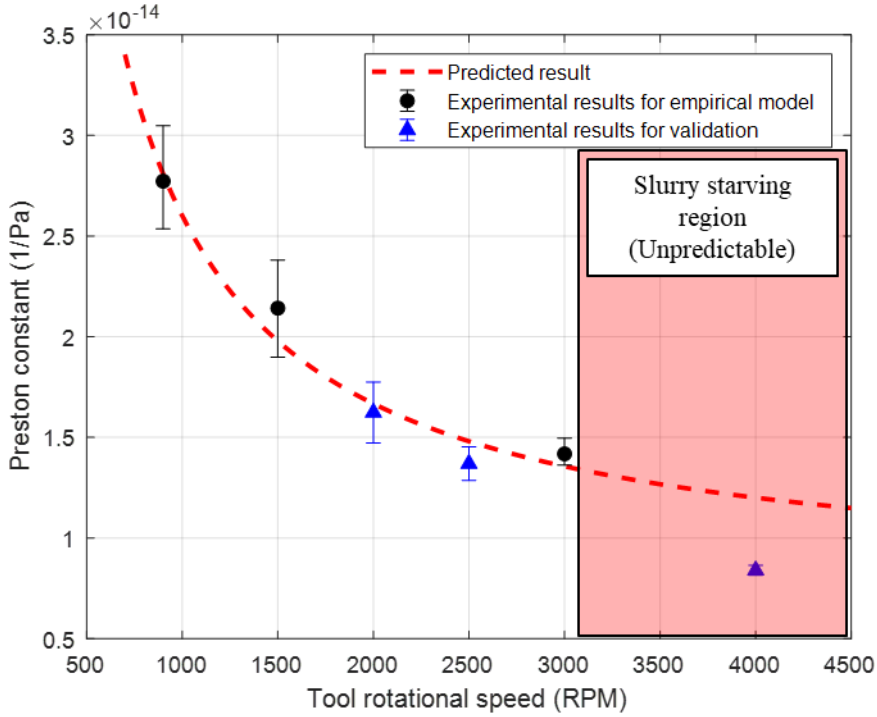

Figure 6.4 Empirical model for Preston constant

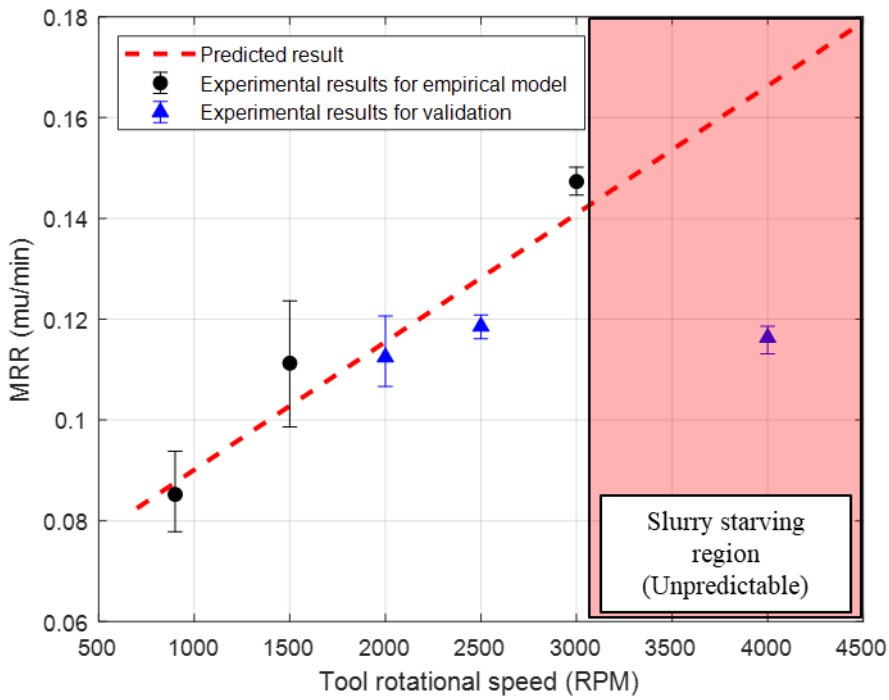

Figure 6.3 Empirical model for MRR

6.4. Power consumption

The power consumption for each supply method was also measured. The power efficiency of the proposed system was compared by measuring the power consumption of the slurry pump, stage, and spindle. The results of measuring the energy consumption of the entire system are shown in Figure 6.5 and Figure 6.6

The energy measurement results for each component are compared as follows. First, in the case of the slurry pump, the power consumption changed according to the supply flow rate regardless of the slurry supply method. An average power consumption of 21.3 W was consumed at 2.5 ml/min, which increased linearly to an average power consumption of 23.3 W at 15 ml/min. The stage exhibited almost the same power consumption throughout the experiment. In the case of the spindle, center-injected polishing consumed an average of approximately 3% more power than conventional polishing. This is a very small increase compared to the improvement value of MRR, and the center-injected polishing had up to 132% greater energy efficiency when comparing the energy efficiency through power consumption versus material removal, as shown in Figure 6.7 and Figure 6.8.

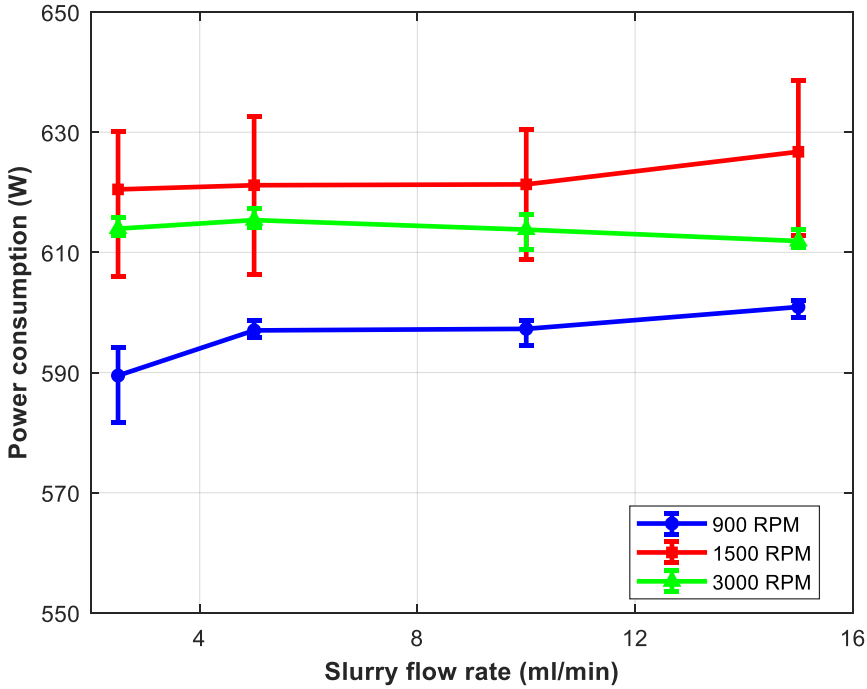

Figure 6.5 Power consumption of center injected polishing

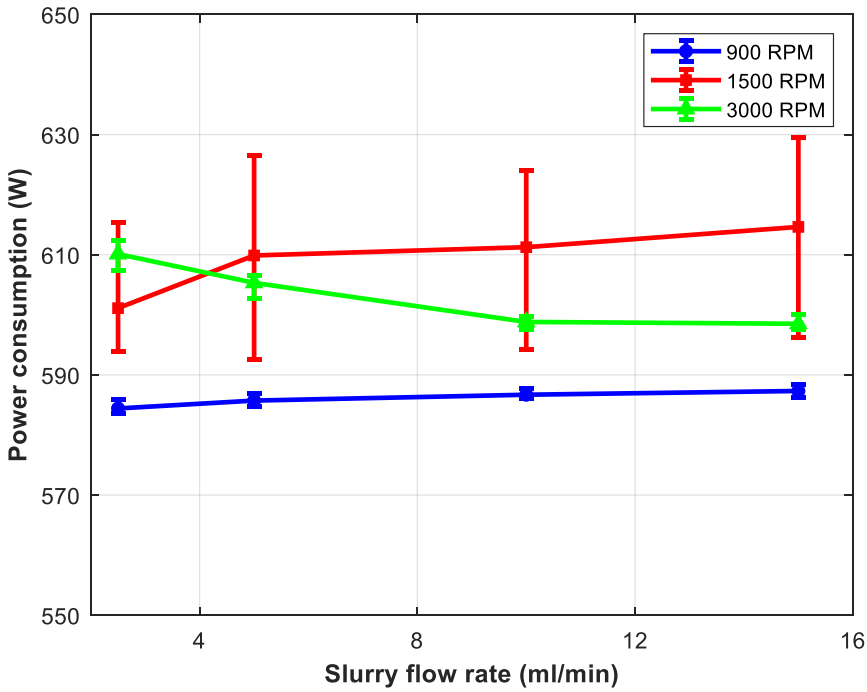

Figure 6.6 Power consumption of conventional polishing

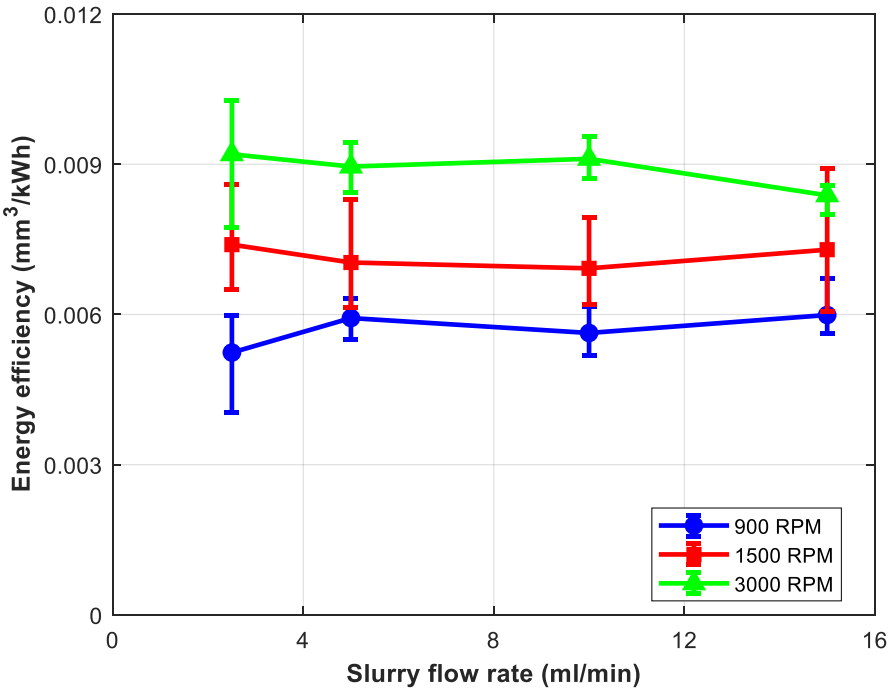

Figure 6.7 Energy efficiency of center injected polishing

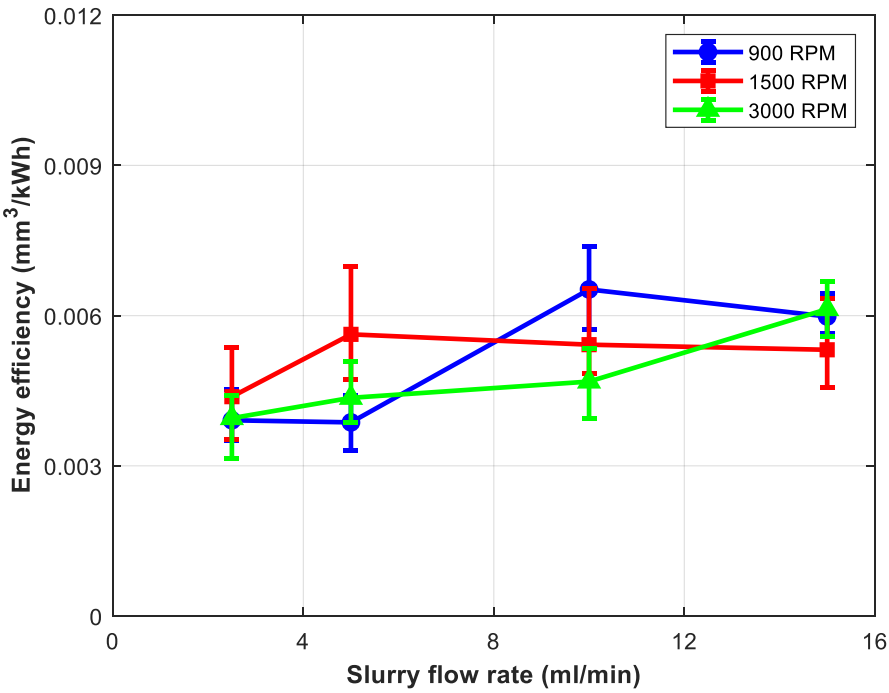

Figure 6.8 Energy efficiency of conventional polishing

Chapter 7. Conclusion

In this dissertation, center-injected polishing is introduced as an approach to improve slurry supply and reduce slurry usage. A polishing tool was developed that uses a rotary union to supply slurry directly to the center of the tool. Polishing experiments were performed using the developed tool under various slurry supply flow rates and rotational speeds. Thus, the effect of center injection on the performance and slurry consumption was evaluated.

The center-injected polishing increased the MRR by up to 138% compared with conventional polishing and obtained a surface with roughness values below 18 nm on both sides after 52 min of polishing. The effect of improving the slurry supply of center-injected polishing was investigated through CFD and flow observation under actual polishing conditions. The slurry supply performance was also compared with the Preston constant. In this comparison, the center-injected polishing showed a maximum improvement in the slurry supply performance at 3000 RPM based on the magnitude of the constant.

Significant process performance improvements and slurry consumption reductions were achieved simultaneously through this study. The MRR increased by 138%, and at the same time, the slurry consumption decreased by 58%.

Bibliography

[1] R. Cheung, *Silicon carbide microelectromechanical systems for harsh environments*. World Scientific, 2006.

[2] H. Morkoc, S. Strite, G. Gao, M. Lin, B. Sverdlov, and M. Burns, "Large-band-gap SiC, III-V nitride, and II-VI ZnSe-based semiconductor device technologies," *Journal of Applied physics,* vol. 76, no. 3, pp. 1363-1398, 1994, doi:https://doi.org/10.1063/1.358463.

[3] N. Jepps and T. Page, "Polytypic transformations in silicon carbide," *Progress in crystal growth and characterization,* vol. 7, no. 1-4, pp. 259-307, 1983, doi:https://doi.org/10.1016/0146-3535(83)90034-5.

[4] T. Ayalew, "SiC semiconductor devices technology, modeling and simulation," 2004. doi:https://doi.org/10.34726/hss.2004.04281063.

[5] T. Muranaka, Y. Kikuchi, T. Yoshizawa, N. Shirakawa, and J. Akimitsu, "Superconductivity in carrier-doped silicon carbide," *Science and Technology of Advanced Materials,* vol. 9, no. 4, p. 044204, 2009, doi:https://doi.org/10.1088/1468-6996/9/4/044204.

[6] S. Sun, M. Brandt, and M. Dargusch, "Thermally enhanced machining of hard-to-machine materials—a review," *International Journal of Machine Tools and Manufacture,* vol. 50, no. 8, pp. 663-680, 2010, doi:https://doi.org/10.1016/j.ijmachtools.2010.04.008.

[7] D.-H. Kim and C.-M. Lee, "A study on the laser-assisted ball-end milling of difficult-to-cut materials using a new back-and-forth preheating method," *The International Journal of Advanced Manufacturing*

Technology, vol. 85, no. 5, pp. 1825-1834, 2016, doi:https://doi.org/10.1007/s00170-015-8014-1.

[8] Z. Li and R. C. Bradt, "Thermal expansion of the hexagonal (4 H) polytype of SiC," *Journal of Applied Physics,* vol. 60, no. 2, pp. 612-614, 1986.

[9] G. L. Harris, *Properties of silicon carbide* (no. 13). Iet, 1995.

[10] M. E. Levinshtein, S. L. Rumyantsev, and M. S. Shur, *Properties of Advanced Semiconductor Materials: GaN, AIN, InN, BN, SiC, SiGe*. John Wiley & Sons, 2001.

[11] C.-M. Zetterling, *Process technology for silicon carbide devices* (no. 2). IET, 2002.

[12] J. D. Reddy, A. A. Volinsky, C. L. Frewin, C. Locke, and S. E. Saddow, "Mechanical properties of 3C-SiC films for MEMS applications," *MRS Online Proceedings Library (OPL),* vol. 1049, 2007, doi:https://doi.org/10.1557/PROC-1049-AA03-06.

[13] H. Pollicove and D. Golini, "Deterministic manufacturing processes for precision optical surfaces," in *Key Engineering Materials*, 2003, vol. 238: Trans Tech Publ, pp. 53-58, doi: https://doi.org/10.4028/www.scientific.net/KEM.238-239.53.

[14] R. Pan, Y. Zhang, J. Ding, C. Huang, and Z. Wang, "Optimization strategy on conformal polishing of precision optics using bonnet tool," *International Journal of Precision Engineering and Manufacturing,* vol. 17, no. 3, pp. 271-280, 2016, doi:https://doi.org/10.1007/s12541-016-0035-7.

[15] Z.-C. Lin, R.-Y. Wang, and Z.-W. Jhang, "Establishing a theoretical model for abrasive removal depth of silicon wafer chemical mechanical polishing

by integrating a polishing times analytical model and specific down force energy theory," *The International Journal of Advanced Manufacturing Technology,* vol. 95, no. 9, pp. 4671-4683, 2018, doi:https://doi.org/10.1007/s00170-017-1532-2.

[16] L. Zhang, D. Huang, W. Zhou, C. Fan, S. Ji, and J. Zhao, "Corrective polishing of freeform optical surfaces in an off-axis three-mirror imaging system," *The International Journal of Advanced Manufacturing Technology,* vol. 88, no. 9, pp. 2861-2869, 2017, doi:https://doi.org/10.1007/s00170-016-8995-4.

[17] S. Wan, X. Zhang, W. Wang, and M. Xu, "Effect of pad wear on tool influence function in robotic polishing of large optics," *The International Journal of Advanced Manufacturing Technology,* vol. 102, no. 5, pp. 2521-2530, 2019, doi:https://doi.org/10.1007/s00170-019-03344-7.

[18] B. Chen, S. Li, Z. Deng, B. Guo, and Q. Zhao, "Grinding marks on ultra-precision grinding spherical and aspheric surfaces," *International Journal of Precision Engineering and Manufacturing-Green Technology,* vol. 4, no. 4, pp. 419-429, 2017, doi:https://doi.org/10.1007/s40684-017-0047-5.

[19] C. R. Dandekar, Y. C. Shin, and J. Barnes, "Machinability improvement of titanium alloy (Ti–6Al–4V) via LAM and hybrid machining," *International Journal of Machine Tools and Manufacture,* vol. 50, no. 2, pp. 174-182, 2010, doi:https://doi.org/10.1016/j.ijmachtools.2009.10.013.

[20] P.-y. Zhao, M. Zhou, Y.-j. Zhang, and G.-c. Qiao, "Surface roughness prediction model in ultrasonic vibration assisted grinding of BK7 optical glass," *Journal of Central South University,* vol. 25, no. 2, pp. 277-286, 2018, doi:https://doi.org/10.1007/s11771-018-3736-5.

[21] Q. Gou, J. Xiong, Z. Guo, J. Liu, L. Yang, and X. Li, "Influence of NbC additions on microstructure and wear resistance of Ti (C, N)-based cermets bonded by CoCrFeNi high-entropy alloy," *International Journal of Refractory Metals and Hard Materials,* vol. 94, p. 105375, 2021, doi:https://doi.org/10.1016/j.ijrmhm.2020.105375.

[22] N. J. Vickers, "Animal communication: when i'm calling you, will you answer too?," *Current biology,* vol. 27, no. 14, pp. R713-R715, 2017, doi:https://doi.org/10.1016/j.cub.2017.05.064.

[23] Z. Dong and H. Cheng, "Study on removal mechanism and removal characters for SiC and fused silica by fixed abrasive diamond pellets," *International Journal of Machine Tools and Manufacture,* vol. 85, pp. 1-13, 2014, doi:https://doi.org/10.1016/j.ijmachtools.2014.04.008.

[24] T. Zhang, Y. Zhao, T. Yu, T. Yu, J. Shi, and J. Zhao, "Study on polishing slurry waste reduction in polishing monocrystalline silicon based on ultrasonic atomization," *Journal of cleaner production,* vol. 233, pp. 1-12, 2019, doi:https://doi.org/10.1016/j.jclepro.2019.06.067.

[25] P. A. Abrego Serrano, M. Kim, D.-R. Kim, D.-H. Kim, G.-H. Kim, and S.-H. Ahn, "Spherical mirror and surface patterning on silicon carbide (SiC) by material removal rate enhancement using CO2 laser assisted polishing," *International Journal of Precision Engineering and Manufacturing,* vol. 21, no. 5, pp. 775-785, 2020, doi:https://doi.org/10.1007/s12541-019-00304-9.

[26] T. Yu, T. Zhang, X. Yu, X. Yang, and J. Sun, "Study on optimization of ultrasonic-vibration-assisted polishing process parameters," *Measurement,* vol. 135, pp. 651-660, 2019,

doi:https://doi.org/10.1016/j.measurement.2018.12.008.

[27] H. Lee, H. Kim, and H. Jeong, "Approaches to Sustainability in Chemical Mechanical Polishing (CMP): A Review," *International Journal of Precision Engineering and Manufacturing-Green Technology,* pp. 1-19, 2021, doi:https://doi.org/10.1007/s40684-021-00406-8.

[28] X. Liu, Y. Liu, Y. Liang, H. Liu, Y. Hu, and B. Gao, "Optimization of slurry components for a copper chemical mechanical polishing at low down pressure using response surface methodology," *Microelectronic engineering,* vol. 88, no. 1, pp. 99-104, 2011, doi:https://doi.org/10.1016/j.mee.2010.09.007.

[29] Y.-J. Seo and W.-S. Lee, "Chemical mechanical polishing of Ba0. 6Sr0. 4TiO3 film prepared by sol–gel method," *Microelectronic Engineering,* vol. 75, no. 2, pp. 149-154, 2004, doi:https://doi.org/10.1016/j.mee.2004.03.086.

[30] S.-W. Park, Y.-J. Seo, and W.-S. Lee, "A study on the chemical mechanical polishing of oxide film using a zirconia (ZrO2)-mixed abrasive slurry (MAS)," *Microelectronic Engineering,* vol. 85, no. 4, pp. 682-688, 2008, doi:https://doi.org/10.1016/j.mee.2007.12.049.

[31] H. Lee and H. Jeong, "Analysis of removal mechanism on oxide CMP using mixed abrasive slurry," *International journal of precision engineering and manufacturing,* vol. 16, no. 3, pp. 603-607, 2015, doi:https://doi.org/10.1007/s12541-015-0081-6.

[32] H. Lee, D. Lee, M. Kim, and H. Jeong, "Effect of mixing ratio of non-spherical particles in colloidal silica slurry on oxide CMP," *International Journal of Precision Engineering and Manufacturing,* vol. 18, no. 10, pp.

1333-1338, 2017, doi:https://doi.org/10.1007/s12541-017-0158-5.

[33] Z. Lu, S.-H. Lee, V. R. Gorantla, S. Babu, and E. Matijević, "Effects of mixed abrasives in chemical mechanical polishing of oxide films," *Journal of materials research,* vol. 18, no. 10, pp. 2323-2330, 2003, doi:https://doi.org/10.1557/JMR.2003.0326.

[34] Y. Lee, Y.-J. Seo, and H. Jeong, "Evaluation of oxide-chemical mechanical polishing characteristics using ceria-mixed abrasive slurry," *Electronic Materials Letters,* vol. 8, no. 5, pp. 523-528, 2012, doi:https://doi.org/10.1007/s13391-012-2056-4.

[35] Y. Lee, Y.-J. Seo, H. Lee, and H. Jeong, "Effect of diluted colloidal silica slurry mixed with ceria abrasives on CMP characteristic," *International Journal of Precision Engineering and Manufacturing-Green Technology,* vol. 3, no. 1, pp. 13-17, 2016, doi:https://doi.org/10.1007/s40684-016-0002-x.

[36] H. Lee, D. Kim, J. An, H. Lee, K. Kim, and H. Jeong, "Hybrid polishing mechanism of single crystal SiC using mixed abrasive slurry (MAS)," *CIRP annals,* vol. 59, no. 1, pp. 333-336, 2010, doi:https://doi.org/10.1016/j.cirp.2010.03.114.

[37] D. Lee, H. Lee, and H. Jeong, "The effects of a spray slurry nozzle on copper CMP for reduction in slurry consumption," *Journal of Mechanical Science and Technology,* vol. 29, no. 12, pp. 5057-5062, 2015, doi:https://doi.org/10.1007/s12206-015-1101-2.

[38] S. Ramakrishnan, S. Janjam, U. Patri, D. Roy, and S. Babu, "Comparison of dicarboxylic acids as complexing agents for abrasive-free chemical mechanical planarization of copper," *Microelectronic engineering,* vol. 84,

no. 1, pp. 80-86, 2007, doi:https://doi.org/10.1016/j.mee.2006.08.011.

[39] G. Yang, P. He, and X.-P. Qu, "Inhibition effect of glycine on molybdenum corrosion during CMP in alkaline H2O2 based abrasive free slurry," *Applied Surface Science,* vol. 427, pp. 148-155, 2018, doi:https://doi.org/10.1016/j.apsusc.2017.08.140.

[40] H. Hara *et al.*, "Novel abrasive-free planarization of 4H-SiC (0001) using catalyst," *Journal of electronic materials,* vol. 35, no. 8, pp. L11-L14, 2006, doi:https://doi.org/10.1007/s11664-006-0218-6.

[41] S. Pandija, D. Roy, and S. Babu, "Chemical mechanical planarization of copper using abrasive-free solutions of oxalic acid and hydrogen peroxide," *Materials chemistry and physics,* vol. 102, no. 2-3, pp. 144-151, 2007, doi:https://doi.org/10.1016/j.matchemphys.2006.11.015.

[42] X. Liao, Y. Sampurno, Y. Zhuang, and A. Philipossian, "Effect of slurry application/injection schemes on slurry availability during chemical mechanical planarization (CMP)," *Electrochemical and Solid-State Letters,* vol. 15, no. 4, p. H118, 2012, doi:https://doi.org/10.1149/2.009205esl.

[43] L. Rayleigh, "Polish," *Transactions of the Optical Society,* vol. 19, no. 1, p. 38, 1917, doi:https://doi.org/10.1088/1475-4878/19/1/302.

[44] R. Aghan and L. E. Samuels, "Mechanisms of abrasive polishing," *Wear,* vol. 16, no. 4, pp. 293-301, 1970, doi:https://doi.org/10.1016/0043-1648(70)90253-X.

[45] C. Evans *et al.*, "Material removal mechanisms in lapping and polishing," *CIRP annals,* vol. 52, no. 2, pp. 611-633, 2003, doi:https://doi.org/10.1016/S0007-8506(07)60207-8.

[46] J. Luo and D. A. Dornfeld, "Material removal mechanism in chemical

mechanical polishing: theory and modeling," *IEEE transactions on semiconductor manufacturing,* vol. 14, no. 2, pp. 112-133, 2001, doi:https://doi.org/10.1109/66.920723.

[47] H. Hertz, "On the contact of rigid elastic solids and on hardness, chapter 6: Assorted papers by H. Hertz," ed: MacMillan, New York, 1882.

[48] K. L. Johnson and K. L. Johnson, *Contact mechanics*. Cambridge university press, 1987.

[49] D. A. Hanaor, Y. Gan, and I. Einav, "Contact mechanics of fractal surfaces by spline assisted discretisation," *International Journal of Solids and Structures,* vol. 59, pp. 121-131, 2015.

[50] I. N. Sneddon, "The relation between load and penetration in the axisymmetric Boussinesq problem for a punch of arbitrary profile," *International journal of engineering science,* vol. 3, no. 1, pp. 47-57, 1965, doi:https://doi.org/10.1016/0020-7225(65)90019-4.

[51] K. J. P. Johnson, Cambridge, "Contact Mechanics Cambridge Univ," 1985.

[52] B. Bhushan, *Principles and applications of tribology*. John Wiley & Sons, 1999.

[53] M. Swain, "Microscopic observations of abrasive wear of polycrystalline alumina," *Wear,* vol. 35, no. 1, pp. 185-189, 1975, doi:https://doi.org/10.1016/0043-1648(75)90152-0.

[54] N. Emori, T. Sasada, and M. Oike, "Effect of Material Combination in Rubbing Parts on 3 Body Abrasive Wear," *Journal of Japan Society of Lubrication Engineers,* vol. 30, no. 1, pp. 53-59, 1985.

[55] M. Jenkins and A. Stamboulis, *Durability and reliability of medical polymers*. Elsevier, 2012.

[56] H. Rahnejat, *Tribology and dynamics of engine and powertrain: fundamentals, applications and future trends*. Elsevier, 2010.

[57] G. Straffelini, "Friction and Wear," *Springer International Publishing, Switzerland. doi,* vol. 10, pp. 978-3, 2015.

[58] E. Rabinowicz and R. Tanner, "Friction and wear of materials," *Journal of Applied Mechanics,* vol. 33, p. 479, 1966.

[59] G. Straffelini, "Friction and wear," *Springer Tracts in Mechanical Engineering. Springer, Cham. doi. org/10.1007/978-3-319-05894-8,* 2015, doi:https://doi.org/10.1007/978-3-319-05894-8.

[60] E. J. Terrell and C. F. Higgs, "Hydrodynamics of slurry flow in chemical mechanical polishing: A review," *Journal of The Electrochemical Society,* vol. 153, no. 6, p. K15, 2006, doi:https://doi.org/10.1149/1.2188329.

[61] F. Preston, "The theory and design of plate glass polishing machines," *J. Soc. Glass Tech.,* vol. 11, p. 214, 1927.

[62] Y. Zhao and L. Chang, "A micro-contact and wear model for chemical–mechanical polishing of silicon wafers," *Wear,* vol. 252, no. 3-4, pp. 220-226, 2002, doi:https://doi.org/10.1016/S0043-1648(01)00871-7.

[63] Y. Wang, B. Lin, S. Wang, and X. Cao, "Study on the system matching of ultrasonic vibration assisted grinding for hard and brittle materials processing," *International Journal of Machine Tools and Manufacture,* vol. 77, pp. 66-73, 2014, doi:https://doi.org/10.1016/j.ijmachtools.2013.11.003.

[64] T. Tawakoli, B. Azarhoushang, and M. Rabiey, "Ultrasonic assisted dry grinding of 42CrMo4," *The International Journal of Advanced Manufacturing Technology,* vol. 42, no. 9, pp. 883-891, 2009, doi:https://doi.org/10.1007/s00170-008-1646-7.

[65] D. Guo, J. Li, G. Xie, Y. Wang, and J. Luo, "Elastic properties of polystyrene nanospheres evaluated with atomic force microscopy: size effect and error analysis," *Langmuir,* vol. 30, no. 24, pp. 7206-7212, 2014, doi:https://doi.org/10.1021/la501485e.

[66] Y.-R. Jeng and P.-Y. Huang, "A material removal rate model considering interfacial micro-contact wear behavior for chemical mechanical polishing," *J. Trib.,* vol. 127, no. 1, pp. 190-197, 2005, doi:https://doi.org/10.1115/1.1828068.

[67] F. Klocke and R. Zunke, "Removal mechanisms in polishing of silicon based advanced ceramics," *CIRP annals,* vol. 58, no. 1, pp. 491-494, 2009, doi:https://doi.org/10.1016/j.cirp.2009.03.120.

[68] M. Kim, S. Bang, D.-H. Kim, H.-T. Lee, G.-H. Kim, and S.-H. Ahn, "Hybrid CO2 laser-polishing process for improving material removal of silicon carbide," *The International Journal of Advanced Manufacturing Technology,* vol. 106, no. 7, pp. 3139-3151, 2020, doi:https://doi.org/10.1007/s00170-019-04846-0.

[69] Y. Xie and B. Bhushan, "Effects of particle size, polishing pad and contact pressure in free abrasive polishing," *Wear,* vol. 200, no. 1-2, pp. 281-295, 1996, doi:https://doi.org/10.1016/S0043-1648(96)07275-4.

[70] J.-Y. Lai, "Mechanics, mechanisms, and modeling of the chemical mechanical polishing process," Massachusetts Institute of Technology, 2001.

[71] Q. Luo, S. Ramarajan, and S. Babu, "Modification of the Preston equation for the chemical–mechanical polishing of copper," *Thin solid films,* vol. 335, no. 1-2, pp. 160-167, 1998, doi:https://doi.org/10.1016/S0040-

6090(98)00896-7.

요약(국문 초록)

실리콘 카바이드는 재료가 지닌 낮은 밀도, 높은 강성, 낮은 열팽창률 등의 우수한 기계적, 화학적 물성 때문에 최근 우주 분야에서 광학 부품으로 많은 주목을 받고 있다. 일반적으로 광학 부품의 제작은 높은 재료 제거율, 낮은 표면 품질을 갖는 공정에서 출발하여, 마지막에는 낮은 재료 제거율과 우수한 표면 품질을 갖는 공정으로 마무리된다. 폴리싱은 이 광학 부품 제작의 마지막 단계에서 광학 부품의 품질을 결정하는 매우 중요한 역할을 수행한다.

매우 낮은 재료 제거율을 갖는 폴리싱의 특성상 폴리싱은 광학 부품 제작 공정 중에 가장 많은 시간이 소요되는 공정 중 하나이다. 이 긴 가공 시간동안 소요되는 소모품의 양 또한 엄청나기 때문에, 이를 줄이는 것이 공정의 비용을 절감하고 환경성을 개선하는데 핵심이다.

폴리싱의 주요 소모품 중의 하나인 슬러리의 경우, 일반적으로 공정에 충분한 양이 공급되는 것을 확실시하기 위하여 별다른 고려 없이 과도한 양의 슬러리를 공급한다. 하지만 이 과도한 공급량 중에 일부만이 실제 폴리싱 공정에 참여하고 나머지는 폐기물로 배출된다. 특히 이 과정에서 회전하는 폴리싱 툴로 인해 발생하는 원심력이 폴리싱 툴과 워크피스의 접촉면으로 슬러리를 공급하는 것을 방해한다.

본 연구에서는 툴 중심부에 슬러리를 직접적으로 공급함으로써, 툴 회전에 의해 발생하는 원심력을 슬러리 공급에 활용하여 슬러리의 공급 상태를 개선하고자 한다. 궁극적으로는 슬러리 공급 개선을 통해 공정 자체의 성능을 개선하고 슬러리의 사용량을 줄이고자 한다. 슬러리는

로터리 유니온과 자체 제작된 폴리싱 툴을 통해 툴 중심부로 공급된다. 슬러리의 툴 중심부/외부 공급 시에 다양한 공급 유량 및 툴 회전 속도에서의 폴리싱 실험을 수행하고, 실험 이후 가공량, 표면 거칠기를 측정하여 공정의 성능을 평가하였다. 재료 제거량에서는 툴 중심부 공급이 툴 외부 공급보다 최대 138% 높은 가공량을 보였다. 3가지 기준에 따라 재료 제거량과 슬러리 사용량을 활용하여 슬러리 저감량을 평가하였을 때는 최고 슬러리 가공 효율 기준 54%, 같은 공정 파라미터 사용 기준 58%, 최대 재료 제거 성능 기준 84%의 슬러리 저감 성능을 보였다.

주요어 : 폴리싱, 슬러리 저감, 녹색 생산, 실리콘 카바이드

학 번 : 2016-20673